

STATUS OF THESIS

Title of thesis

AMINO-*N*-(3-(DIMETHYLAMINO)PROPYL)ACETAMIDE
AS AN ABSORBENT FOR CARBON DIOXIDE CAPTURE
AND UTILIZATION

I HANAN BINTI MOHAMED MOHSIN

hereby allow my thesis to be placed at the Information Resource Center (IRC) of the Universiti Teknologi PETRONAS (UTP) with the following conditions:

1. The thesis becomes the property of UTP
2. The IRC of UTP may make copies of the thesis for academic purposes only.
3. This thesis is classified as

Confidential

Non-confidential

If this thesis is confidential, please state the reason:

The contents of the thesis will remain confidential for _____ years.

Remarks on disclosure:

Endorsed by

Signature of Author

Signature of Supervisor

Name of Author:
Hanan binti Mohamed Mohsin
Permanent address:
730, Lorong 22/2, Lavender Heights,
70450, Senawang,
Negeri Sembilan, Malaysia.

Name of Supervisor:
Dr. Khairiraihanna binti Johari

Date: _____

Date: _____

APPROVAL PAGE

UNIVERSITI TEKNOLOGI PETRONAS

AMINO-*N*-(3-(DIMETHYLAMINO)PROPYL)ACETAMIDE AS AN
ABSORBENT FOR CARBON DIOXIDE CAPTURE AND UTILIZATION

by

HANAN BINTI MOHAMED MOHSIN

The undersigned certify that they have read and recommend to the Postgraduate Studies Programme for acceptance of this thesis for the fulfilment of the requirements for the degree stated.

Signature:

Main Supervisor:

Signature:

Co-Supervisor:

Signature:

Head of Department:

Date:

AMINO-*N*-(3-(DIMETHYLAMINO)PROPYL)ACETAMIDE
AS AN ABSORBENT FOR CARBON DIOXIDE
CAPTURE AND UTILIZATION

by

HANAN BINTI MOHAMED MOHSIN

A Thesis

Submitted to the Postgraduate Studies Programme
as a Requirement for the Degree of

MASTER OF SCIENCE
CHEMICAL ENGINEERING
UNIVERSITI TEKNOLOGI PETRONAS
BANDAR SERI ISKANDAR,
PERAK

MARCH 2020

DECLARATION OF THESIS

Title of thesis

AMINO-*N*-(3-(DIMETHYLAMINO)PROPYL)ACETAMIDE
AS AN ABSORBENT FOR CARBON DIOXIDE CAPTURE
AND UTILIZATION

I HANAN BINTI MOHAMED MOHSIN

hereby declare that the thesis is based on my original work except for quotations and citations which have been dully acknowledged. I also declare that it has not been previously or concurrently submitted for any other degree at UTP or other institutions.

Witnessed by

Signature of Author

Permanent address: _____
730, Lorong 22/2,
Lavender Heights,
70450, Senawang,
Negeri Sembilan, Malaysia

Date: _____

Signature of Supervisor

Name of Supervisor
Dr. Khairiraihanna binti Johari

Date: _____

ACKNOWLEDGEMENT

With the grace of Almighty, I am able to finish this thesis study. This work would not have been possible without the assistance and encouragement of various individuals from the beginning until the end of this master journey. I would like to take this opportunity to convey my uttermost gratitude to my main supervisor, Dr. Khairiraihanna Johari for the persistence guidance, inspiration, and motivational support in ensuring that I completed this master thesis. My appreciation also goes to my co-supervisor, Prof Dr. Azmi Mohd Shariff for sharing his knowledge and wisdom in the subject matter. To my family members, especially my parents and my siblings, thank you for the support and words of encouragement that helped keep me motivated throughout my study period. To my housemates and friends, Nur Afiqah, Siti Suhailah, Anisah, Norliza, and Khaliesah, I really appreciate the knowledge and experience shared with me which assisted towards the completion of my thesis. The same amount of gratitude goes to the lab technologies, Mr. Adli, Ms. Shahidah, and Mr. Samad who are always available to lend a helping hand when handling equipment in the laboratories. Last but not least, I would like to thank the university and CO₂ Research Center (CO2RES) in particular, for the financial support and facilities provided for me to carry out my research activities.

ABSTRACT

Monoethanolamine (MEA) is a conventional absorbent used for CO₂ capture in the industry. However, MEA has limited CO₂ absorption capacity. Moreover, high energy input is required to separate CO₂ from MEA after the absorption process. In this study, the CO₂ desorption process was eliminated through integration of CO₂ capture and utilization. The high energy requirement during CO₂ utilization can also be reduced through the integration process. The performance of 3-dimethylaminopropylamine (DMAPA) neutralized with glycine as potential absorbent for CO₂ capture was evaluated in this study by measuring the CO₂ loading capacity of the absorbent. The physical properties of the absorbent were evaluated by measuring the density, viscosity, refractive index, and surface tension of the absorbent. The absorbent formed through the neutralization process was analyzed by using Fourier transform infrared (FTIR) spectroscopy. The possibility of CO₂ utilization was also studied through addition of ethanol into the CO₂-saturated absorbent. The FTIR results indicated that amino-N-(3-(dimethylamino)propyl)acetamide was formed when glycine was added into DMAPA. The CO₂ loading capacities of the absorbent were found to decrease as the concentration of the absorbent increased. However, the net CO₂ loading capacity showed an opposite trend such that the total amount of CO₂ absorbed by the solution increased as the concentration of the absorbent increased. This was supported by the results obtained for CO₂ utilization which indicated that the amount of solids recovered increased as concentration of the absorbent increased. At 5 bar and 303.15 K, the optimum concentration of absorbent for CO₂ capture and subsequent utilization was 1.0 M, with CO₂ loading capacity of 1.6 mol CO₂/ mol of absorbent, which was higher than the conventional monoethanolamine (MEA) absorbent (0.77 mol CO₂/ mol MEA). The solids recovered contained carbamate salt. Based on this study, the CO₂ loading capacity of the amino-N-(3-(dimethylamino)propyl)acetamide showed significant improvement, in comparison to MEA. Moreover, the formation of solid products indicated the possibility of CO₂ conversion at low pressure and temperature conditions, and hence reduction in energy requirement during CO₂ utilization process.

ABSTRAK

Monoethanolamina (MEA) ialah penyerap konvensional yang digunakan untuk menangkap karbon dioksida (CO_2) di industri. Namun begitu, MEA mempunyai kadar penyerapan CO_2 yang terhad. Tambahan pula, input tenaga yang tinggi diperlukan untuk mengasingkan CO_2 daripada MEA selepas proses penyerapan. Dalam kajian ini, proses penyahherapan CO_2 disingkatkan melalui proses integrasi antara penangkapan dan penggunaan CO_2 . Keperluan tenaga yang tinggi semasa penggunaan CO_2 juga boleh dikurangkan melalui proses integrasi ini. Prestasi 3-dimetilaminopropilamina (DMAPA) yang dineutrasiasi dengan glisina sebagai penyerap untuk penangkapan dan penggunaan CO_2 telah dinilai dengan mengukur kadar penyerapan CO_2 . Sifat fizikal cecair dinilai dengan mengukur ketumpatan, kelikatan, indeks biasan, dan ketegangan permukaan. Penyerap yang dihasilkan melalui proses neutralisasi dianalisa menggunakan spektroskopi inframerah transformasi Fourier (FTIR). Kemungkinan penggunaan CO_2 juga dikaji dengan menambah etanol ke dalam penyerap yang telah tepu dengan CO_2 . Keputusan FTIR menunjukkan amino-N-(3-(dimetilamino)propil)asetamida terhasil apabila glisina ditambah kepada DMAPA. Kadar muatan CO_2 oleh penyerap didapati menurun apabila kepekatan penyerap meningkat. Namun begitu, jumlah bersih kapasiti muatan menunjukkan arah aliran yang berbeza iaitu jumlah keseluruhan CO_2 yang diserap oleh penyerap meningkat apabila kepekatan penyerap meningkat. Penemuan ini disokong oleh keputusan kajian penukaran CO_2 , iaitu jumlah pepejal yang dihasilkan meningkat apabila kepekatan penyerap meningkat. Pada 5 bar dan 303.15 K, kepekatan optimum penyerap untuk proses penangkapan dan penukaran CO_2 kepada produk baru ialah 1.0 M, dengan kadar larutan CO_2 sebanyak 1.6 mol CO_2 /mol penyerap yang didapati lebih tinggi daripada penyerap konvensional MEA (0.77 mol CO_2 /mol MEA). Pepejal yang dihasilkan mengandungi garam karbamat. Melalui kajian ini, kadar muatan CO_2 amino-N-(3-(dimetilamino)propil)asetamida menunjukkan peningkatan berbanding dengan MEA. Tambahan pula, penghasilan pepejal menunjukkan kemungkinan proses penukaran CO_2 pada suhu dan tekanan gas yang rendah, malah, menurunkan penggunaan tenaga semasa proses penukaran CO_2 .

In compliance with the terms of the Copyright Act 1987 and the IP Policy of the university, the copyright of this thesis has been reassigned by the author to the legal entity of the university,

Institute of Technology PETRONAS Sdn. Bhd.

Due acknowledgement shall always be made of the use of any materials contained in, or derived from, this thesis.

© Hanan binti Mohamed Mohsin, 2020

Institute of Technology PETRONAS Sdn. Bhd.

All rights reserved.

TABLE OF CONTENT

ABSTRACT	vi
ABSTRAK	vii
TABLE OF CONTENT	ix
LIST OF TABLES	xii
LIST OF FIGURES	xv
LIST OF ABBREVIATIONS	xviii
LIST OF SYMBOLS	xix
CHAPTER 1: INTRODUCTION	
1.1 Overview	1
1.2 Research Background	1
1.3 Problem Statement	3
1.4 Objective	4
1.5 Scope of Study	4
1.6 Thesis Organization	5
CHAPTER 2: LITERATURE REVIEW	
2.1 Overview	7
2.2 CO ₂ Mitigation to Reduce the Impacts of Global Warming on the Environment	7
2.2.1 Sources of CO ₂	8
2.2.2 CO ₂ mitigation from point sources	9
2.3 Carbon Capture and Utilization (CCU) Technology	15
2.3.1 Types of CO ₂ utilization	16
2.3.2 Opportunities and challenges in CO ₂ utilization process	19
2.3.3 Integration of CO ₂ capture and utilization	20
2.3.4 The use of alcohol as reagent for CO ₂ utilization	21
2.4 Absorbents for CO ₂ Capture and Utilization	23
2.4.1 Types of absorbent for CO ₂ capture and utilization	23

2.4.2	Amine as an absorbent for CO ₂ capture and utilization	42
2.5	Mechanism of Study for CO ₂ Capture and Utilization	47
2.5.1	Mechanisms for CO ₂ capture for amine solution	47
2.5.2	Mechanisms for CO ₂ utilization	52
2.6	Summary	54
CHAPTER 3: METHODOLOGY		
3.1	Overview	55
3.2	Research Flow	55
3.3	Materials and Chemicals	56
3.4	Preparation and Characterization of Absorbent	57
3.4.1	Preparation of absorbent	57
3.4.2	Physical characterization	58
3.4.3	Fourier transform infrared (FTIR) spectroscopy	61
3.5	CO ₂ Solubility Measurement	61
3.6	CO ₂ Utilization and Characterization Study	64
3.6.1	CO ₂ utilization study	64
3.6.2	Characterization of solid particles	65
3.7	Summary	66
CHAPTER 4: RESULTS AND DISCUSSION		
4.1	Overview	67
4.2	Characterization of Absorbent	67
4.2.1	Physical properties of the absorbent	68
4.2.2	Correlation studies for physical properties of the absorbent	71
4.2.3	Surface functional groups of the absorbent	75
4.3	CO ₂ Solubility Study	78
4.3.1	Experimental data for CO ₂ solubility study	78
4.3.2	Comparison of CO ₂ solubilities of the absorbent with other absorbents	81
4.3.3	Interactions between CO ₂ and the absorbent	83

4.4	CO ₂ Utilization and Characterization Study	87
4.4.1	CO ₂ utilization performances	87
4.4.2	Characterization of solid particles	91
4.5	Summary	97
CHAPTER 5: CONCLUSION		
5.1	Conclusion	99
5.2	Recommendations	100
REFERENCES		102
APPENDIX A		114
APPENDIX B		116
APPENDIX C		119
APPENDIX D		122
APPENDIX E		123
APPENDIX F		124
APPENDIX G		125
APPENDIX H		126

LIST OF TABLES

Table 2.1:	Various methods for CO ₂ capture.	11
Table 2.2:	Advantages and disadvantages of various technologies available for CO ₂ capture.	12
Table 2.3:	List of chemicals derived from CO ₂ and their uses.	18
Table 2.4:	Different type of carbamate or carbonate products obtained from CO ₂ utilization by using alcohol as a reagent.	22
Table 2.5:	List of absorbents, media, and additional reagents used for CO ₂ capture and subsequent utilization.	25
Table 2.6:	Advantages and disadvantages of absorbents and reaction media/ reagents for CO ₂ capture and utilization.	40
Table 2.7:	CO ₂ solubilities of different types of monosubstituted amine at 313.15 K.	42
Table 2.8:	CO ₂ solubilities of different types of diamines at 313.15 K.	44
Table 2.9:	CO ₂ solubility of potassium glycinate at 0.9 M and 313.15 K [126].	46
Table 2.10:	CO ₂ absorption studies for different types of amino acid and amine solutions at 313.15 K.	47
Table 3.1:	The properties of chemicals used in this experiment.	57
Table 3.2:	Experimental conditions for CO ₂ capture process.	64
Table 4.1:	A _i values based on Equation (3.2) for density, refractive index, and surface tension of the absorbent.	72
Table 4.2:	Fitting parameters based on Equations (3.3) and (3.4) to predict viscosity of the absorbent.	72
Table 4.3:	Standard deviations (σ) and regression coefficients (R^2) of the physical properties of the absorbent.	72
Table 4.4:	Surface functional groups and vibration modes for each peak detected in the FTIR spectra of aqueous GLY, DMAPA, and the absorbent.	77

Table 4.5:	The characteristics peaks of the absorbent before and after CO ₂ absorption process.	85
Table 4.6:	The characteristics peaks of solids obtained after addition of ethanol.	93
Table 4.7:	Binding energy detected by the XPS spectra and the corresponding moiety.	95
Table A1:	Comparison of experimental (Exp.) physical properties of deionized water with previous literature (Lit.) [133] at various temperatures (<i>T</i>).	114
Table A2:	Densities of the absorbent at different temperatures (<i>T</i>).	114
Table A3:	Refractive indices of the absorbent at different temperatures (<i>T</i>).	115
Table A4:	Surface tensions of the absorbent at different temperatures (<i>T</i>).	115
Table A5:	Viscosities of the absorbent at different temperatures (<i>T</i>).	115
Table B1:	Variables a, b, A, and B based on Peng Robinson Equation.	117
Table B2:	Variables a ₂ , a ₁ , and a ₀ based on cubic equation $Z^3 + a_2Z^2 + a_1Z + a_0 = 0$	117
Table B3:	Data and measured values for determination of CO ₂ loading capacity of 5.0 M MEA.	118
Table C1:	The standard deviations for pressure and CO ₂ loading capacities of 5.0 MEA measured at 313.15 K.	120
Table C2:	The standard deviations for pressure and CO ₂ loading capacity of 1.0 M GLY-KOH measured at 313.15 K.	121
Table D1:	The CO ₂ loading capacities (α) of 1.0 M amino-N-(3(dimethylamino) propyl) acetamide measured at different temperature and pressure (<i>P</i>).	122
Table D2:	The CO ₂ loading capacities (α) of 0.1 M to 2.0 M amino-N-(3-(dimethylamino)propyl)acetamide measure at different pressure (<i>P</i>) and 303.15 K.	122

Table E1:	Total moles of CO ₂ absorbend by the absorbent.	123
Table F1:	Table F1: The average mass of solids recovered and standard deviations based on 1 mol ethanol.	124

LIST OF FIGURES

Figure 2.1:	Sources of CO ₂ released into the atmosphere [26 - 29].	8
Figure 2.2:	Process flow diagram of the amine scrubbing process, adopted from Bottoms [5].	13
Figure 2.3:	One-step conversion process (in-situ utilization).	24
Figure 2.4:	Two-step conversion process.	24
Figure 2.5:	Type of absorbents, reaction media, and additional reagents used for CO ₂ capture and utilization.	39
Figure 2.6:	Structures of various diamines.	43
Figure 2.7:	Performance of various diamine solutions in comparison to MEA. Reprinted with permission from Rui Zhang et al. Energy & Fuels 2017 31 (10), 11099-11108. Copyright (2019) American Chemical Society.	45
Figure 2.8:	Zwitterion structure of glycine in aqueous form.	45
Figure 3.1:	Flow of research methodology used in this study.	56
Figure 3.2:	Process flow diagram of solubility cell.	62
Figure 3.3:	Two-step method for CO ₂ capture and utilization study.	65
Figure 4.1:	Densities of the absorbent at different temperatures.	69
Figure 4.2:	Refractive indices of the absorbent at different temperatures.	69
Figure 4.3:	Surface tensions of the absorbent at different temperatures.	70
Figure 4.4:	Viscosities of absorbent at different temperatures.	70
Figure 4.5:	Comparison between experimental and predicted density of the absorbent.	73
Figure 4.6:	Comparison between experimental and predicted refractive index (RI) of the absorbent.	73
Figure 4.7:	Comparison between experimental and predicted surface tension of the absorbent.	74
Figure 4.8:	Comparison between experimental and predicted viscosity of the absorbent.	74

Figure 4.9:	The proposed interaction between glycine (GLY) and DMAPA molecules.	75
Figure 4.10:	The FTIR spectra of (a) aqueous glycine (GLY), DMAPA, and the absorbent, amino-N-(3-(dimethylamino)propyl)acetamide and (b) close-up spectra between 2000 to 600 cm^{-1} .	76
Figure 4.11:	CO_2 loading capacities of 1.0 M amino-N-(3-(dimethylamino) propyl)acetamide at different temperatures.	79
Figure 4.12:	CO_2 loading capacity of different concentrations of the absorbent (Temperature: 303.15 K).	80
Figure 4.13:	Net CO_2 absorbed by the absorbent (Temperature:303.15 K).	81
Figure 4.14:	CO_2 loading capacity of amino-N-(3-dimethylamino)propyl)acetamide absorbent in comparison with 30 w/w % MEA measured at 303.15 K.	82
Figure 4.15:	The CO_2 loading capacity of 0.1 and 1.0 M amino-N-(3-(dimethylamino)propyl)acetamide measured at 303.15 K, in comparison with GLY-KOH.	83
Figure 4.16:	FTIR spectra of (a) the absorbent before and after the absorption process (b) close-up spectra between 1750 to 600 cm^{-1} .	84
Figure 4.17:	Amount of solids from CO_2 utilization based on different concentrations of absorbent (Ethanol concentration: 1 mol).	88
Figure 4.18:	CO_2 loading capacities and the total amount of solids recovered during utilization process.	89
Figure 4.19:	The effect of amount of ethanol on the product formation (absorbent concentration = 1 mol; time = 3 hours).	90
Figure 4.20:	The effect of conversion time on the product formation (absorbent concentration = 1 mol; ethanol concentration = 1 mol).	90
Figure 4.21:	Full FTIR spectra of the solids, ethanol, and CO_2 -saturated absorbent, for wavenumber ranging from 4000 to 600 cm^{-1} .	92

Figure 4.22:	The close up spectra of the solid products at wavenumber ranging from 1800 cm^{-1} to 600 cm^{-1} .	92
Figure 4.23:	XPS spectrum of solids obtained after addition of ethanol into CO_2 -saturated solution.	94
Figure 4.24:	XPS spectra of (a) oxygen; (b) carbon; and (c) nitrogen, of the solids.	96
Figure B1:	Pressure in solubility cell and premixed tank during the CO_2 absorption process.	116
Figure C1:	CO_2 loading capacities of 5.0 M monoethanolamine (MEA) in comparison with previous literatures (Temperature: 313.15 K).	119
Figure C2:	CO_2 loading capacities of 1.0 M GLY-KOH in comparison with previous literature (Temperature: 313.15 K).	120

LIST OF ABBREVIATIONS

AMP	2-amino-2-methyl-propanol
Ca(OH) ₂	Calcium hydroxide
CaO	Calcium oxide
CCS	Carbon capture and storage
CCU	Carbon capture and utilization
CO	Carbon monoxide
CO ₂	Carbon dioxide
DEA	Diethanolamine
ECBM	Enhanced coal bed methane recovery
EDA	Ethylenediamine
EG	1,2-ethylene glycol
EOR	Enhanced oil recovery
FTIR	Fourier transform infrared spectroscopy
H ₂	Hydrogen gas
MDEA	N-methyldiethylaminoamine
MEA	Monoethanolamine
N ₂	Nitrogen gas
Na ₂ CO ₃	Sodium carbonate
NaCl	Sodium chloride
NaHCO ₃	Sodium bicarbonate
PEG	Polyethylene glycol
PZ	Piperazine
w/w%	Weight percentage
XPS	X-ray photoelectron spectroscopy

LIST OF SYMBOLS

Symbols	Descriptions	Units
α	CO ₂ loading capacity	mol CO ₂ / mol absorbent
ρ	Density	g/cm ³
RI	Refractive Index	nD
γ	Surface tension	mN/m
η	Viscosity	mPa.s
σ	Standard deviation	-
ν	Wavenumber	cm ⁻¹
T	Temperature	K
t	Time	hours

This page is intentionally left blank

CHAPTER 1

INTRODUCTION

1.1 Overview

This chapter provides an overall summary of the thesis study. This research focused on carbon dioxide (CO₂) capture and utilization, as one of the methods for CO₂ mitigation. CO₂ absorption is currently the most advanced technology available for CO₂ capture. However, limited CO₂ absorption capacity of the absorbent and high regeneration energy during the CO₂ desorption process were identified as the limitations for CO₂ absorption technology. Moreover, the high energy requirement during CO₂ utilization process was also addressed in this research. The main aim of this research is to identify a potential absorbent with high CO₂ capacity compared to the conventional monoethanolamine (MEA). This research also investigates the possibility of integrating the CO₂ capture with CO₂ utilization process to eliminate the CO₂ desorption process and hence reduce the energy requirement during CO₂ utilization.

1.2 Research Background

Global warming is a natural phenomenon driven by high emissions of CO₂ into the atmosphere. Increasing of the Earth's surface temperature, melting of ice glaciers, droughts, and floods are contributed by excessive anthropogenic emissions of CO₂. Carbon capture and utilization (CCU) was identified as one of the methods for CO₂ mitigation. Several methods have been reported for CO₂ capture such as absorption [1], adsorption [2], membrane technology [3], and cryogenic distillation [4]. Based on the amine scrubbing process patented by Bottoms [5] in 1930, absorption process is regarded as the most mature and well understood technology with high CO₂ removal efficiency. The absorption process relies on chemical interactions

between CO₂ molecules to separate CO₂ from natural gas [6], followed by solvent regeneration process to release CO₂ and recycle the solvent back into the system. The solvent regeneration process is usually performed by heating the solvent at temperature ranging between 100 to 120 °C [1]. The desorption process contributes to significant energy requirement during the CO₂ capture process. Various alternatives were considered to reduce the energy requirement during solvent regeneration process which include replacing amine with other types of absorbent [7-9] and mixing the absorbent with organic solvents [10, 11]. Apart from that, CO₂ desorption process can also be eliminated through simultaneous CO₂ capture and conversion process [12, 13], which will be further explored in this research.

The use of CO₂ as a building block for the synthesis of carbon-based materials were discussed by various authors [6, 14, 15]. High purity CO₂ usually obtained from CO₂ capture process can be converted into value-added products such as urea, salicylic acid, methanol, and cyclic carbonates [15] which provides an alternative pathway for CO₂ storage. At present, the industrial application of CO₂ fixation is limited by the high activation energy during the synthesis of low energy carbon-based products [14]. Thus, the existing technology for CO₂ conversion requires large energy input, which increases the cost of CCU technology. This can be seen in the production of urea which occurs at temperature of approximately 185 to 190 °C and pressure of 180 to 200 atm [15]. Similarly, salicylic acid is produced at high temperature and pressure through the Kolbe-Schmitt method [14]. One of the methods which was identified to lower the energy requirement during CO₂ fixation is by reacting CO₂ with co-reactants such as hydroxide or amine solution which can lower the activation energy and hence allow conversion to occur at reduced temperature [15].

Organic media such as alcohol was identified as one of the reagents which can be used to convert CO₂ into value-added products such as carbamates which are useful for drug synthesis and agrochemical products [16, 17]. Apart from carbamates, ethanol can also be converted to carbonates in the presence of CO₂ gas [18]. The conventional method for generating carbamates involves the use of toxic chemicals such as isocyanates and chloroformates [16]. Moreover, the conversion process usually occurs at high temperature and pressure conditions. CO₂ capture and subsequent utilization by using ethanol was proposed as one of the methods to reduce the energy requirement during the CO₂ conversion process.

1.3 Problem Statement

Monoethanolamine (MEA) is the most common type of absorbent used in the oil and gas industry for removing CO₂ from flue gas. The chemistry behind the MEA absorption process is well understood and MEA is also available at reasonable cost [19]. Despite that, MEA has limited CO₂ absorption capacity which requires large absorption tank to attain high removal efficiency [19]. Diamines such as N-methylpropane-1,3-diamine (MAPA) and 3-dimethylaminopropylamine (DMAPA) demonstrated significantly higher CO₂ absorption capacity compared to other types of amines [20]. The neutralization of diamine with amino acid were also studied to further increase the CO₂ absorption capacity of the absorbent [21, 22]. Moreover, the addition of amino acid provides additional advantages such that amino acid is known to have low toxicity, low volatility, and high oxidation stability [23].

In spite of the advantages of diamine neutralized with amino acid, the high energy requirement during absorbent regeneration process remains a challenge which needs to be overcome to ensure competitiveness of the CO₂ absorption technology. The high regeneration energy during the desorption process can be eliminated by integrating the CO₂ capture with CO₂ utilization process. The integration process is also expected to address the issue of high thermodynamic stability of the CO₂ molecules which requires high energy input during the conversion process.

In CCU, organic media such as ethanol has been found to successfully convert CO₂ into value-added products [24]. However, the study conducted by Han and Wee [24] indicated that the addition of organic media (ethanol) into the absorbent increased the viscosity of the absorbent, which hinders diffusion of CO₂ molecules into the absorbent during absorption process. To overcome this problem, a two-step CO₂ capture and subsequent utilization method was employed where in the organic solvent was added directly after the CO₂ capture process, thus the high viscosity of the ethanol may not affect the CO₂ diffusion process. Previous studies on diamines [21, 22] also focused on CO₂ capture at lower pressure, which focused on post-combustion technology.

In this study, the performance of 3-dimethylaminopropylamine (DMAPA) neutralized with glycine as a potential absorbent for CO₂ capture was evaluated at higher pressure ranging from 5 to 25 bar, focusing on pre-combustion technology. The possibility of utilization CO₂ was also investigated by mixing the CO₂-saturated absorbent with ethanol as a reagent.

1.4 Objective

This study covered the following aims:

- i. To prepare and characterize the amino-N-(3-(dimethylamino)propyl)acetamide as an absorbent for CO₂ capture.
- ii. To evaluate the CO₂ absorption capacity of the prepared absorbent.
- iii. To study the utilization of CO₂ by using the prepared absorbent and ethanol.

1.5 Scope of Study

The preparation of amino-N-(3-(dimethylamino)propyl)acetamide was carried out through basic neutralization of glycine with aqueous DMAPA solution. The concentrations of amino-N-(3-(dimethylamino)propyl)acetamide prepared were within the range of 0.1 to 2.0 mol/L (M). The absorbents were characterized by using density meter, viscometer, refractometer, and tensiometer to measure the physical properties of the absorbent which will affect the CO₂ solubility in the absorbent, particularly viscosity of the absorbent. The surface functional groups available in the absorbent were identified by using Fourier transformation infrared (FTIR) spectrometer, to indicate the neutralization reaction between glycine and DMAPA.

The solubility of CO₂ in the prepared absorbent was evaluated using a high pressure solubility cell, by bubbling CO₂ gas into the absorbent. The CO₂ loading capacity of the absorbent was calculated by using pressure differential technique. The solubility study was conducted at pressure ranging from 5 to 25 bar and temperature between 303.15 K to 323.15 K.

CO₂ utilization study was carried out by using two-step CO₂ capture and conversion method. After the CO₂ absorption process, ethanol was added into the CO₂-saturated amino-N-(3-(dimethylamino)propyl)acetamide absorbent. The solids produced from the reaction was characterized by using FTIR, and X-ray photoelectron spectroscopy (XPS) to determine the functional groups and chemical binding available in the absorbent.

1.6 Thesis Organization

This thesis is divided into five (5) chapters as outlined:

Chapter 1 covers the background of study, problem statements, as well as objectives and scope of research. This introduction section is aimed to provide readers with general overview on the proposed research topic.

Chapter 2 presents the literature reviews on the importance of CO₂ mitigation and methods which can be adopted to reduce CO₂ content in the atmosphere. Carbon capture and storage (CCS) as well as carbon capture and utilization (CCU) were also briefly outlined in this chapter. Methods for CO₂ separation process were also highlighted. Moreover, the different types of solvent previously studied as potential absorbents for CO₂ capture and subsequent utilization were also listed in the literature reviews. Finally, the mechanisms involved in CO₂ capture and the reaction pathways for CO₂ utilization were also briefly discussed.

Chapter 3 describes the experimental procedures used in this research which covers the absorbent preparation and characterization, CO₂ solubility study, and CO₂ utilization study.

Chapter 4 reports the results obtained from the experimental work. The results were also compared with outcomes reported in previous literatures to validate the methodology used in this thesis study.

Chapter 5 provides a general conclusion based on the experimental data collected as well as future work required for this research followed by a list of references cited in this thesis.

This page is intentionally left blank

CHAPTER 2

LITERATURE REVIEW

2.1 Overview

High emissions of CO₂ into the atmosphere is an environmental concern which needs to be addressed to reduce the impacts of global warming. The different sources of CO₂ were identified in this chapter. Carbon capture is one of the methods which can be applied for CO₂ mitigation process. CO₂ capture technologies include absorption, adsorption, membrane technology, and cryogenic distillation. This chapter also highlights various types of CO₂ utilization technology (CCU) and the opportunities as well as challenges in CO₂ conversion process. The integration of CO₂ capture with CO₂ utilization process and the use of ethanol as a reagent for CO₂ was proposed as a method to eliminate the energy intensive CO₂ desorption and to reduce energy requirement during CO₂ utilization. Different types of absorbents previously used for CO₂ capture and subsequent utilization were also discussed in this chapter. The final section of this chapter describes the mechanisms for CO₂ capture and utilization process.

2.2 CO₂ Mitigation to Reduce the Impacts of Global Warming on the Environment

CO₂ is one of the greenhouse gases present in the atmosphere which plays a significant role in heating up the Earth's surface through the greenhouse effect. Excessive emission of CO₂ into the atmosphere was identified as the main contributor of global warming. It was reported that the Earth's temperature increased by an average of 1.7 °C per century over the last 45 years mainly contributed by emissions from human activities [25]. Apart from increased in atmospheric temperature, global warming also causes drastic climate changes which include melting of snow and

ice glaciers, droughts, floods, and rising of the sea levels [26, 27]. Thus, there is a crucial need for CO₂ mitigation to ensure the Earth's sustainability for current and future generations.

2.2.1 Sources of CO₂

Sources of CO₂ are divided into two categories namely natural sources or anthropogenic sources [26-29] as indicated in Figure 2.1. The concentration of CO₂ in the atmosphere is maintained by the natural carbon cycle such that CO₂ emitted through respiration of living organisms, ocean release, and organic material decompositions are re-absorbed through natural mechanisms such as photosynthesis, forestation, and ocean uptake [27]. Apart from natural emissions, CO₂ is also released from large point sources such as power plants and manufacturing facilities. The combustion of fossil fuels, iron and steel production, cement production, ammonia production, and hydrogen production contributed to the most significant increase in CO₂ levels in the atmosphere.

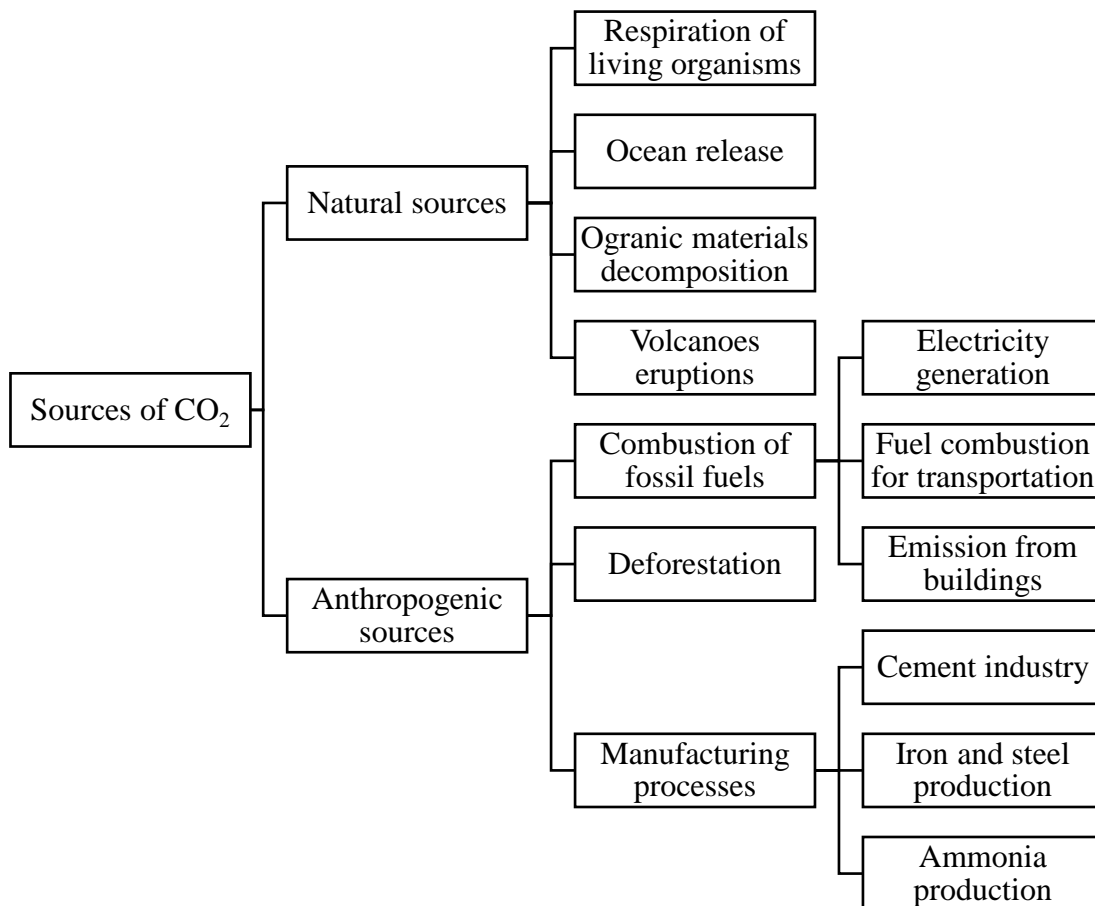


Figure 2.1: Sources of CO₂ released into the atmosphere [26-29].

As the anthropogenic CO₂ gases continue to be emitted, the carbon cycle may not be able to cope with the excessive amount of CO₂, thus results in accumulation of CO₂ in the atmosphere. Statistic published by the United States Environmental Protection Agency [30] indicated that anthropogenic gases accelerated global warming by approximately 37% from the year 1990 to 2015, of which 30% was attributed by CO₂ alone.

2.2.2 CO₂ mitigation from point sources

In parallel with the efforts to reduce the impacts of global warming contributed by the combustion of fossil fuels and industrial activities, several strategies were adopted such as enhancing the energy generated from combustion of fossil fuels and introduction of low-carbon or carbon-free fuels [26, 27]. Another method which can be implemented for CO₂ mitigation is by capturing CO₂ from large point sources such as power plants and manufacturing facilities, followed by injection of the CO₂ gas into underground reservoirs. This process is known as carbon capture and storage (CCS).

2.2.2.1 Carbon Capture and Storage (CCS) Technology

CCS is a highly proven technology based on its commercial application for natural gas sweetening process [31, 32]. The earliest large scale CCS plant, Val Verde natural gas plants commenced operation in the year 1972 with CO₂ capture capacity of 1.3 million tonnes per annum [31]. Examples of large scale CO₂ capture facilities from large point sources which are currently in operation include the Boundry Dam CCS facility in Canada, which captures CO₂ from coal-fired power plant, the Abu Dhabi CCS facility in United Arab Emirates which captures CO₂ from iron and steel production, and the Quest plant in Canada which captures CO₂ from hydrogen production plant [33].

CCS is divided into a few categories namely pre-combustion, post-combustion, and oxy-fuel combustion [34]. The pre-combustion technology involves decarbonization of fuel prior to the energy generation process [32]. Through gasification process, fuels are converted into syngas which primarily contained hydrogen (H₂) and carbon monoxide (CO). The syngas is then converted into mixtures

of H₂ and CO₂ through water-gas shifting reaction, which increases the CO₂ concentration in gas stream. The pre-combustion CO₂ capture technology which occurred at elevated pressure of approximately 2 to 14 bar [35], which offers a number of benefits such as higher driving force during the separation process, lower energy requirement during compression process, as well as low emissions of sulphur and nitrogen oxides [32].

Post-combustion process is another CCS technology which focused on capturing CO₂ released after combustion of fuels. This process can be easily retrofitted to any existing power plants or industrial manufacturing plants to reduce downstream CO₂ emissions [32], with minimal plant modification. However, the low concentration of flue gas in power plants (atmospheric pressure) limits the efficiency of CO₂ separation process. Nonetheless, this technology is widely applied to capture CO₂ from industrial facilities such as ammonia, hydrogen, and methane production which release exhaust gas at higher pressure ranging from 5 to 27 bar [36].

Apart from pre-combustion and post-combustion technology, oxy-fuel is also has potential to reduce CO₂ emissions from large point sources. By reacting hydrocarbon fuels with pure oxygen, flue gas generated, mainly composed of CO₂ can be directly send for sequestration. However, the main challenge of this technology is the high energy requirement for production of oxygen (O₂).

Among all the CCS technologies discussed, both pre-combustion and post-combustion technology at elevated pressure of more than 2 bar is a promising option for capturing CO₂ from large point sources due to higher driving force during the separation process. Hence, this research will focus on capturing CO₂ at elevated pressure.

2.2.2.2 Methods for CO₂ capture

Several methods for CO₂ separation process were reported in the literatures namely absorption [6, 19, 37], adsorption [37-39], membrane [40, 41], and cryogenic distillation [42-44]. Descriptions for each method are as presented in Table 2.1. The advantages and disadvantages of different CO₂ capture methods are also summarized in Table 2.2. Chemical-based absorption is the earliest existing technology and is the

most mature technology available up-to-date. Meanwhile, adsorption and cryogenic distillation technologies are still in development stage and it will take years before they can be fully commercialized for large scale application for CO₂ capture. Membrane is another technology which is fully commercialized, but its application is limited by flowrate up to 700 million standard cubic feet per day (MMscfd) and high maintenance requirements.

Table 2.1: Various methods for CO₂ capture.

Methods	Descriptions	References
Absorption	<ul style="list-style-type: none"> Divided into two – chemical and physical absorption. Separation process relies on the physical or chemical interactions between an absorbent and the feed gas. Examples of chemical solvent: monoethanolamine (MEA), diethanolamine (DEA), diglycolamine (DGA), and methyldiethanolamine (MDEA). Examples of physical solvent: Flour Solvent™, Selexol, Purisol, Rectisol, and Ifpexol. 	[6, 19, 37]
Adsorption	<ul style="list-style-type: none"> Molecules adhere to onto the surface of solid materials based on strong affinity of CO₂ towards certain functional groups. Divided into two – chemical and physical adsorption. Examples of adsorbents: amine-modified activated carbon, zeolites, metal-organic-framework (MOF), and silica. 	[37-39]
Membrane	<ul style="list-style-type: none"> Membrane operates based on transportation of gas molecules across a thin layer film composed of organic or inorganic materials. Membranes available include porous membrane transport process, solution-diffusion membrane, and ion transport membrane 	[40, 41]
Cryogenic separation	<ul style="list-style-type: none"> Cryogenic refers to the extremely low temperature condition during the separation process. Consist of three stages – compression, refrigeration, and cryogenic distillation. The technology has been patented (Ryan/Homes process, Controlled FreezeZone™, and CryoCell) 	[42-44].

Table 2.2: Advantages and disadvantages of various technologies available for CO₂ capture.

Technologies	Advantages	Disadvantages	References
Absorption (chemical and physical)	<ul style="list-style-type: none"> • Mature technology • High separation efficiency (80 -90 % separation efficiency). • High reactivity. • Commercially available solvent. 	<ul style="list-style-type: none"> • High solvent regeneration energy for chemical absorption - solvent is heated between 100 to 120 °C). • High capital, operation, and maintenance cost. • Limited capacity (for MEA – 0.5 mol MEA/ mol CO₂) • Bulky equipment 	[29, 32, 45-47]
Adsorption (chemical and physical)	<ul style="list-style-type: none"> • Simple process and easy to handle. • Lower regeneration energy. • No liquid required – reduce risk of corrosion. 	<ul style="list-style-type: none"> • Limited flowrate. • Larger equipment size when CO₂ content is more than 2%. 	[29, 32, 37, 38]
Membrane technology	<ul style="list-style-type: none"> • Mature technology • Compact and modular design (low footprint). • Flexible process operation conditions (CO₂ concentration from 3 to 90 %; Feed flow between 3 to 700 MMscfd). • No chemicals required. • Low capital cost. 	<ul style="list-style-type: none"> • Limited gas processing volume (700 MMscfd). • High maintenance due to fouling. 	[29, 32, 41, 42]
Cryogenic distillation	<ul style="list-style-type: none"> • Used in production of industrial gases. • Generate CO₂ in liquid form. • No gas compression is required for CO₂ transportation. • No chemicals required. • Suitable for CO₂ concentration of more than 50%. 	<ul style="list-style-type: none"> • High energy requirement for refrigeration process. • Formation of CO₂ solids at low temperature. • Still in development stage. 	[4, 29, 37, 42, 46]

In the near future, absorption is still regarded as the most efficient removal technology for CO₂ capture plant based on its historic performances and high reliability. However, there are several issues related to absorption technology which need to be addressed to ensure that the technology remains competitive for CO₂ capture process. This includes the high energy requirement during the CO₂ desorption process as well as the performance of the absorbent used for CO₂ capture. Researchers have come out with various methods to enhance the operation of CO₂ absorption system which include the elimination of the highly intensive solvent regeneration process. This can be done through integration of CO₂ capture with CO₂ utilization process which will be further discussed in Section 2.3.

2.2.2.3 Absorption process as a method for CO₂ mitigation from point sources

The absorption process is a separation method based on physical or chemical interactions between CO₂ molecules and liquid absorbent. The acidic nature of CO₂ allows the molecules to react chemically with amine absorbent and hence separate CO₂ molecules from feed gas. On top of that, organic solvent can also be used to capture CO₂ through physical binding [6]. Figure 2.2 demonstrates the absorption technology used for CO₂ removal process. The main processes involved in this technology are CO₂ absorption process and solvent regeneration process.

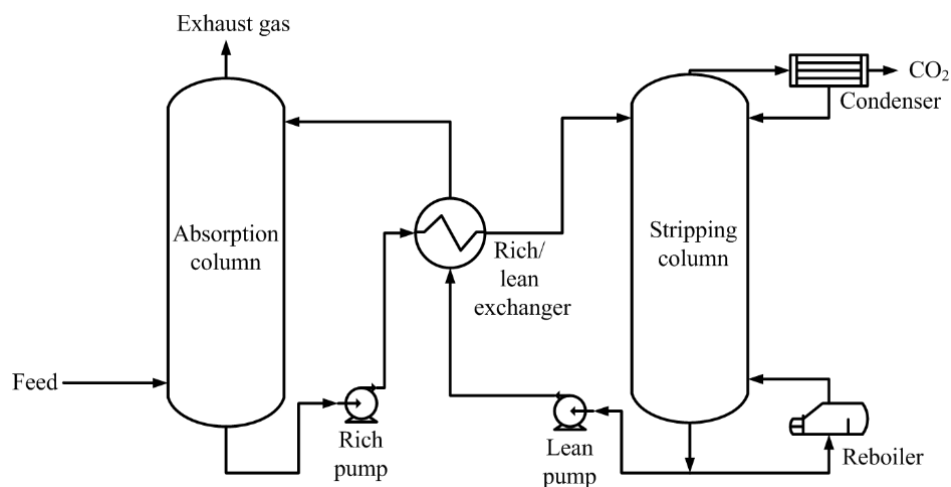


Figure 2.2: Process flow diagram of the amine scrubbing process, adopted from Bottoms [5].

Monoethanolamine (MEA) is the most well established solvent used for CO₂ capture [32]. MEA is widely utilized as an absorbent in gas sweetening process due to the properties of MEA such as low cost, availability, and high reactivity [32]. Apart from MEA, other amine solvents such as diethanolamine (DEA), diglycolamine (DGA), and methyldiethanolamine (MDEA) also demonstrated significant performances as CO₂ capture absorbents [45-47]. Amine solvent contains amino functional group (-NH) which is responsible for the reaction between the absorbent and CO₂ molecules. This process may be reversed by heating action to regenerate the solvent for recycling. However, due to high thermal stability of the compound formed during the reaction, a large amount of heat is required for CO₂ desorption process. Typically the temperature requirement for the solvent regeneration process is approximately 100 to 120 °C [1, 32]. This is main limitation of the absorption technology, which contributes to high operational cost for CO₂ separation process. On top of that, limited CO₂ loading capacity, high volatility, as well as high thermal and oxidation degradation of amine solutions also need to be addressed to ensure that the absorbent is economically competitive [48].

Physical solvents such as Fluor Solvent™, Selexol, Purisol, Rectisol, and Ifpexol were commercially developed based on various organic chemicals [42] to reduce the high energy requirement during solvent regeneration process. Nonetheless, the disadvantage of this type of solvent is the low absorption capacity compared to amine solution. This leads to increase in the amount of solvent required to remove CO₂ molecules which contributes to larger size of absorption column and hence larger capital cost. Alternatively, mixed solvents which incorporate both the chemical and physical absorption mechanisms may be used to reduce regeneration energy while maintaining high absorption capacity.

Numerous research were carried out to identify an alternative solvent with high absorption capacity, low solvent regeneration energy, high thermal and oxidation stability, and low vapor pressure [48-50]. Apart from that, integration of CO₂ capture with CO₂ utilization was identified as one of the strategies which can be adopted to reduce energy requirement or eliminate the highly intensive CO₂ regeneration process.

2.2.2.4 CO₂ compression and sequestration

Apart from CO₂ capture process, the CCS technology involves additional steps namely compression and transportation followed by sequestration. In order to transport CO₂ into underground reservoirs, the CO₂ separated from feed gas needs to be compressed to higher pressure within the range of 100 to 150 bar [1]. This contributes to higher energy requirement for both the compression and transportation process. Moreover, CCS technology is also associated with both high capital and operating cost mainly attributed to compression of CO₂, construction of additional infrastructures and continuous monitoring of CO₂ behavior. The high cost incurred by this technology can be compensated by the increase in production of crude oil and methane through the EOR and ECBM technology, respectively. Nonetheless, the abundant of CO₂ available from the natural gas sweetening process coupled with shorter distances between CO₂ sources and geological reservoirs contributed to lower demand for CO₂ captured from other sources such as power plants and industrial manufacturing facilities. For long term storage of CO₂ in deep saline aquifers and ocean storage, no value-added products are generated and hence the CCS technology is not economically attractive. On the other hand, CCU was introduced to enhanced the economic competitiveness of the carbon capture technology.

2.3 Carbon Capture and Utilization (CCU) Technology

The term carbon capture and utilization (CCU) refers to the process of capturing CO₂ from feed gas and reutilizing the gas either in its original form or by converting the CO₂ gas into other commercial products. At present, CO₂ is already widely used in various industries such as pharmaceutical [14], chemical manufacturing [14, 51], food and beverages [52, 53], textile [53], oil and gas [53] and electronic industries [53]. The most common applications of CO₂ utilization include enhanced oil recovery (EOR) process, and production of chemicals such as inorganic carbonates [14, 51], urea, as well as salicylic acid [54]. The shift from CCS to CCU is seen as a better alternative to address the shortcomings of CCS technology particularly the high cost for CO₂ sequestration [55].

2.3.1 Types of CO₂ utilization

CO₂ utilization are categorized into two types namely direct and indirect utilization. Direct utilization refers to the process of utilizing CO₂ directly in its original state, without any conversion process [15]. Meanwhile, indirect utilization refers to the process of converting CO₂ molecules into other carbon-based products [15]. In the following subsection, the direct and indirect uses of CO₂ are discussed.

2.3.1.1 Direct utilization of CO₂

Enhanced oil recovery (EOR) and enhanced coal bed methane recovery (ECBM) technologies are examples of direct utilization such that CO₂ is directly used to enhance the production of oil and methane, by injecting the gas into underground reservoirs. Established in 1986, EOR is one of the earliest form of direct CO₂ utilization technology available in the market and widely used in oil-producing countries such as Norway, Canada and the USA [52, 56]. In contrast, the ECBM technology is still in development stage [57].

Food and beverages industry is the second largest application of direct CO₂ utilization up-to-date [56]. High purity CO₂ can be used as carbonating agent and as seal gas during production of wines. On the other hand, supercritical CO₂ can be used as fluids for the removal of caffeine from coffee. In the food industry, CO₂ is mainly used in packaging and preservation processes to protect food against bacteria. On top of that, CO₂ is also used to provide inert atmosphere during food manufacturing processes to prevent contamination.

Another existing direct CO₂ utilization is urea yield boosting [56]. The synthesis of urea from natural gas generate excess amount of ammonia, which decreases production output. On top of that, CO₂ is also released as a by-product. Instead of venting the gas into the atmosphere, the CO₂ can be captured and reacted with ammonia to boost urea production. This application has been successfully proven by a number of projects around the world [56].

Apart from the large-scale direct CO₂ utilization, small scale uses of CO₂ are also commercially available in the market, namely for physical solvent application. This include the use of CO₂ for pulp and paper processing, production of dry ice, water treatment, steel manufacturing, dry cleaning solvent, welding, refrigerant gas, and as fire extinguishers [52, 55].

2.3.1.2 Indirect utilization of CO₂

Indirect utilization of CO₂ involves chemical reactions between CO₂ molecules and other materials for the formation of new products. CO₂ is an attractive feedstock for many chemical and fuel conversions due to the abundance of CO₂ supply, non-toxic, and non-flammable properties [58]. Moreover, CO₂ contains the element carbon which is the building block of many essential chemicals such as urea, methanol, salicylic acid, formic acid, and cyclic carbonates [15].

Mineral carbonation is another type of indirect CO₂ utilization, such that CO₂ is reacted with metal oxides found in silicate minerals such as serpentine, olivine, and wollastonite [57] to produce metal carbonates. Mineral carbonation involves direct or indirect carbonation process. For direct carbonation process, CO₂ is reacted with mineral silicates under pressurized condition. In contrast, indirect mineral carbonation occurs through a series of steps which include metal extraction using hydrochloric acid or molten salt, followed by hydration process to produce metal hydroxide, and finally the carbonation process which involves reacting CO₂ gas with the metal hydroxide solution [57].

The cultivation of microalgae using CO₂ molecules also creates an opportunity for CO₂ utilization for production of biofuels. Microalgae can be used for both capturing CO₂ from gas streams and converting CO₂ into value-added biofuels [57]. Moreover, the nitrogen gas from flue gas can also be used as a nutrient source for the cultivation process [57]. The cultivation of microalgae can be performed in an open pond or by using a photo-bioreactor. The microalgae can then be converted into fuels by harvesting the biomass, followed by thermochemical or biochemical conversion process.

Table 2.3 shows the different types of chemicals which can be synthesis indirectly from CO₂ molecules, along with their potential applications in the industries. The vast amount of products which can be produced from CO₂ molecules created a higher demand for indirect CO₂ utilization as compared to direct CO₂ utilization [56].

Table 2.3: List of chemicals derived from CO₂ and their uses.

Chemicals derived from CO₂	Uses	References
Urea	Agricultural fertilizers Moisturizer in pharmaceutical industry	[14]
Formic acid	Leather processing Textile industry Food preservation Hydrogen storage media (fuel)	[59]
Salicylic acid	Pharmaceutical	[54]
Synthesis gas (CO and H ₂)	Synthesis of hydrocarbon fuel Production of methanol Transportation fuel	[14]
Carbamates	Drug design Medicinal chemistry Agrochemical	[17, 60]
Inorganic carbonates	Building and cement manufacturing industry Paper making industry Pharmaceutical industry Raw materials for optical glasses	[14, 51]
Cyclic carbonates	Manufacturing of polymers Used as solvents – (ethylene carbonate and propylene carbonates)	[14]
Polycarbonates	Building material Building foam Insulating materials Plastics	[14]
Dimethyl carbonates	Intermediates for organic synthesis Intermediates for polymer production	[14]

2.3.2 Opportunities and challenges in CO₂ utilization process

EOR, ECBM, utilization of CO₂ in the production of food and beverages, as well as urea yield boosting are currently dominating the industry for direct CO₂ utilization, with well proven technologies currently available in the market. Despite its wide application in various industries, the volume of CO₂ utilized through physical means are limited at industrial level [55]. For the EOR and ECBM technologies, geological constraints and the possibility of CO₂ leakages are issues which need to be addressed when considering these technologies for CCU application. Moreover, due to stringent industry requirements, high purity CO₂ is required for utilization of CO₂ in the food and beverages industry. On the other hand, utilization of CO₂ to boost the production urea, does not require external supply of CO₂, as the gas is obtained on-site from the urea manufacturing plant. Although direct utilization of CO₂ through physical means open up new pathways for a more sustainable production approach through recycling of captured CO₂, the large-scale industrial application is currently limited by several factors which include geological constrains and CO₂ supply.

Existing large scale indirect CO₂ utilization technologies include the production of urea and salicylic acid [54]. The annual production of urea and salicylic acid were reported to be approximately 150 million tons and 70 thousand tons respectively [15]. However, the conversion of these products are usually carried out at very high temperature and pressure [61]. This can be seen in the production of urea which involves the reaction between CO₂ and ammonia at temperature ranging between 185 to 190 °C and pressure of 190 to 200 atmosphere [15]. This is due to the high thermodynamic stability of CO₂ molecules, being the most oxidized state of carbon. Moreover, the demand for urea and salicylic acid is not expected to grow in the next few years [54]. Nonetheless, other types of chemicals such organic and inorganic carbonates have huge potential for CCU application as reported by Brinckerhoff [56], based on its various industrial applications. However, despite the opportunities available for CO₂ conversion, the large-scale commercialization of CCU technology is still subject to the high energy requirement during the conversion process due to the high thermodynamic barrier of CO₂ molecules.

2.3.3 Integration of CO₂ capture and utilization

To maximize the potential application of CCU, researchers conducted studies to identify methods to overcome the high thermodynamic barrier of CO₂. One of the methods which can be applied to reduce the activation energy during CO₂ conversion process is by introducing catalyst during the reaction [6]. Examples of catalyst which can be used during CO₂ conversion process include aluminum oxide, platinum, and zirconium dioxide [15]. The use of these catalyst is a promising method to reduce the activation energy during conversion process [15]. However, for commercialization of large-scale CO₂ utilization plant the use of expensive metal catalyst is not economically attractive option.

Another strategy which can be implemented to reduce the energy requirement during CO₂ conversion process is by reacting CO₂ in its ionic form such as carbamate or carbonate ions [61]. This is because carbamate and carbonate ions have higher energy levels compared to CO₂ molecules, thus reduce the activation energy required during conversion process [61]. The ionic form of CO₂ molecules can be obtained by reacting CO₂ molecules directly with amine solutions. Depending on the CO₂ capture mechanisms, CO₂ capture and subsequent utilization leverage on the formation of carbamates, or carbonates in aqueous solutions [61] during the absorption process. In the conventional process, carbamates are formed when CO₂ are absorbed by the amine solution. These carbamates are regenerated to allow the solvent to be recycled back into the system. However, due to the high thermal stability of carbamates, high energy is required to breakdown the carbamates into its original constituents [62]. Converting this carbamate ions into valuable products such as calcium and magnesium carbonates can be done at atmospheric temperature and pressure as reported by Galvez-Martos et al. [63] and Lee et al. [51]. Through CO₂ capture and subsequent utilization, carbamate can be recovered without the use of harmful chemicals.

Carbon capture and subsequent utilization is expected to benefit both the capture and utilization process. The utilization process allows the elimination of solvent regeneration and hence the high energy requirement during CO₂ capture process. Furthermore, the utilization also eliminates the gas compression and transportation processes for direct and indirect CCU application.

2.3.4 The use of alcohol as reagent for CO₂ utilization

Carbonates and carbamates were identified as potential products of CO₂ utilization with various industrial applications as indicated in Table 2.3. Carbamates are primarily used for manufacturing of polymers and agrochemical products as well as drug designs [14, 17, 60]. Carbamates can be synthesized by using a few different routes as discussed by Ghosh and Brindisi [17]. However, the traditional methods for production of carbamates involve the use of highly toxic materials such as isocyanates, acyl azides, and nitroaromatic compounds [17]. Green synthesis of carbamates by using amines and alcohols were previously studied by Ion et al. [16], by reacting CO₂ with amines and alcohol, in the presence of a metal catalyst such as tin (Sn) and nickel (Ni). This study indicated that alcohol is a potential reagent which can be used to transform CO₂ into carbamates.

Apart from production of carbamates, alcohol can also be utilized for the production of carbonates. Both organic and inorganic carbonates have high demand in the industry, particularly in the manufacturing and construction industries as previously listed in Table 2.3. Previous studies indicated that linear carbonates can also be derived by reacting alcohol with CO₂ with the use of metal catalyst such as tin oxides and ceria-zirconia oxides [64].

The main drawback for the production of carbamates or carbonates using ethanol and CO₂ is the use of expensive metal catalyst. To eliminate the use of catalyst during production of organic carbonates and carbamates, the integration of CO₂ capture process with CO₂ utilization process using alcohol as a reagent were studied by various authors [18, 65, 66]. Table 2.4 indicates some of the products which can be obtained from the CO₂ conversion process. In general, alcohol such as methanol, ethanol, and 1-propanol can be utilized along with CO₂ to produce various precursors of carbamate or carbonate depending on the mechanism during CO₂ capture and utilization process. For the purpose of simplification in this, ethanol was selected as a reagent for CO₂ utilization study. Moreover, alcohol has lower toxicity compared to methanol and also is easily available.

Table 2.4: Different type of carbamate or carbonate products obtained from CO₂ utilization by using alcohol as a reagent.

Absorbent (reacted with CO₂)	Medium/ reagent	Rate of CO₂ absorption (%)	Products	Maximum yield of products (%)	References
NH ₃	Ethanol	90	Ammonium carbamate	94 ^a	[66]
	1-propanol	88	Ammonium carbamate	98 ^a	[66]
Triethylenetetramine (TETA)	Ethanol	82	TETA-carbamate	Not available	[67]
Piperazine	Methanol	Not available	Piperazine dicarbamate	Not available	[68]
Potassium proline	Ethanol	Not available	Bicarbonate and proline carbamate	Not available	[18]
2-amino-2-methyl-1-propanol	Ethylene glycol + ethanol/ Ethylene glycol + 1-propanol	75 – 95	AMP-carbamate Alcohol carbonate	Not available	[69]
Sodium hydroxide	Ethanol	Not available	Sodium ethyl carbonate	Not available	[24]
Sodium hydroxide	Methanol	55	Sodium methyl carbonate	45 ^b	[65]

^a with respect to absorbent

^b with respect to CO₂

2.4 Absorbents for CO₂ Capture and Utilization

The absorbents which were studied for CO₂ capture and utilization were listed discussed in this section. Among all the solvents reported, amine is the most widely studied absorbent. However, amine such as monoethanolamine (MEA) has limited absorption capacity. Literature reviews suggested that amine can be potentially replaced with diamines based on its high CO₂ absorption capacity. Moreover, the neutralization of amine with amino acid salt also showed significant improvement in terms of CO₂ loading capacity of the absorbent.

2.4.1 Types of absorbent for CO₂ capture and utilization

Various absorbents were reported for CO₂ capture and subsequent utilization namely amines [62, 70, 71], strong bases [24, 65, 72], weak bases [73-75], ionic liquids [76, 77] and amino acid salts [18], as summarized in Table 2.5. The transformation process is divided into two types namely one-step transformation process or two-step process as indicated in Figures 2.3 and 2.4, respectively. The products obtained from the conversion process are dependent on the media used during CO₂ capture as well as additional reagents added before or after the CO₂ capture process as also indicated in Table 2.5.

In the one-step process, organic medium such as methanol [65, 68], ethanol [78], and vegetable oils [79, 80] was mixed with absorbent and used as medium for CO₂ capture. The organic medium can be substituted with other non-aqueous solvents namely deep eutectic solvent [81] and ionic liquid [82]. During the CO₂ absorption process, the absorbents are directly converted into solid carbamate salts in a non-aqueous environment. Other than organic medium, inorganic carbonates can be instantaneously generated through a one-pot reaction when solvents such as calcium hydroxide [72] and aqueous ammonia [75] are used as absorbents for CO₂ capture. Cyclic carbonates were also generated through addition of epoxides into ionic liquids using one-step reaction [76, 77]. Alternatively, two-step reaction can also generate carbamate salts and carbonated products through additions of reagents into CO₂-saturated absorbents.

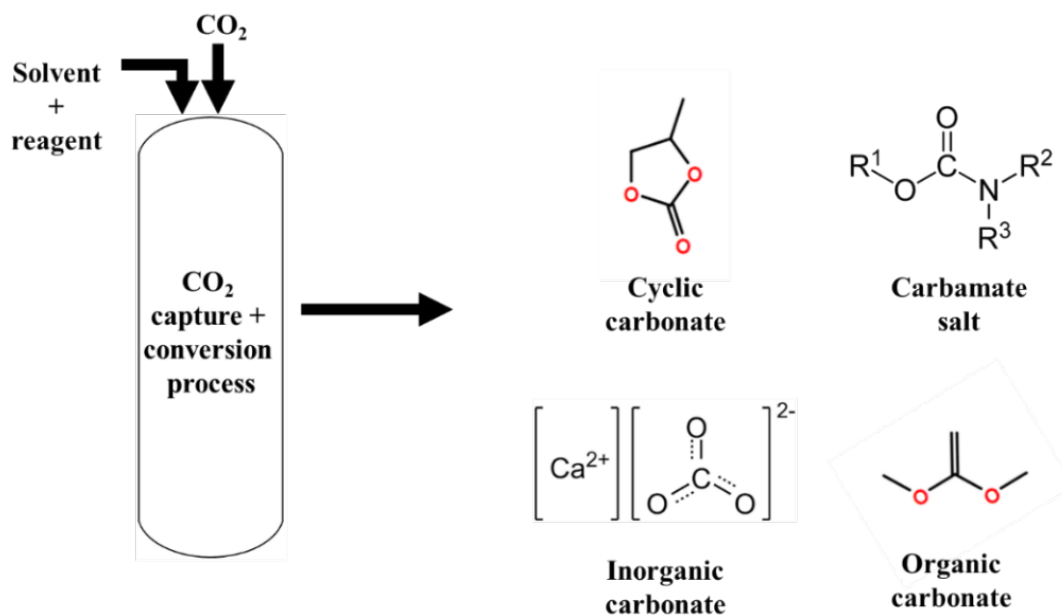


Figure 2.3: One-step conversion process (in-situ utilization).

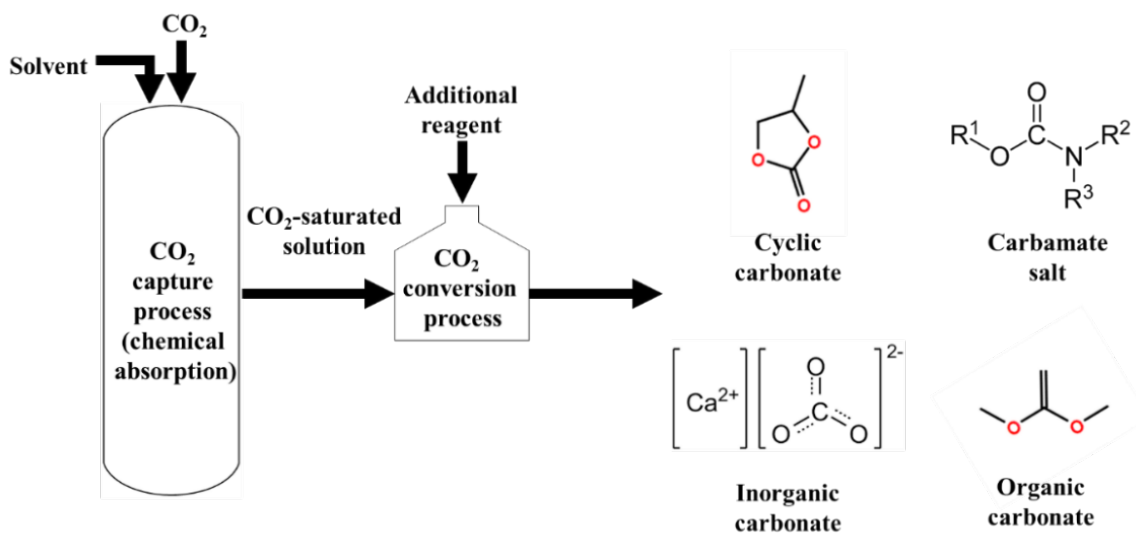


Figure 2.4: Two-step conversion process.

Table 2.5: List of absorbents, media, and additional reagents used for CO₂ capture and subsequent utilization.

Absorbents	Media for CO ₂ capture	Additional reagents/ catalysts	Products of CO ₂ conversion	Conditions during CO ₂ conversion process			Type of conversions		CO ₂ loading capacity (mol CO ₂ /mol absorbent)	Product yield ^a / conversion rate ^b (%)	Ref.
				P (atm)	T (K)	Time (hours)	One-step	Two-step			
Amine (Aqueous Phase)											
MEA	Water	Aqueous calcium chloride, CaCl ₂	Calcium carbonate	1	303.15	24	/		Not available	Not available	[62]
25 MEA/ DEA/ PZ/ AMP/ MDEA	Brine (aqueous NaCl)	Not applicable	Sodium bicarbonate	1	313.15	24	/		0.94	85 ^a	[83]
MEA/ DEA/ MDEA	Water	Aqueous calcium oxide (CaO)	Calcium carbonate	1	303.15	24		/	0.18 – 0.40	17 - 84	[84]
EDA	PEG	Aqueous calcium hydroxide, Ca(OH) ₂	Calcium carbonate	1	363.15	2		/	Not available	Not available	[85]

Table 2.5: List of absorbents, media, and additional reagents used for CO₂ capture and subsequent utilization (continued)

Absorbents	Media for CO ₂ capture	Additional reagents/ catalysts	Products of CO ₂ conversion	Conditions during CO ₂ conversion process			Type of conversions		CO ₂ loading capacity (mol CO ₂ / mol absorbent)	Product yield ^a / conversion rate ^b (%)	Ref.
				P (atm)	T (K)	Time (hours)	One-step	Two-step			
Amine (Aqueous Phase) - continued											
MEA/ DEA/ MDEA	Water	Aqueous barium chloride	Barium carbonate	1	303.15	2		/	Not available	60 – 90 ^b	[86]
MEA/ DEA/ MDEA/ AMP	Water	Anhydrous calcium chloride, CaCl ₂	Calcium carbonate	1	313.15	6		/	0.65 – 0.75	0.25 – 0.75 g CaCO ₃ / CaCl	[87]
EDA	1,2-ethylene glycol (EG)	Aqueous calcium hydroxide, Ca(OH) ₂	Calcium carbonate	1	373.15	1		/	1.26	46 ^a	[71]
MEA/ DEA/ MDEA	Water	Ca ²⁺ ions (industrial wastewater)	Inorganic metal carbonate	1	298.15	3		/	0.30 – 0.40	30 - 40 ^b	[12]

Table 2.5: List of absorbents, media, and additional reagents used for CO₂ capture and subsequent utilization (continued)

Absorbents	Media for CO ₂ capture	Additional reagents/ catalysts	Products of CO ₂ conversion	Conditions during CO ₂ conversion process			Type of conversions		CO ₂ loading capacity (mol CO ₂ / mol absorbent)	Product yield ^a / conversion rate ^b (%)	Ref.
				P (atm)	T (K)	Time (hours)	One-step	Two-step			
Amine (Aqueous Phase)											
MEA/ EDA/ DEA/ TEA/ MDEA/ AMP	Water	Metal ions (Ca ²⁺ /Sr ²⁺ / Ba ²⁺ / Mn ²⁺ / Cd ²⁺ / Pb ²⁺)	Metal carbonates	1-6 Mpa	293.15 -303.15	0.5 - 3	/		Not available	Not available	[88]
MEA	Water	Ca(OH) ₂ (industrial wastewater)	Calcium carbonate	1	298.15	3	/		0.45 – 0.50	Not available	[70]
Amine (Non-Aqueous Phase)											
DEA	Ionic liquid	Not applicable	DEA carbamate	1	298.15	6	/		0.50	Not available	[82]
AMP	EG + ethanol/ EG + 1-propanol	Not applicable	AMP-carbamate, alcohol carbonates	1	293.15 -313.15	24	/		Not available	Not available	[69]

Table 2.5: List of absorbents, media, and additional reagents used for CO₂ capture and subsequent utilization (continued)

Absorbents	Media for CO ₂ capture	Additional reagents/ catalysts	Products of CO ₂ conversion	Conditions during CO ₂ conversion process			Type of conversions		CO ₂ loading capacity (mol CO ₂ /mol absorbent)	Product yield ^a / conversion rate ^b (%)	Ref.
				P (atm)	T (K)	Time (hours)	One-step	Two-step			
Amine (Non-Aqueous Phase) - continued											
MEA/ DEA/ AMP/ TEA) MAE	Vegetable oil	Not applicable	Carbamates	1-8 bar	298.15 -338.15	0.5 - 2.5	/		0.94	53 ^a	[80]
AMP	Deep eutectic solvent	Not applicable	AMP carbamate	1-10 bar	298.15 -338.15	0.5 - 2.5	/		0.48	82 ^a	[81]
EDA/ DETA/ TETA	Vegetable oil	Not applicable	Carbamates	1.5, 10	298.15	0.5 - 1.5	/		1.40	72 ^a	[79]
PZ	Water/ ethanol	Not applicable	PZ carboxamide	1	298.15	168	/		Not available	Not available	[78]
PZ	Methanol	Not applicable	PZ-dicarbamate	1	298.15	Few hours	/		Not available	Not available	[68]

Table 2.5: List of absorbents, media, and additional reagents used for CO₂ capture and subsequent utilization (continued)

Absorbents	Media for CO ₂ capture	Additional reagents/ catalysts	Products of CO ₂ conversion	Conditions during CO ₂ conversion process			Type of conversions		CO ₂ loading capacity (mol CO ₂ /mol absorbent)	Product yield ^a / conversion rate ^b (%)	Ref.
				P (atm)	T (K)	Time (hours)	One-step	Two-step			
Metal Hydroxide Solution (Strong Base)											
Calcium hydroxide	Water	Not applicable	Calcium Carbonate	1	298.15	NM	/		Not available	Not available	[72]
Sodium hydroxide (NaOH)	Ethanol	Not applicable	Sodium ethyl carbonate	1	298.15	NM	/		Not available	99 ^a	[24]
Sodium hydroxide (NaOH)	Methanol	Not applicable	Sodium methyl carbonate	1	298.15	0.5	/		4.36 g CO ₂ /500 mL methanol	45 ^b	[65]
Ionic Liquid											
Urea derivative-based ionic liquid	Not applicable	Propylene oxide	Propylene carbonate	0.5 - 2.5	373.15 - 413.15	0.5 - 3	/		1.40 - 2.20	99 ^a	[77]
Bifunctionalized ionic liquid	Water	Styrene oxide	Styrene carbonate	1	373.15	12	/		1.00 - 1.20	20 - 94 ^b	[13]

Table 2.5: List of absorbents, media, and additional reagents used for CO₂ capture and subsequent utilization (continued)

Absorbents	Media for CO ₂ capture	Additional reagents/ catalysts	Products of CO ₂ conversion	Conditions during CO ₂ conversion process			Type of conversions		CO ₂ loading capacity (mol CO ₂ /mol absorbent)	Product yield ^a / conversion rate ^b (%)	Ref.
				P (atm)	T (K)	Time (hours)	One-step	Two-step			
Ionic liquid - continued											
Histidine derived ionic liquid	Dimethyl carbonate	Epoxide	Cyclic carbonates	1	353.15	5	/		0.84	55 - 98 ^a	[76]
Weak Base											
Chilled ammonia	Water	Not applicable	Ammonium carbonate and bicarbonate	NA	275.15 - 283.15	NM	/		0.1 – 0.1	Not available	[89]
Aqueous ammonia	Water	Zinc sulfate heptahydrate/ zinc chloride/ barium chloride dehydrate	Metal carbonates	1	293	< 1	/		0.29 – 1.86	Not available	[90]

Table 2.5: List of absorbents, media, and additional reagents used for CO₂ capture and subsequent utilization (continued)

Absorbents	Media for CO ₂ capture	Additional reagents/ catalysts	Products of CO ₂ conversion	Conditions during CO ₂ conversion process			Type of conversions		CO ₂ loading capacity (mol CO ₂ /mol absorbent)	Product yield ^a / conversion rate ^b (%)	Ref.
				P (atm)	T (K)	Time (hours)	One-step	Two-step			
Amino Acid Salt											
Potassium Proline	Ethanol	Not applicable	Bicarbonate and proline salts	0.5	303.15	4	/		0.64 – 1.13	45 – 59 ^b	[18]
Others											
Superbase (Diazabicyclo 5.4.0-undec-7-ene (DBU))	PEG	N-butylamine	Dibutyl urea	1	373.15 -403.15	12 - 24	/		0.74 – 1.09	47 – 97 ^a	[91]
Weak acid (Ammonium nitrate + calcium oxide)	Water	Not applicable	Calcium carbonate	1	298.15	24	/		0.58	99 ^a	[51]

2.4.1.1 Amine

Amine such as monoethanolamine (MEA), diethanolamine (DEA), ethylenediamine (EDA), 2-amino-2-methyl-1-propanol (AMP), and piperazine (PZ) are the most widely studied types of absorbent for CO₂ capture and direct conversion into value-added products (Table 2.5). The chemical reaction between amine and CO₂ is well understood based on its application for CO₂ removal from natural gas. Moreover, amine has high reactivity and it can be easily obtained at reasonable cost [92]. In theory, the reactions between CO₂ and aqueous amine solution are divided into three steps. The first step involved dissolution of CO₂ molecules into liquid phase (aqueous CO₂), followed by formation of bicarbonate, and finally formation of carbamate ions [46].

The ionic CO₂ molecules can be easily converted into metal carbonates through addition of metal ions in an aqueous medium. This process was demonstrated through studies performed by various researchers [12, 62, 70, 71, 83-88] which reported that metal carbonates such as calcium, barium, and magnesium carbonates can be produced at low pressure (mostly 1 atmosphere) and moderate temperature. However, the source of metal ions for the carbonation process is a crucial factor which determines the commercial viability of this technology. In a study reported by Park et al. [62] and Arti et al. [87], calcium ion was obtained by dissolving solid calcium chloride in water. Meanwhile, Kang et al. [84] used calcium oxide to provide metal ions for the conversion process. Similarly, other metal ions such as barium, and magnesium were also obtained from their respective metal oxides which were subsequently converted to metal hydroxides [71, 85, 88]. Production of these metal oxides usually involve energy intensive processes such as mining, conversion process, and transportation [93]. Alternatively, the metal oxides can be replaced with metal ion waste available from desalination process. The concept of utilizing industrial waste as a source of metal ions was investigated by Dindi et al. [83], Kang et al. [12], and Yoo et al. [70]. Reject brine from desalination process contained high amount of metal ions which can be recycled instead of being released back into the seawater. This provides a more sustainable approach for the carbonation process. However, the use of reject brine is subject to the concentration of chlorine ions in the waste solution, as high concentration of chlorine ions can cause equipment corrosion.

Dilution of concentrated amine by using water for the purpose of CO₂ capture was identified as one of the main causes of pipeline corrosion. According to Hasib-ur-Rahman et al. [82], aqueous amine solution which contained 15 weight percentage (w/w%) DEA showed high corrosion activity compared to DEA-ionic liquid emulsion which indicated almost negligible corrosion activity. This was due to the absence of water which prevented the formation of carbonic acid when water molecules reacted with CO₂, thus reduced its interaction with iron surface [82]. Moreover, the non-aqueous environment hindered the formation of bicarbonate and carbonate ions and hence allowed the formation of solid carbamates. The study conducted by Hasib-ur-Rahman et al. [82] has prompted other authors to investigate the performances of CO₂ capture and subsequent utilization by using amine-based solvent mixed with organic solutions such as methanol [68], ethanol [78], ethylene glycol, and ethanol mixtures [69], as well as vegetable oils [79, 80]. Deep eutectic solvent [81] was also studied as a potential non-aqueous medium for CO₂ capture.

Apart from generation of solid carbamates, the non-aqueous medium may contribute to higher CO₂ loading capacity, depending on the nature of the solvent. Uma Maheswari and Palanivelu [81], reported that the CO₂ loading capacity of amine mixed with deep eutectic solvent was higher compared to aqueous alkanoamine solutions. This may be due to the high polar nature of deep eutectic solvents which attracted more CO₂ molecules to dissolve in the solution [81]. However, in the case of vegetable oil, the CO₂ absorption capacity is subjected to the oil's viscosity [79, 80]. In general, vegetable oils such as sunflower oil, gingelly oil, groundnut oil, and palm oil have high viscosities [94] which hindered the desorption of CO₂ molecules within the solution. Nonetheless, amine solution especially AMP reported some improvement in CO₂ loading capacity when mixed with coconut oil [80]. This is due to the lower viscosity of coconut oil [95] compared to other types of vegetable oil [94]. The effect of viscosity on the CO₂ loading capacity of the absorbent was observed in the work reported by Shamiri et al. [96]. At lower concentrations of glycerol in the MEA-glycerol mixtures, higher CO₂ loading capacities were recorded compared to 30 w/w% MEA [96]. However, as concentration of glycerol increased, the CO₂ absorption capacities of MEA-glycerol mixtures were reported to be lower than the 30 w/w% MEA due to higher viscosity of the organic medium [96].

The addition of non-aqueous medium into pure amine solution resulted in the formation of immiscible liquids which are easier for product separation [82]. Two-phase flow system is a common phenomenon in many industrial processes particularly in the oil and gas industry. However, despite advances in technology, the mechanism of CO₂ capture in a two-phase media is not fully understood. Moreover, characterization of two phase flow requires complex mathematical calculations [97] which are both time consuming and costly. Current study focuses on batch process [79, 80, 82] which is direct and straight forward. In contrast, the CO₂ capture process in the industry involves continuous flow and transportation of immiscible liquid would be more complicated. Hence, despite the formation of value-added product, the use of non-aqueous solvent mix with amine solution may not be suitable for large scale commercial application. In contrary, the carbonation of CO₂ using aqueous amine solution mixed with metal ions is regarded to bring a positive impact in the production of metal carbonates due to lower temperature and pressure requirement during conversion process.

2.4.1.2 Metal hydroxide solution

Metal hydroxide solution was also reported as a potential absorbent for CO₂ capture due to its high absorption capacity and fast capture rate [98]. Aqueous calcium hydroxide was previously studied for its application in CO₂ capture and subsequent utilization [72]. In an aqueous environment, calcium hydroxide dissolved into calcium and hydroxide ions. Calcium carbonate was form instantaneously when calcium ions reacted with CO₂ the in the aqueous phase. This process occurred at room temperature of 298.15 K and pressure of 1 atm [72]. Sodium hydroxide is another type of strong base which can be used for CO₂ capture. In the presence of CO₂, aqueous sodium hydroxide produced sodium carbonate (Na₂CO₃) which was subsequently converted to sodium bicarbonate (NaHCO₃) [98]. In comparison with calcium hydroxide solution, the bicarbonate obtained from sodium hydroxide solution was not recovered as solid product due to its high solubility in water [98].

Han and Wee [24, 65] proposed the use of alcohol such as ethanol [24] and methanol [65] as a medium for CO₂ capture and utilization. This method was successfully proven to generate sodium ethyl carbonate and sodium methyl carbonate

when sodium hydroxide was dissolved in ethanol and methanol, respectively. The advantage of using alcohol is the presence of -OH functional group, which can participate in physical absorption of CO₂ [65]. However, the use of organic medium is limited by its high viscosity, which hinders the CO₂ absorption process. Another drawback of using sodium hydroxide dissolved in ethanol as an absorbent is the high concentration of sodium hydroxide is required for efficient removal of CO₂ [65]. Similarly, the production of methyl carbonate only occurred at higher concentrations of sodium hydroxide solution [65]. Considering the fact that sodium hydroxide is produced from expensive metal ions, this process may not be economically viable. Industrial waste was utilized as source of metal ions as reported by Kang et al. [12]. However, in order to attain high purity product, the metal ions needs to be segregated since industrial waste usually contained more than one type of metal ions [12]. Moreover, metal hydroxide is also known to be highly corrosive [6] and hence it is an unattractive choice of absorbent for CO₂ capture and subsequent utilization application.

2.4.1.3 Ionic liquid

Ionic liquid is an emerging solvent for CO₂ capture which has gained significant attention mainly based on its properties such as low volatility, high thermal stability, and tunable structures [99]. On top of being an absorbent, ionic liquid can also be used as a catalyst for the production for cyclic carbonate. Cycloaddition of epoxides with CO₂ using ionic liquids were investigated by a few authors such as Kumar et al. [76], Luo et al. [13], and Lui et al. [77]. Experimental results revealed that epoxides were transformed into cyclic carbonates at atmospheric pressure. Moreover, the ionic liquid can be recycled up to six times with yield more than 95% was reported by Kumar et al. [76].

Despite the positive aspects of ionic liquid as an absorbent for CO₂ capture and utilization, the absorbent also has certain drawbacks. The synthesis of ionic liquid involves complex steps and occurred at high temperature, increasing its production cost [100]. On top of that, the synthesis of ionic liquid as well as CO₂ conversion process occurred in the presence of organic media such as toluene, acetonitrile [77], and dimethylformamide [76]. These solvents are highly flammable and volatile, thus release toxic fumes into the environment. Moreover, the production of ionic liquid generates

organic waste product. Hence, the development of ionic liquid for CO₂ capture and utilization remains a challenge mainly due to high cost and the use of organic media during conversion process.

2.4.1.4 Weak base

The transformation of metal ions into metal carbonates through CO₂ capture and utilization can also be performed by using weak base as an absorbent. This process was studied by Gaur et al. [90], in which metal carbonate was successfully synthesized when CO₂ reacted with a mixture containing metal salt and aqueous ammonia. In comparison to strong base (metal hydroxide solution) which produced carbonated products at higher concentration of absorbent [24, 65], smaller concentration of weak base was sufficient to transform CO₂ into solid products [90]. Weak base can also be replaced by alkaline industrial waste, which was also capable of generating metal carbonates when reacted with CO₂ and metal salts [90]. Weak base can generate precipitates directly during the CO₂ capture process without additional reagent or the use of organic medium. Solids crystals such as ammonium bicarbonate and ammonium carbonate can be easily generated using aqueous ammonia as an absorbent depending on pH of the solution [73]. However, the pH of the solution needs to be controlled to prevent the formation of by-products [73]. Nonetheless, the carbonated products have high commercial values as they are sources of fertilizers [101].

The disadvantage of using aqueous ammonia as an absorbent for CO₂ capture and utilization is the high volatility of the solvent which leads to vapor loss to the environment. This problem was resolved by decreasing temperature of the absorbent by using the chilled ammonia technology [89]. In this process, ammonia is cooled down to a temperature ranging between 2 to 10 °C before entering the absorption column, thus prevented the evaporation of ammonia [89]. Products which were recovered through chilled ammonia CO₂ capture process include ammonium bicarbonate, ammonium carbonate, and ammonium carbamate [89]. However, the major drawback of chilled ammonia process is that the absorption and conversion process occurred at very low temperature, and hence more energy is required for refrigeration and cooling processes.

2.4.1.5 Amino acid salt

Amino acid salt is another type of absorbent which was investigated for the purpose of CO₂ capture [23, 102]. The properties of amino acid salt include low oxidation degradation, high reactivity, and low volatility which makes it a good absorbent for CO₂ capture [23]. Similar to aqueous ammonia, pH of the absorbent plays an important role in the formation of precipitates during CO₂ capture which leads to reduction in energy during solvent regeneration process through phase separation method [102]. However, these solids are regenerated to allow amino acid salt to be recycled back into the system. Currently, there are limited studies on CO₂ capture and utilization using amino acid salt.

In study conducted by Shen et al. [18], amino acid salt was mixed with ethanol which increased the rate of CO₂ capture compared to aqueous amino acid salt. Although the study focused on phase change method through regeneration of precipitates, the formation of carbamate proline, bicarbonate, and ethyl carbonate salts proved that amino acid salt in organic medium has the capability to be used as an absorbent for CO₂ capture and subsequent utilization. However, the viscosity of the solution in ethanol was reported to be higher than in water [18] which limits the dissolution of CO₂ in the absorbent. The CO₂ loading capacity of the amino acid salt mixed with ethanol was reported to be lower when compared to aqueous amino acid salt solution [18]. Nonetheless, as an environmentally friendly solvent, amino acid salt is an alternative absorbent which can potentially replace other types of absorbent for CO₂ capture and utilization application.

2.4.1.6 Other types of absorbent

Superbase [91] and weak acid [51] were also reported as absorbents for CO₂ capture and utilization. Superbase namely diazabicyclo[5.4.0]-undec-7-ene (DBU) dissolved in PEG solution was reacted with CO₂ to produce liquid amidinium carbonate salt, which was subsequently converted into urea in the presence of amine solution. The reaction occurred at 1 bar and temperature between 100 to 130 °C [91] compared to conventional process which occurred at temperature of 185 to 190 °C and pressure of 180 to 200 atm [15]. Weak acid was also studied as a potential absorbent [51] such that

ammonium nitrate was used to extract metal ions from solid industrial waste. When ammonium nitrate was mixed with calcium oxide (solid industrial waste), ammonium hydroxide was produced which increased the capacity of the mixture to absorb CO₂. Simultaneously, calcium ions from industrial waste were directly converted to metal carbonates [51].

Superbase has high CO₂ absorption capacity of approximately twice compared to the conventional MEA solution [91]. However, superbase has high basicity which can cause equipment and pipeline corruptions. Moreover, the use of organic medium increases the viscosity of the absorbent. Nonetheless, these studies [51, 91] suggested that apart from solvents listed in the previous categories, there are other types of absorbent which are also capable of capturing CO₂ and directly converting CO₂ into value-added products at moderate temperature and pressure conditions. This includes the production of urea from superbase and amine mixture.

2.4.1.7 Advantages and disadvantages of different types of absorbent

The potential absorbents which can be used for CO₂ capture and utilization are as illustrated in Figure 2.5. The solvents are divided into a few categories namely amine solution, metal hydroxide solution (strong base), weak base, ionic liquid, amino acid salt, and others. Direct carbonation of CO₂ into metal carbonates can be achieved through addition of solution containing metal ions. In the absence of water molecules, solid carbamate can be generated. Certain absorbents such as calcium hydroxide and aqueous ammonia are able to transform CO₂ directly into solid products without the use of organic media or additional reagents. Amino acid salt is an environmentally friendly absorbent which can also be utilized for CO₂ capture and conversion process. Nonetheless, amino acid salt has limited absorption capacity. Moreover, cyclic carbonates can be generated without the use of expensive metal complexes by using ionic liquid as CO₂ absorbent and catalyst for the conversion process. However, the cycloaddition process may require the presence of highly toxic organic medium such as toluene, acetonitrile, and dimethylformamide.

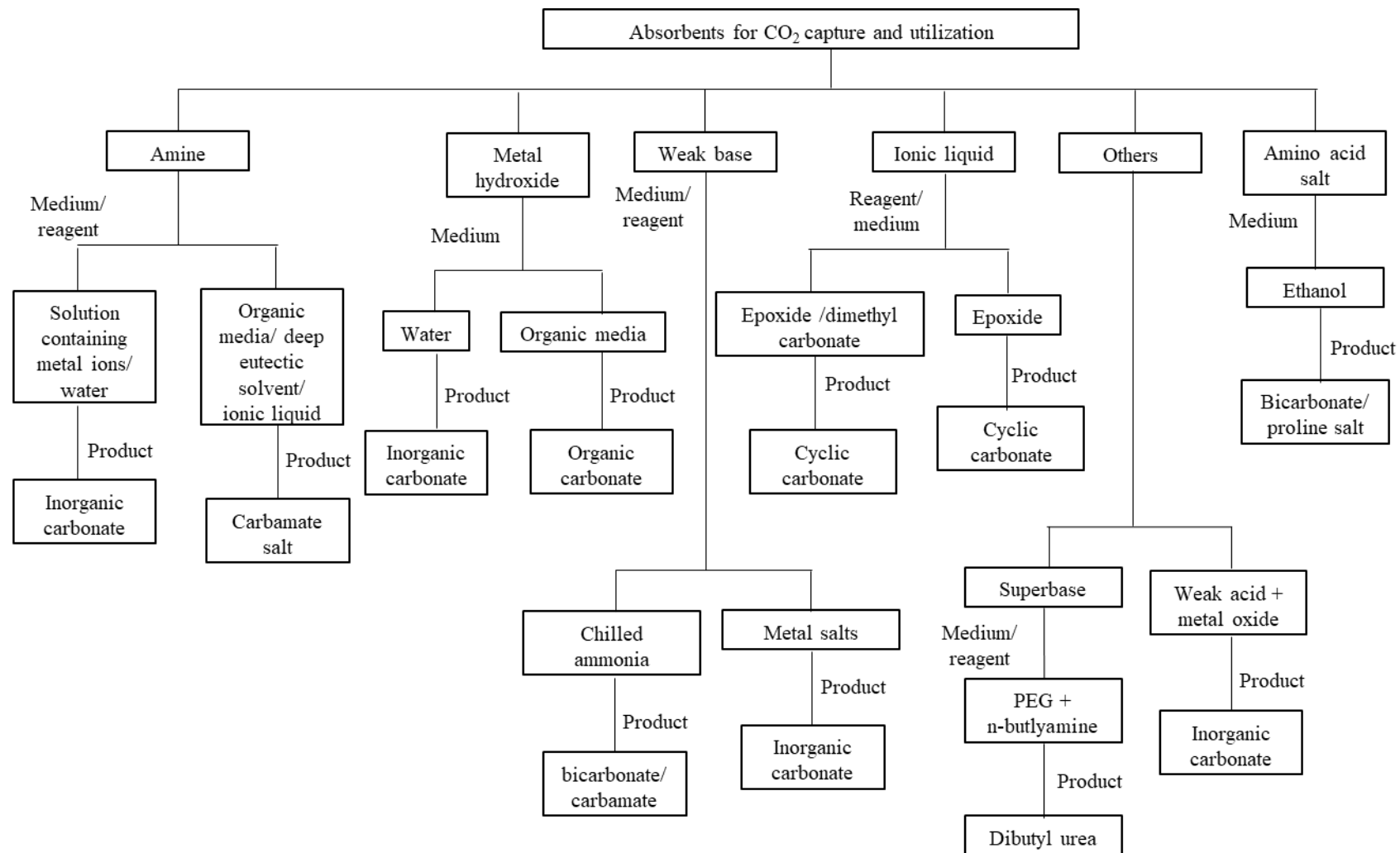


Figure 2.5: Type of absorbents, reaction media, and additional reagents used for CO₂ capture and utilization.

The advantages and disadvantages of each types of absorbents are summarized in Table 2.6. Among all the absorbents, aqueous amine is the most mature absorbent available for CO₂ capture. On top of that, the addition of metal ions generated inorganic carbonates at low temperature and pressure. The expensive cost of metal ions can be replaced with industrial waste which provides a more sustainable approach for the production of metal carbonates. However, the CO₂ capture capacity of amine solvent is much lower compared to other types of absorbents such as ionic liquid, and superbase. The use of organic media such as methanol and ethanol are also attractive for the purpose of CO₂ capture and subsequent utilization. The high viscosity of absorbent which may reduce the diffusivity of CO₂ can be overcome by using the two-step conversion method instead of one-step utilization process.

Table 2.6: Advantages and disadvantages of absorbents and reaction media/ reagents for CO₂ capture and utilization.

Type of absorbents	Reaction Media/ reagents	Advantages	Disadvantages	Ref.
Amine solution	Metal ion solutions/ industrial waste	<ul style="list-style-type: none"> • Mature solvent • Generate metal carbonates at low temperature and atmospheric pressure 	<ul style="list-style-type: none"> • Energy intensive process for production of metal ions • High concentration of chlorine ions in industrial waste • Metal ions in industrial waste needs to be segregated to obtain high purity product 	[12, 62, 71, 83-88]
	Organic media	<ul style="list-style-type: none"> • Produces organic carbamate without the use of toxic chemicals • Low capital cost (one-step reaction) 	<ul style="list-style-type: none"> • Organic media has high viscosity • Formation of two-phase liquid 	[68, 69, 79-81, 103]
Metal hydroxide	Water	<ul style="list-style-type: none"> • Generate metal carbonate at low temperature and atmospheric pressure • Low capital cost 	<ul style="list-style-type: none"> • Energy intensive process for production of metal ions/ metal salts • Absorbent is highly corrosive 	[72]

Table 2.6: Advantages and disadvantages of absorbents and reaction media/ reagents for CO₂ capture and utilization (continued).

Type of absorbents	Reaction Media/ reagents	Advantages	Disadvantages	Ref.
Metal hydroxide	Organic media	<ul style="list-style-type: none"> • Produces organic carbonate in liquid form (organic solvent) 	<ul style="list-style-type: none"> • Organic media has high viscosity • Absorbent is highly corrosive 	[24, 65]
Ionic liquid	Organic solvent/ Epoxide	<ul style="list-style-type: none"> • High CO₂ absorption capacity • Transform epoxides into cyclic carbonate at low temperature and atmospheric pressure 	<ul style="list-style-type: none"> • The use highly toxic organic media (toluene, DMF) during synthesis of ionic liquid and during conversion process • Ionic liquid is expensive • Ionic liquids have high viscosity 	[13, 76, 77]
Weak base	Water	<ul style="list-style-type: none"> • No additional media/ reagent is required for conversion process 	<ul style="list-style-type: none"> • High energy requirement for cooling process 	[89]
	Metal salt	<ul style="list-style-type: none"> • Generate metal carbonates at low temperature and atmospheric pressure 	<ul style="list-style-type: none"> • Energy intensive process for production of metal ions/ metal salts • Aqueous ammonia has high volatility 	[90]
Amino acid salt	Organic solvent	<ul style="list-style-type: none"> • Environmentally friendly absorbent 	<ul style="list-style-type: none"> • Low absorption capacity 	[18]
Others (Superbase and weak acid)	PEG/ metal oxide	<ul style="list-style-type: none"> • Superbase has high CO₂ absorption capacity 	<ul style="list-style-type: none"> • Organic media has high viscosity • High toxicity • Corrosive 	[51, 91]

2.4.2 Amine as an absorbent for CO₂ capture and utilization

As previously discussed in Section 2.4, amine is the most widely type of absorbent used for CO₂ capture and utilization. However, one of the disadvantages of using amine such as monoethanolamine (MEA) is the limited CO₂ absorption capacity of the absorbent. In this section, the different types of amines were reviewed to identified a potential amine which can be used as an absorbent for CO₂ capture and utilization.

2.4.2.1 CO₂ solubility of monosubstituted amine

This section will compare the performance of different types of monosubstituted amine commonly reported for CO₂ absorption studies at various absorption conditions as shown in Table 2.7. The studies revealed that amine such as MEA, DEA, and TEA has limited absorption capacity (less than 1.0 mol CO₂ / mol amine) due to limited amino functional group to interact with CO₂ molecules.

Table 2.7: CO₂ solubilities of different types of monosubstituted amine at 313.15 K.

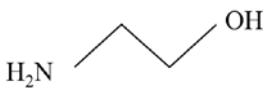
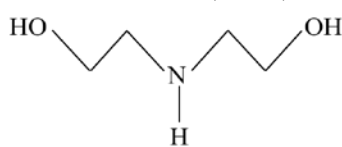
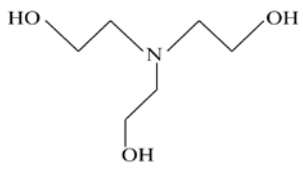
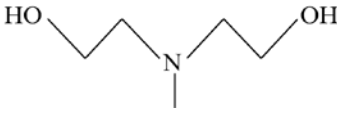

Amine	Concentration of amine (M)	P (bar)	CO ₂ solubility (mol CO ₂ /mol amine)	Reference
Monoethanolamine (MEA) 	2.0	1.01	0.676	[104]
	5.0	1.01	0.594	[105]
	5.0	1.15	0.469	[7]
	5.0	1.40	0.620	[105]
	5.0	5.52	0.676	[105]
	5.0	5.04	0.653	[106]
	5.0	8.83	0.728	[105]
	5.0	15.04	0.784	[106]
	5.0	25.12	0.842	[106]
Diethanolamine (DEA) 	2.0	1.01	0.727	[104]
	2.9	1.15	0.502	[7]
	2.0	1.04	0.727	[107]
	4.0	1.02	0.639	[107]
	3.8	34.47	0.880	[108]
	3.8	41.37	1.04	[108]
Triethanolamine (TEA) 	3.0	1.15	0.266	[7]
	3.0	1.06	0.425	[109]

Table 2.7: CO₂ solubilities of different types of monosubstituted amine at 313.15 K (continued).

Amine	Concentration of amine (M)	P (bar)	CO ₂ solubility (mol CO ₂ /mol amine)	Reference
 Methyldiethanolamine (MDEA)	2.0	1.01	0.805	[104]
	2.8	2.00	0.930	[110]
	2.8	4.50	0.990	[110]
	2.8	8.00	1.060	[110]
	2.8	12.5	1.100	[110]
 2-amino-2methyl-1-propanol (AMP)	3.4	1.15	0.626	[7]
	2.0	1.59	0.991	[111]
	2.0	0.94	0.940	[112]
	3.0	0.94	0.875	[112]
	2.0	5.60	1.26	[113]
	3.0	5.30	1.06	[113]

2.4.2.2 Diamine as potential absorbent for CO₂ capture and utilization

To further improve the absorption capacity of monosubstituted amines, the CO₂ solubilities of diamines were investigated as by various authors [43, 47]. The structures of several diamines are as shown in Figure 2.6. The enhancement in CO₂ absorption performance was mainly based on the additional -NH functional group present in diamine solutions which provided further attachment sites for binding of CO₂ molecules [20].

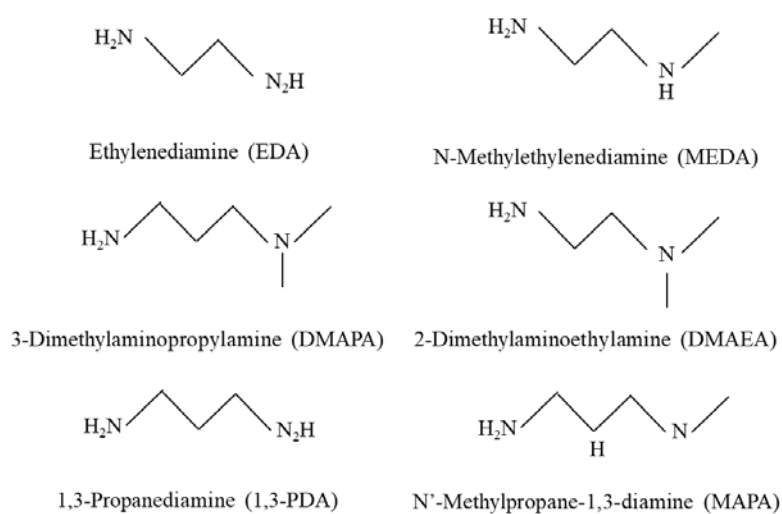


Figure 2.6: Structures of various diamines.

In Table 2.8, the CO₂ solubilities of at different types of diamines at various conditions were reviewed. The results indicated diamine generally have higher CO₂ loading capacity in comparison to monosubstituted amine solution.

Table 2.8: CO₂ solubilities of different types of diamines at 313.15 K.

Diamine	Concentration of amine (M)	P (bar)	CO₂ solubility (mol CO₂/ mol amine)	Reference
MAPA	2.0	0.98	1.365	[114]
	2.0	1.67	1.455	[114]
	2.0	2.57	1.523	[114]
	2.0	3.29	1.584	[114]
DMAPA	1.0	0.07	0.970	[115]
	1.5	1.24	1.300	[116]
	1.5	1.75	1.350	[116]
	1.5	2.25	1.400	[116]
	1.5	2.75	1.450	[116]
EDA	1.0	0.07	0.980	[115]
	2.0	5.00	1.100	[117]
	2.0	2.00	1.080	[117]
	2.0	0.45	0.990	[117]
DMEA	1.0	0.07	0.780	[115]

Apart from the presence of additional -NH functional group, other factors which affects the CO₂ loading capacity are diamine chain length and the presence of additional methyl group attached to the N atom. In a study performed by Zhang et al. [20], it was suggested that DMAPA exhibited the highest performance for CO₂ capture based on high removal efficiency and high CO₂ cyclic capacity (Figure 2.7). Despite that, the high volatility of DMAPA remains an obstacle for further development of this solvent. Diamines were reported to have significant vapor pressure which contributed to solvent loss and emissions of toxic fumes into the environment [118, 119]. Moreover, DMAPA is also associated with substantial regeneration energy, although it was reported to be lower than MEA [20].

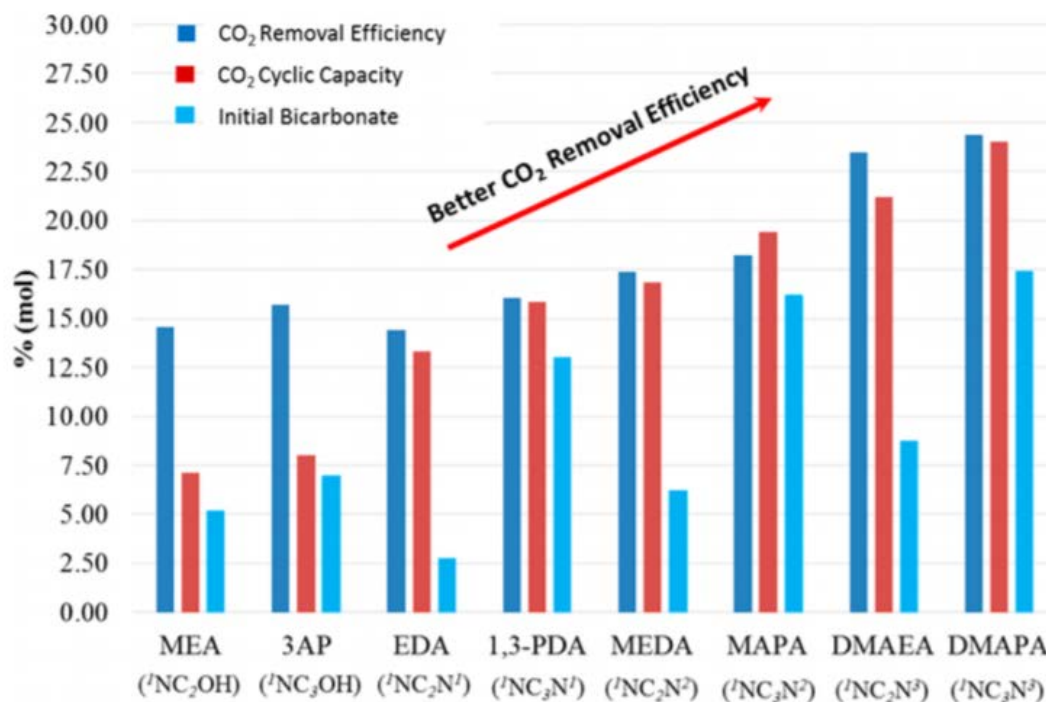


Figure 2.7: Performance of various diamine solutions in comparison to MEA. Reprinted with permission from Rui Zhang et al. *Energy & Fuels* 2017 31 (10), 11099-11108. Copyright (2019) American Chemical Society.

2.4.2.3 Neutralization of amine with aqueous amino acid

One of the methods which was studied to reduce the vapor pressure of alkaline solution is through neutralization with aqueous amino acid as reported by Yang et al. [120]. Amino acid salt was reported as potential absorbent for CO₂ capture based on its low toxicity and non-volatile properties [121]. The simplest form of amino acid reported for CO₂ capture is glycine [122-125], which has the following zwitterion structure in aqueous form as illustrated in Figure 2.8.

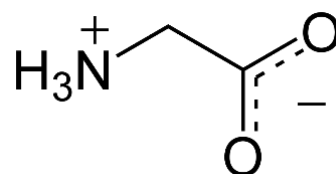


Figure 2.8: Zwitterion structure of glycine in aqueous form.

In order to activate the amino group for CO₂ absorption process, glycine needs to be activated by neutralizing the molecules with a basic solution such as potassium hydroxide (KOH). The CO₂ solubility of potassium glycinate at various absorption conditions are tabulated in Table 2.9.

Table 2.9: CO₂ solubility of potassium glycinate at 0.9 M and 313.15 K [126].

P (bar)	CO₂ solubility (mol CO₂/ mol absorbent)
1.68	0.629
2.99	0.721
5.85	0.796
8.60	0.873
15.11	0.988
21.42	1.125

Although potassium glycinate has high potential to be used as and absorbent for CO₂ capture, it has limited absorption capacity. Apart from inorganic base, amino acid can also be neutralized with organic base namely amine to reduce the vapor pressure of amine solution. The neutralization of aqueous amino acid with MEA and MAPA were investigated by Aronu et al. [22], which revealed that amine amino acid salts have higher CO₂ absorption capacity compared to amino acid neutralized with potassium hydroxide.

Previous CO₂ solubility studies by using amine and amino acid were reported in the literatures as shown in Table 2.10. These studies were limited to low pressure of CO₂ at 10 kPa. Hence, this research focused on the use of DMAPA neutralized with amino acid at higher pressure (between 5 to 25 bar) for pre-combustion CO₂ capture application. For amino acid, glycine was selected as a basis in this experiment, glycine-MEA absorbent was reported to have highest amino acid carbamate formation compared to other amino acids [127]. This would benefit the CO₂ utilization process due to formation of more carbamate ion.

In parallel with the efforts to reduce the high regeneration energy during the CO₂ desorption process, integration of CO₂ capture and utilization using diamine and amino acid as an absorbent was proposed. Based on Section 2.3, ethanol was identified as a potential reagent which can transform CO₂ into carbon-based products. However, due to high viscosity of the absorbent, the CO₂ capture and utilization was performed by using a two-step utilization method.

Table 2.10: CO₂ absorption studies for different types of amino acid and amine solutions at 313.15 K.

Base solution	Amino Acid	CO₂ Capture Concentration (M)	Conditions P (kPa)	CO₂ loading capacity (mol CO₂/ mol absorbent)	Ref
MEA	Serine	0.5	10	0.700	[127]
MEA	Glycine	2.0	10	0.700	[127]
MEA	L-proline	1.0	10	0.890	[127]
KOH	Sarcosine	2.5	10	0.509	[22]
MAPA	Sarcosine	2.5	10	0.527	[22]
MAPA	Glycine	2.5	10	0.519	[22]
MAPA	B-alanine	2.5	10	0.518	[22]
MAPA	Sarcosine	5.0	10	0.51	[128]

2.5 Mechanism of Study for CO₂ Capture and Utilization

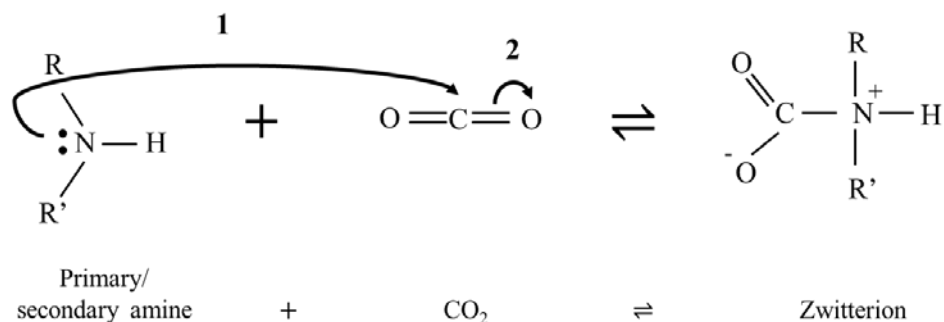
The mechanism of study describes the movements of electrons as well as the proton transfer during the formation of a new compound. In this section, the mechanism study is divided into two parts, namely the mechanisms for CO₂ capture using amine solution (Section 2.5.1) and the mechanisms for CO₂ utilization (Section 2.5.2).

2.5.1 Mechanisms for CO₂ capture for amine solution

The interactions between CO₂ and amines can be described by using a few different mechanisms such as the zwitterion [129], and carbamic acid mechanism [130], depending upon the types of amine used as absorbent. For primary and secondary amines, the CO₂ absorption process is commonly explained through the zwitterion mechanism [79, 80]. Meanwhile, for tertiary amine, the absorption process was defined through the carbamic acid mechanism [79, 80].

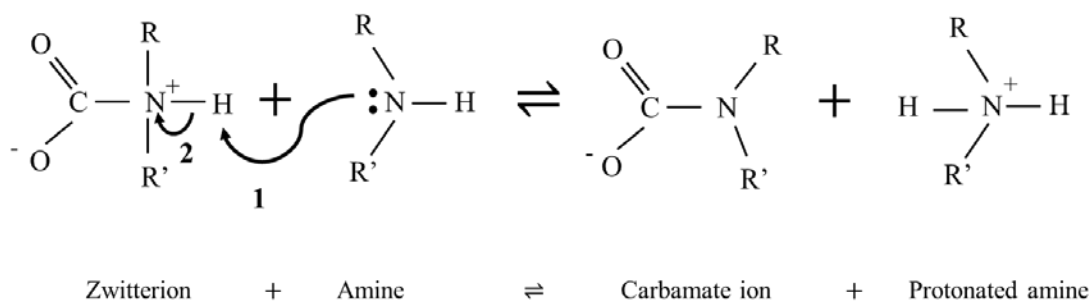
2.5.1.1 Mechanisms of CO₂ capture for monoamine

Based on the zwitterion mechanism [129], CO₂ will interact nitrogen atom from the primary or secondary amino functional group to form an intermediate zwitterion structure as indicated in Scheme 2.1.

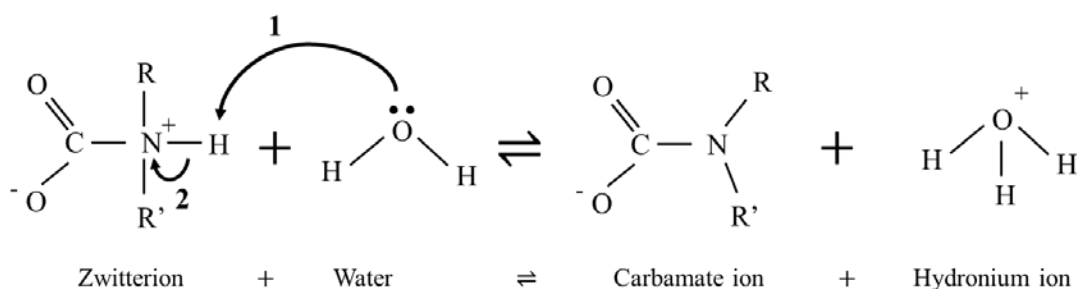


Scheme 2.1: The formation of zwitterion structure from primary or secondary amine (adopted from [80]).

The zwitterion intermediate will then react with another base molecule (base catalyst) such as amine or water to form a carbamate ion as described by Scheme 2.2 and Scheme 2.3.



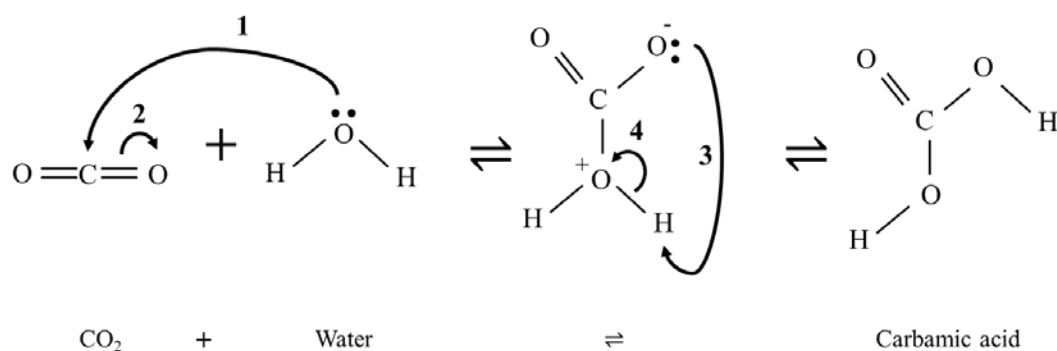
Scheme 2.2: The formation of protonated amine and carbamate ion by reaction between zwitterion and amine (adopted from [80]).



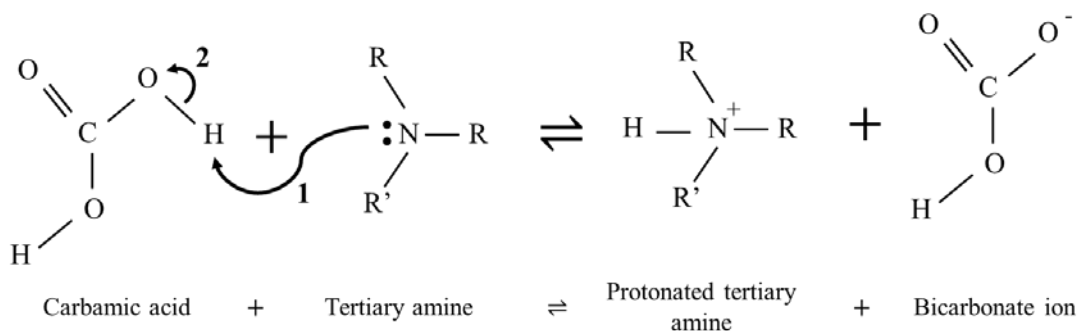
Scheme 2.3: The formation of protonated amine and hydronium ion by reaction between zwitterion and water (adopted from [80]).

The mechanisms based on Schemes 2.2. and 2.3 suggested that the primary and secondary amino group will result in the formation of carbamate ion. However, for tertiary amino group, due to lack of proton, the formation of zwitterion not be feasible [80]. Instead, CO₂ will react with water molecule to form carbamic acid which will interact with tertiary amine group to produce protonated tertiary amine along with

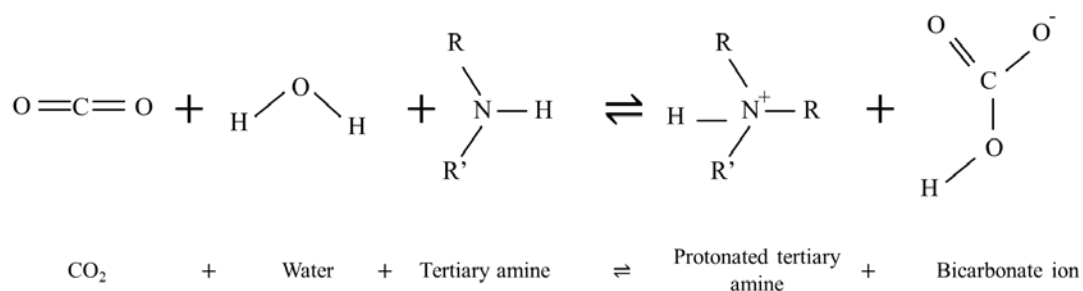
bicarbonate ion. The formation of carbamic acid and its reaction with tertiary amine are described by Scheme 2.4 and Scheme 2.5, respectively. The overall reactions between CO₂ and tertiary amines are illustrated by Scheme 2.6.



Scheme 2.4: Formation of carbamic acid from CO₂ and water molecule (adopted from [80]).



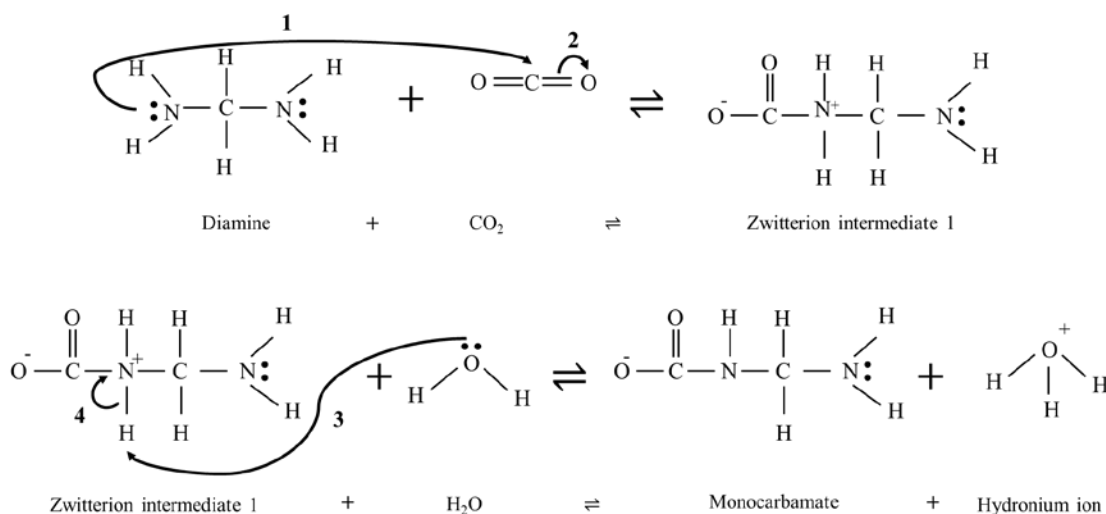
Scheme 2.5: Formation of protonated tertiary amine and bicarbonate ion (adopted from [80]).



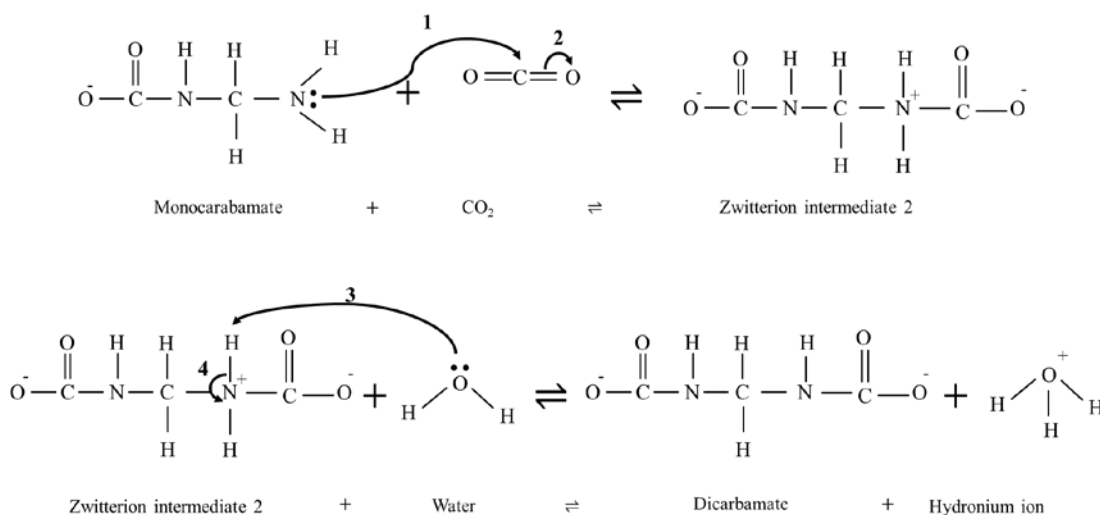
Scheme 2.6: Overall reaction between CO₂ and tertiary amine (adopted from [80]).

2.5.1.2 Mechanisms of CO₂ capture for diamines

The general mechanisms for CO₂ capture using diamines briefly proposed by Zhang et al. [20] and Ciftja et al. [127]. The mechanisms described suggested that in diamine solution, the primary or secondary amino group will be transformed into monocarbamate (Scheme 2.7), followed by a dicarbamate (Scheme 2.8).

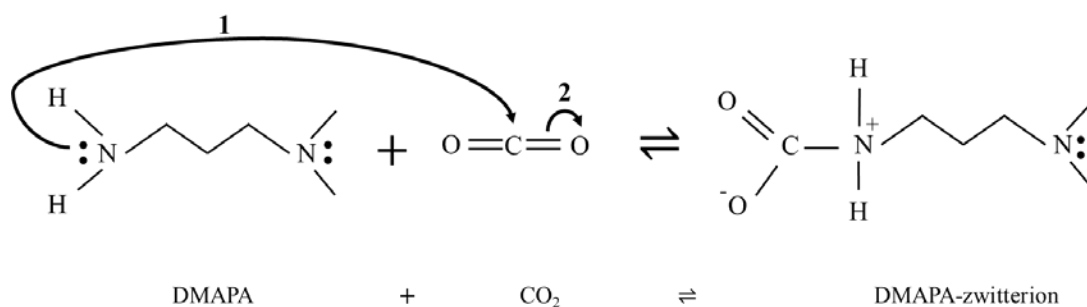


Scheme 2.7: The formation of monocarbamate from a diamine molecule (adopted from [20]).



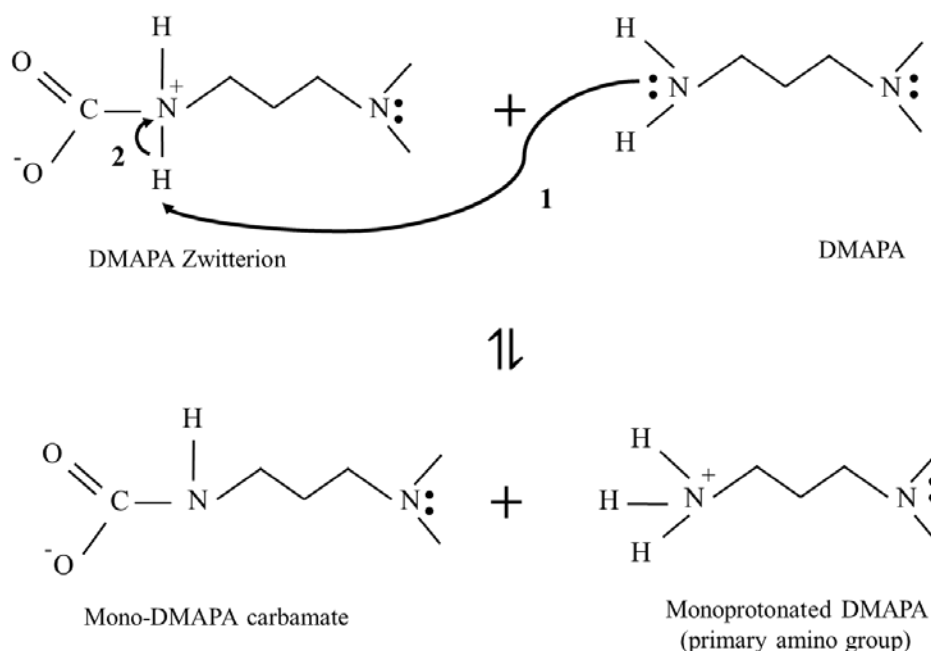
Scheme 2.8: Formation of dicarbamate from a diamine molecule (adopted from [20]).

For a diamine molecule containing tertiary amino group, the formation of dicarbamate is inhibited due to lack of proton from the amino group. A mechanism of CO₂ absorption using DMAPA which contains both primary and tertiary amino group was studied by [131]. The primary amino group will react with CO₂ to form a DMAPA-zwitterion intermediate as illustrated in Figure 2.9.

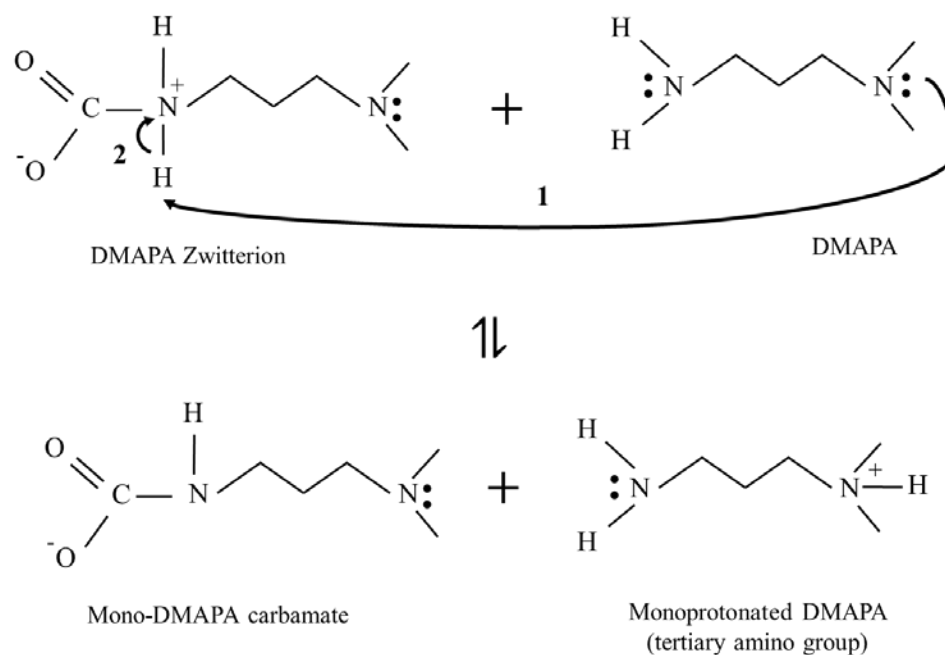


Scheme 2.9: Formation of DMAPA-zwitterion from DMAPA and CO₂ molecule (adopted from [131]).

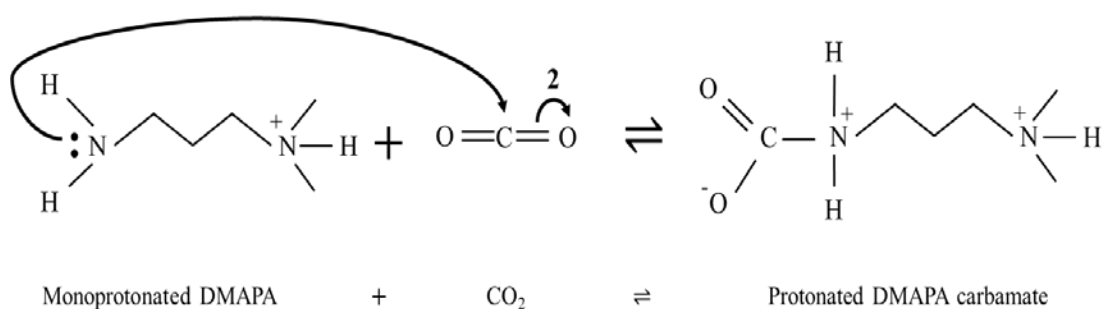
The DMAPA-zwitterion will undergo further deprotonation through reaction between primary or tertiary amino group of a neighboring DMAPA molecule to produce a protonated DMAPA carbamate as shown in Schemes 2.10 and 2.11. The monoprotonated DMAPA molecule will then react continuously with CO₂ to generate protonated DMAPA carbamate as designated by Scheme 2.12. Finally, the mono DMAPA carbamate will also undergo protonation with water via its tertiary amino group to give protonated DMAPA carbamate.



Scheme 2.10: Formation of DMAPA carbamate and monoprotonated DMAPA from primary amino group (adopted from [131]).



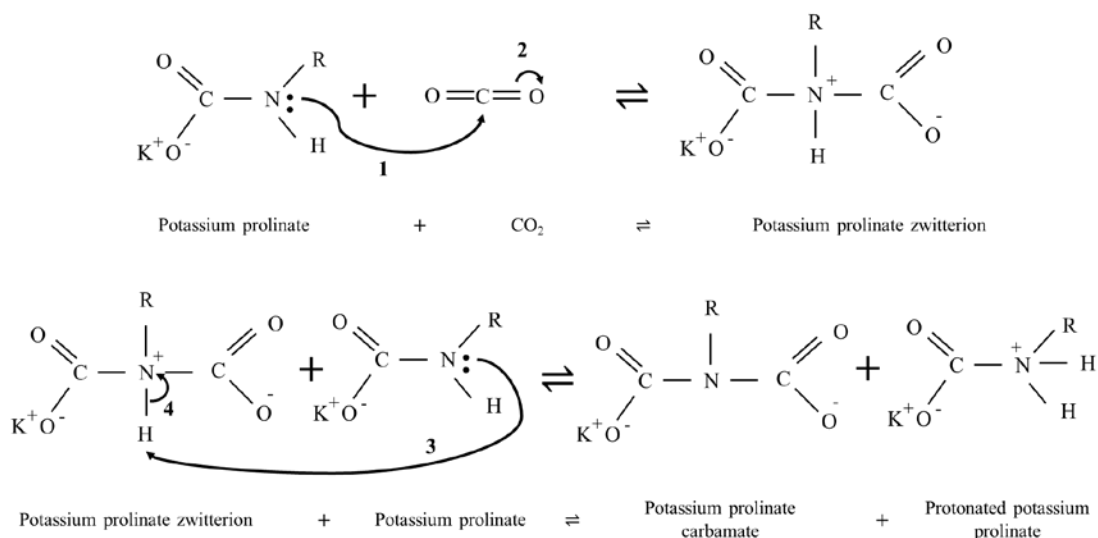
Scheme 2.11: Formation of DMAPA carbamate and monoprotonated DMAPA from tertiary amino group (adopted from [131]).



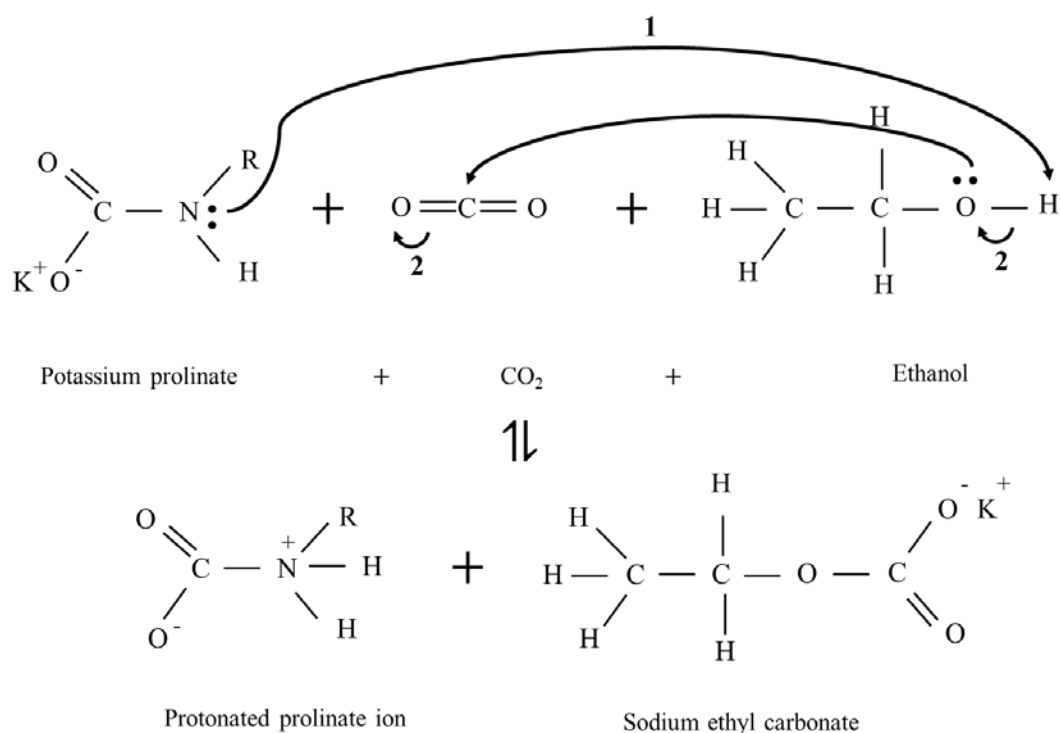
Scheme 2.12: Reaction between monoprotonated DMAPA with CO₂ to produce protonated DMAPA carbamate (adopted from [131]).

2.5.2 Mechanisms for CO₂ utilization

The mechanisms for reaction between CO₂, ethanol and amino acid salt was previously reported by Shen et al. [18]. The mechanisms suggested the formation of two main products namely proline carbamate and sodium ethyl carbonate as demonstrated by Schemes 2.13 and 2.14, respectively.



Scheme 2.13: Reaction between potassium prolinatate and CO₂ to produce potassium prolinatate carbamate (adopted from [18]).



Scheme 2.14: Formation of sodium ethyl carbonate through reactions between potassium prolinatate, CO₂ and water (adopted from [18]).

2.6 Summary

Based on the literature reviews, carbon capture and storage (CCS) from large point sources was identified as one of the strategies which can be implemented to reduce CO₂ content in the atmosphere. CO₂ capture at elevated pressure above 2 bar (for pre-combustion and post-combustion technology) offers a higher CO₂ separation efficiency. Absorption process was identified as the most promising method for CO₂ capture based on its high efficiency, maturity, and reliability. Aqueous amine is the most common type of absorbent reported for CO₂ absorption studies. However, the major drawback of using amine solution is the limited absorption capacity of the solvent (MEA) and the high regeneration energy during solvent regeneration process. Previous research indicated that the high energy requirement during solvent regeneration problem can be resolved by integrating the CO₂ capture with CO₂ utilization process. This offers two advantages, such that the elimination of the CO₂ desorption process and reduction in energy requirement during CO₂ conversion process. Diamine was namely 3-dimethylamino-1-propanol (DMAPA) was identified as a promising absorbent for CO₂ capture, based on its high CO₂ absorption capacity. Moreover, the neutralization with diamine with amino acid was proposed to reduce the vapor pressure of DMAPA. The use of ethanol for CO₂ utilization process was also proposed based previous research which suggested that reaction of CO₂ with ethanol and amine solution will generate carbamate salt which is a useful product for agrochemical and medicinal chemistry industries.

CHAPTER 3

METHODOLOGY

3.1 Overview

This chapter provides an overview of the research methodology used in this study. The flow of research methodology was divided into three main sections namely absorbent preparation and characterization, CO₂ solubility measurement, and CO₂ utilization study. All the materials used in this research were listed in this chapter along with their purity and sources. The preparation and characterization of DMAPA neutralized with glycine as an absorbent for CO₂ capture were also described in this chapter. Empirical correlations was used to analyze the relationship between the concentration and temperature of the absorbent with its physical properties. The CO₂ solubility measurement was conducted using solubility cell, such that the CO₂ loading capacity was calculated by using the pressure differential method. Finally, the CO₂ utilization study was performed by using DMAPA neutralized with glycine as an absorbent for CO₂ capture and the product obtained was characterized to identify the nature of the product.

3.2 Research Flow

Figure 3.1 illustrates the research flow for this study. The research activities were performed based on the three main objectives as listed in Section 1.4. The methodologies for each of the objectives are detailed out in Sections 3.4 to 3.6.

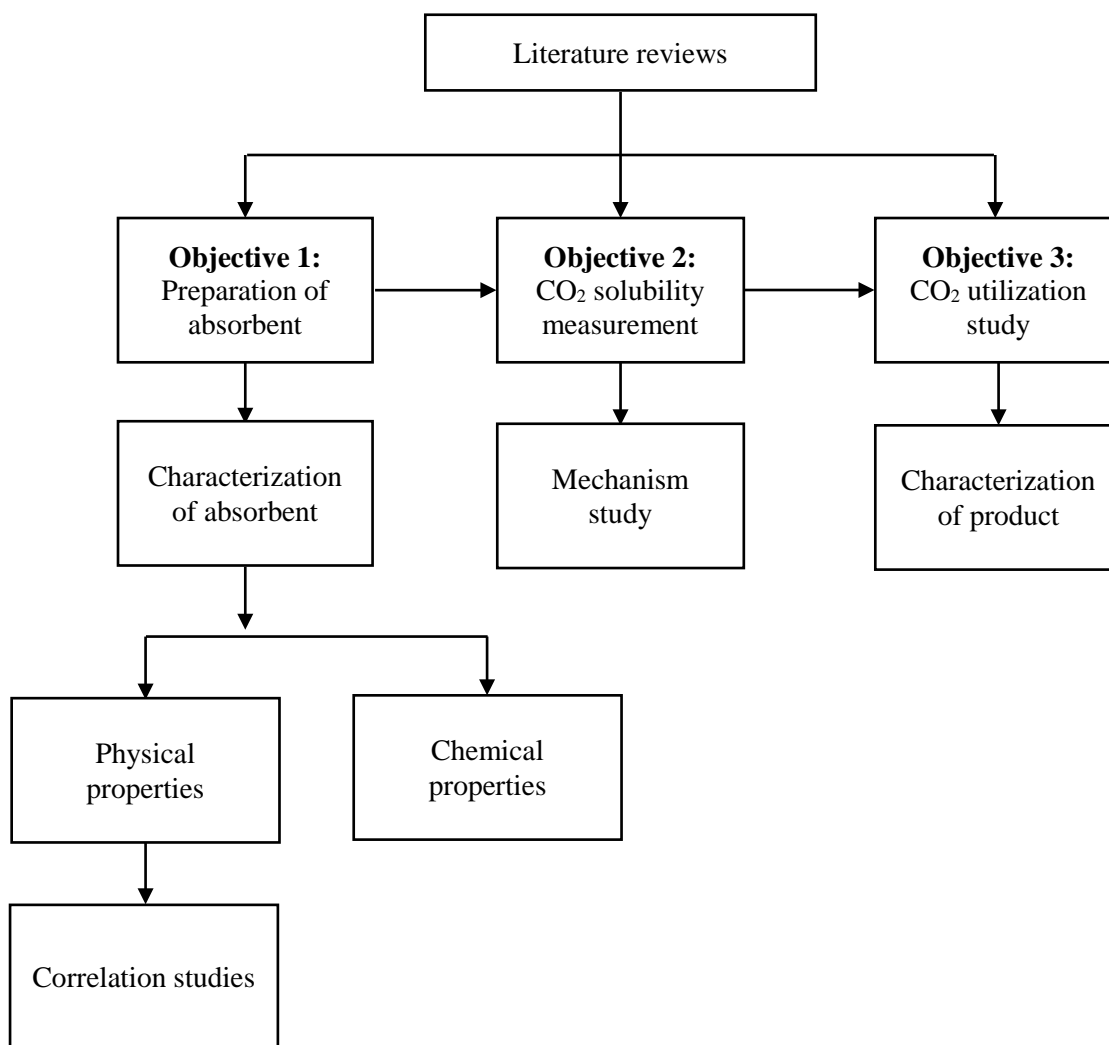


Figure 3.1: Flow of research methodology used in this study.

3.3 Materials and Chemicals

Chemicals used for the preparation of absorbent include monoethanolamine (MEA), glycine (GLY), 3-dimethylaminopropylamine (DMAPA), and potassium hydroxide (KOH). Ethanol was added as a reagent during the CO₂ conversion process. The properties of all the chemicals used in this experiment are presented in Table 3.1. Deionized water was produced through double distillation process (purity $\geq 99.99\%$), while the remaining materials were purchased from respective sources and used without further purification.

Table 3.1: The properties of chemicals used in this experiment.

Chemicals/ materials	Chemical formulas	Molecular weights (g/mol)	Purity (%)	Sources
MEA	NH ₂ CH ₂ CH ₂ OH	61.08	≥ 99.00	Merck
Glycine	H ₂ NCH ₂ COOH	75.06	≥ 99.00	Merck
DMAPA	H ₂ NCH ₂ CH ₂ CH ₂ N(CH ₃) ₂	102.18	≥ 99.00	Sigma Aldrich
KOH	KOH	56.11	≥ 85.00	Merck
Ethanol	C ₂ H ₅ OH	46.07	≥ 99.50	R&M Chemicals
CO ₂ gas	CO ₂	44.01	≥ 99.98	Linde
Nitrogen gas	N ₂	14.00	≥ 99.99	Linde

3.4 Preparation and Characterization of Absorbent

The absorbent used in this thesis was prepared based on Section 3.4.1. The physical properties of the absorbent were measured by using density meter, tensiometer, refractometer, and viscometer. The absorbent was analyzed chemically by using Fourier transform infrared radiation (FTIR) to identify the surface functional groups present in the absorbent.

3.4.1 Preparation of absorbent

The absorbent was prepared through basic neutralization method by mixing equimolar amount of glycine with DMAPA in a 100 mL volumetric flask. The solids were then dissolved in deionized water. The absorbent was prepared for concentrations of 0.1, 0.5, 1.0, 1.5, and 2.0 mol/L (M). The concentration was selected up to 2.0 mol/L since the absorbent is fully saturated and glycine cannot be dissolved in the absorbent beyond 2.0 mol/L. To confirm the reliability of solubility cell in measuring the CO₂ absorption capacity of the absorbent, 5.0 M MEA (equivalent to 30 w/w% MEA) and 1.0 M GLY-KOH (equivalent to 10 w/w% potassium glycinate) were also prepared. Both the concentrations were selected based on data readily available from the literature. Moreover, 5.0 M MEA is usually used in benchmark in many absorption studies [96, 126, 132]. Apart from readily available data, 1.0 M GLY-KOH was also selected as it has higher CO₂ absorption capacity compared to 5.0 M MEA, at lower absorbent concentration. The solutions were then transferred into storage bottles for further characterization, CO₂ solubility and utilization study.

3.4.2 Physical characterization

The physical characterization of the absorbent was studied at temperature ranging from 298.15 to 323.15 K and pressure of 1 atm by using density meter, viscometer, refractometer, and tensiometer. At the start of each measurement, the equipment was washed with acetone to remove any impurities. Each of the equipment was calibrated using deionized water and the results were compared with previous experimental data available from the literature [133]. The average absolute deviation (AAD) was calculated based on Equation (3.1):

$$\% \text{ AAD} = \frac{1}{n} \sum \left| \frac{X_{exp} - Y_{lit}}{Y_{lit}} \right| \times 100 \quad (3.1)$$

where X_{exp} is the experimental data and Y_{lit} is the corresponding value reported by the literature [133]. To ensure consistency of experimental data, the measurements were repeated at least three times (with the exception of surface tension where measurements were repeated five times) and average values were reported in this work.

3.4.2.1 Density

Density of the absorbent was measured using a digital U-tube density meter (Anton Paar, DMA-4500 M) with an accuracy of $\pm 5 \times 10^{-5} \text{ g/cm}^3$. Compressed air was blown into the U-tube pipe to ensure the pipe is dried. Then, approximately 2 mL of the sample was injected into the U-tube pipe and the equipment was set to measure density at desired temperature as mentioned in Section 3.4.2. The uncertainty of temperature measured was reported to be within the range $\pm 0.01 \text{ K}$.

3.4.2.2 Surface tension

Surface tension was measured using an optical contact angle tensiometer (Dataphysics, OCA 15EC). The measurement was conducted based on the pendant drop method. The solution was injected drop wise inside a thermostat chamber by using a syringe attached to a needle (diameter = 0.525 mm). The chamber was connected to a water bath which controlled the temperature of the air inside the chamber to the desired value (with an accuracy of $\pm 0.2 \text{ K}$). A digital camera was used to capture images of the

droplet inside the chamber. The camera was set to record images of 20 frames per second with resolution of 725 x 480 pixels [134]. The equipment was connected to a computer software (SCA 20) which displayed the image of the droplet. Based on the image and density of the solution, the software calculated the surface tension using the Young-Laplace equation.

3.4.2.3 *Refractive index*

Refractive index measures the speed of light travelled in a vacuum compared to the speed of light travelled in a selected medium [135]. The attenuation of light varies according to the amount of molecules in a medium. Hence, refractive index can be used indirectly to determine the concentration of the absorbent. The refractive index of the absorbent was measured using a refractometer (Anton Paar, Abbemat-WR) with an accuracy of $\pm 5 \times 10^{-5}$ nD. The sample was transferred drop wise on to the prism surface using a 1 mL syringe. The uncertainty of temperature of the solution recorded was within the range of ± 0.01 K.

3.4.2.4 *Viscosity*

An electromagnetic viscometer (Cambridge Viscometer, VISCOPro 2000) was used to determine viscosity of the absorbent with an accuracy of $\pm 5 \times 10^{-3}$ mPa.s. A piston was inserted into a measurement cell preloaded with approximately 5 mL of the absorbent. The piston size was selected based on the viscosity range of the solution. In this experiment, the piston selected corresponded to viscosity range of 0.2 to 2 mPa.s. After inserting the piston, the measurement chamber was tilted at an angle of 45°. The equipment was then set to measure viscosity of the absorbent at desired temperatures, with an accuracy of ± 0.01 K.

3.4.2.5 *Correlation studies of physical properties of GLY-DMAPA*

Empirical correlations were used to study the relationships between temperature and concentration of the absorbent with physical properties of the absorbent. Sheikh et al. [136] predicted the correlation of density, refractive index, and

surface tension based on a single parameter. The correlation is a relatively simple equation which correlates the temperature of the absorbent with its physical properties [136]. Nonetheless, the equation did not include the effect of concentration on the physical properties of the absorbent [136]. On the other hand, Graber et al. [137] derived an equation which included temperature and concentration of the solutions to predict selected physical properties of the solution. Graber's equation was then modified [133, 138, 139] to provide a better representation of the physical properties of an aqueous solution as indicated in Equation (3.2).

$$Z=x \times \exp(A_1+ A_2T^{0.5}+A_3x^{0.5})+A_4+A_5T^{0.5}+A_6x^{0.5} \quad (3.2)$$

where Z is density, refractive index, or surface tension of the absorbent, x is the concentration the absorbent, T is the temperature of the solution, and A_1 to A_6 are the fitting parameters which were determined using the least-square method. In this experiment, the parameters were directly obtained through the curve fitting function in MATLAB (version R2015b).

A different correlation (Equation (3.3)) was used to predict viscosity of the absorbent based on different temperature and concentration of the solution as described by Grag et al. [133].

$$\eta = \exp \left[B_0 + \frac{B_1}{T} + \frac{B_2}{T^2} \right] \quad (3.3)$$

where η represents viscosity of the absorbent and B_j are fitting coefficients which are dependent on the concentration of the absorbent (x). The values of B_j were determined based Equation (3.4):

$$B_j = b_{j,0} + b_{j,1}(x) + b_{j,2}(x^2) \quad (3.4)$$

where $b_{j,i}$ are fitting parameters which were obtained by using curve the fitting function in Matlab (version R2015b).

The empirical correlations were validated through statistical analysis by calculating the standard deviations (σ) and least-square regression coefficient (R^2) values for each physical property based on Equations (3.5) and (3.6), respectively.

$$\sigma = \sqrt{\frac{\sum_{i=1}^{i=n} (Z_{exp} - Z_{cor})^2}{n-1}} \quad (3.5)$$

$$R^2 = \frac{\sum_{i=1}^{i=n} (Z_{exp} - \bar{Z}_{cor})^2 - \sum_{i=1}^{i=n} (Z_{exp} - Z_{cor})^2}{\sum_{i=1}^{i=n} (Z_{exp} - \bar{Z}_{cor})^2} \quad (3.6)$$

where, Z_{exp} is the density, refractive index, surface tension, and viscosity measured experimentally, Z_{cor} is the physical properties predicted by the correlation and n is the number of experimental data.

3.4.3 Fourier transform infrared (FTIR) spectroscopy

The surface functional groups present in the absorbent were identified by using Fourier transform infrared (FTIR) spectrometer (PerkinElmer) based on the attenuated total reflectance (ATR) method. A drop of the sample was loaded onto a glass plate and light was transmitted directly on the sample. The transmittances of each absorbent were recorded at wavenumber ranging between 4000 cm^{-1} to 400 cm^{-1} .

3.5 CO₂ Solubility Measurement

The CO₂ solubility study was performed by reacting CO₂ with the prepared absorbent in a solubility cell (DIXSON, SN-0115). The process flow diagram of the equipment is as shown in Figure 3.2. At the beginning of each experiment, the premixed tank and the solubility cells (cell 1 to 3) were purged with N₂ to remove traces of contaminants. The solubility cells were subsequently vacuumed. Pressurized CO₂ gas was then introduced into the 5000 mL premixed tank, while 5 mL absorbent was injected into the 50 mL solubility cell. An automated chiller (JUBALO) and solenoid valves (SMC, VXZ2230) were used to maintain a constant temperature in the premixed tank and solubility cells. The temperature and pressure inside the equilibrium cell were measured using a digital thermometer (YOKOGAWA-7653 with an accuracy of $\pm 0.2 \text{ K}$) and pressure indicator (Druck DPI 150 with an accuracy of $\pm 0.01 \text{ bar}$), respectively. The sample was injected into each cell and stirred at 300 rotations per minute (rpm). Then the pressurized CO₂ was transferred from the premixed tank into

the solubility cell and the temperature and pressure were monitored by using the Sim-coder Basic Software. The CO₂ absorption was assumed to reach equilibrium state when the total pressure in the equilibrium cell remained constant for more than 4 hours.

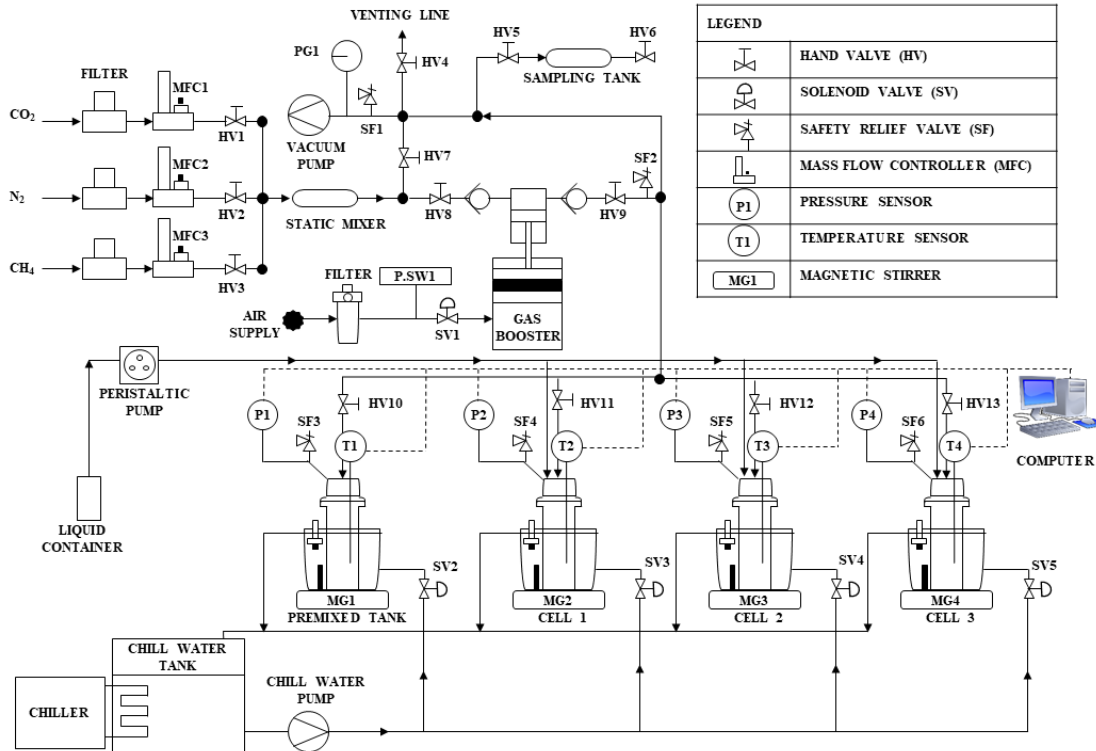


Figure 3.2: Process flow diagram of solubility cell.

The amount of CO₂ gas transferred from the premixed tank into the solubility cell (n_{CO_2}) was calculated based on the pressure change in the premixed tank, temperature, and size of the tank as per Equation (3.7):

$$n_{CO_2} = \frac{V_{pt}}{RT_{pt}} \left(\frac{P_i}{z_i} - \frac{P_f}{z_f} \right) \quad (3.7)$$

where V_{pt} is the volume of the premixed tank, R is the gas constant, T_{pt} is the temperature in the premixed tank, P_i and P_f are the pressure in the premixed tank at the initial and final stages, respectively, and z is the compressibility factor at respective pressure. The compressibility factor was calculated using the Peng Robinson Equation of State (sample calculation can be found in Appendix B). Once equilibrium was achieved in the cell, the equilibrium pressure was determined using Equation (3.8).

$$P_{co_2} = P_T - P_v \quad (3.8)$$

where P_{co_2} is the equilibrium pressure, P_T is the total pressure in the solubility cell, and P_v is the vapor pressure of the solution recorded prior to CO₂ being pumped into the cell. In this experiment, P_v was assumed to be negligible. The amount of CO₂ in the gas phase ($n_{co_2(g)}$), was calculated based on Equation (3.9):

$$n_{co_2(g)} = \frac{V_g P_{co_2}}{Z_{CO_2} RT} \quad (3.9)$$

where V_g is the volume in the gas phase and T is temperature in the solubility cell. The number of moles of CO₂ absorbed by the liquid ($n_{co_2(l)}$) was determined by using Equation (3.10):

$$n_{co_2(l)} = n_{co_2} - n_{co_2(g)} \quad (3.10)$$

The CO₂ loading capacity (α) measured in mol CO₂/ mol of absorbent was then calculated based on Equation (3.11):

$$\alpha = \frac{n_{co_2(l)}}{n_{liquid}} \quad (3.11)$$

where n_{liquid} is the number of moles of the absorbent.

The experimental conditions during the CO₂ absorption process are listed in Table 3.2. Experiments A1 and A2 were performed to determine the reliability of the solubility cell in generating results for the CO₂ solubility study based on the data readily available from the literature at selected pressure range. 5.0 M MEA (equivalent to 30 w/w% MEA) was selected for comparison since it widely used as a benchmark in numerous CO₂ absorption studies [106, 126, 132, 140]. Moreover, 1.0 M GLY-KOH has higher CO₂ loading capacity compared to 5.0 M MEA, even with lower solute concentration. For experiment A3, the concentration of absorbent was fixed at 1.0 M of the absorbent as a basis to study the effect of temperature in the equilibrium cell on the CO₂ solubility of the absorbent, by varying the temperature in the equilibrium cell from 303.15 to 323.15 K. Meanwhile, experiment A4 was conducted to study the effect of concentration on the CO₂ solubility of the absorbent. In all the experiments, the pressure was varied from 5 to 25 bar to investigate the relationship between pressure and CO₂ loading capacity of the absorbent.

Table 3.2: Experimental conditions for CO₂ capture process.

No.	Absorbent	Concentration of absorbent (mol/L)	Pressure (bar)	Temperature (K)
A1	MEA	5.0	5	313
A2	GLY-KOH	1.0	5	313
A3	GLY-DMAPA	1.0	5	303, 313, 303
A4	GLY-DMAPA	0.1	5-25	303
A5	GLY-DMAPA	0.5	5-25	303
A6	GLY-DMAPA	1.0	5-25	303
A7	GLY-DMAPA	1.5	5-25	303
A8	GLY-DMAPA	2.0	5-25	303

3.6 CO₂ Utilization and Characterization Study

The utilization study was carried after the CO₂ absorption process, by adding ethanol into the CO₂-saturated absorbent. The solids were then characterized by using FTIR and X-ray photoelectron spectroscopy (XPS).

3.6.1 CO₂ utilization study

CO₂ utilization was carried out by using the two-step method of CO₂ capture and subsequent utilization (Figure 3.3). Similar method was described by Yang et al. [91] such that CO₂ was captured by using an absorbent (superbase mixed with polyethylene glycol) to activate the CO₂ molecules. Once the absorption process was completed, fresh amine solution was added to produce urea. In this experiment, DMAPA neutralized with glycine was used as an absorbent during CO₂ capture while organic medium (ethanol) was added after the CO₂ capture process. CO₂-saturated solution was obtained from the solubility study experiment in Section 3.5, followed by addition of 1mol of ethanol into the solution. The mixture was left idle for three hours to allow the formation of solids. Next, the sample was filtered in order to recover the solids formed during CO₂ conversion. The product is then oven-dried at 343.15 K for approximately 6 hours. The solid particles were collected, weighted, and analyzed by using FTIR and XPS.

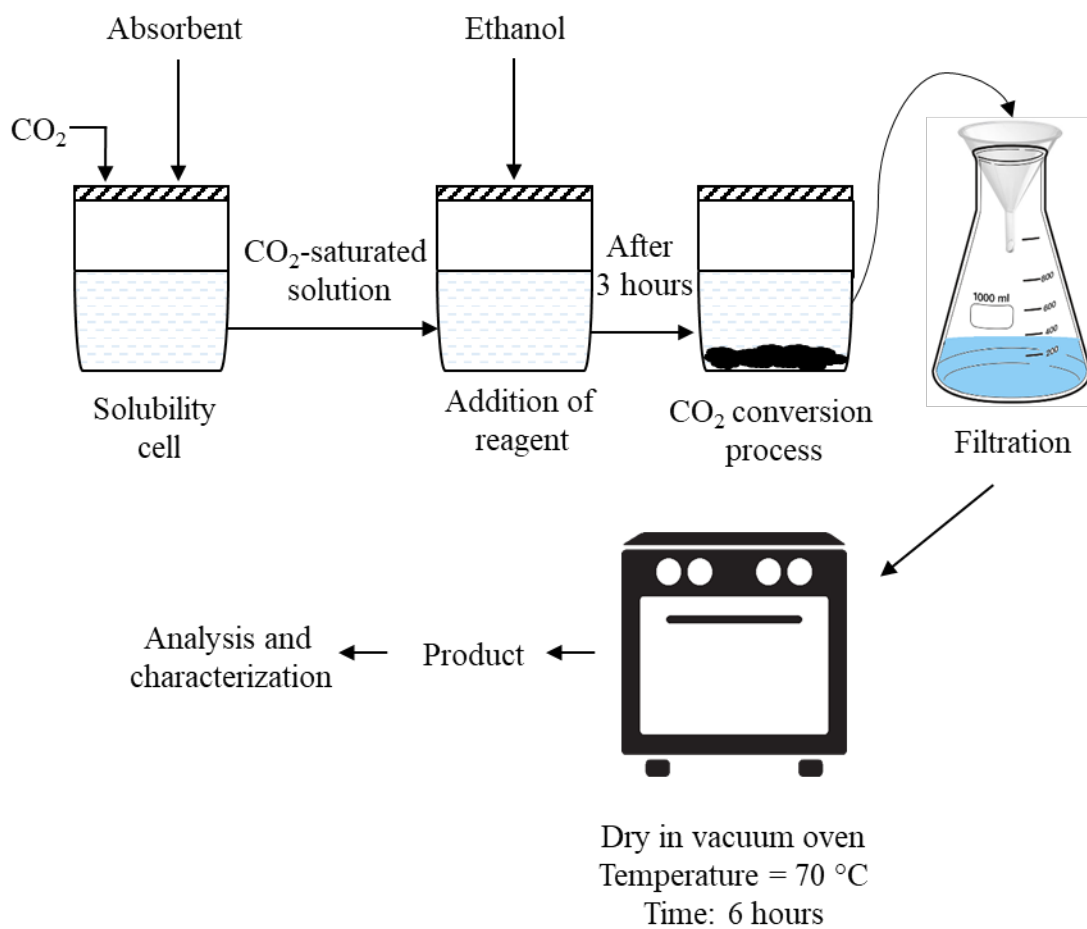


Figure 3.3: Two-step method for CO₂ capture and utilization study.

3.6.2 Characterization of solid particles

The solids product obtained were characterized by using two methods namely the FTIR spectroscopy and the X-ray photoelectron spectroscopy as described in the following subsections.

3.6.2.1 Surface functional group analysis

The nature of the product was identified by observing the surface functional groups present in the solids by using FTIR spectroscopy. The methodology for FTIR analysis is similar to the method previously outlined in Section 3.4.3.

3.6.2.2 *Surface chemical binding*

X-ray photoelectron spectroscopy (XPS) was used to determine the surface chemical binding of the final product. The XPS spectra were recorded by using Thermo Scientific, K-alpha. The overall scan was performed based on pass energy of 200 eV for binding energy ranging from 0 to 1400 eV. The pass energy was then reduced to 50 eV to obtain a high resolution for each surface element present in the solids. The surface element detected by the XPS include carbon (280 - 294 eV), nitrogen (392 - 410 eV), and oxygen (525 - 545 eV).

3.7 **Summary**

The absorbent was prepared by using the basic neutralization method with concentrations ranging from 0.1, 0.5, 1.0, 1.5, and 2.0 mol/L (M). The absorbent was characterized physically by using density meter, refractometer, tensiometer, and viscometer. The surface functional groups found in the absorbent were analyzed by using the FTIR. 5.0 MEA and 1.0 M glycine neutralized with inorganic base (GLY-KOH) was selected to calibrate the CO₂ solubility cell based on publish data readily available from the literature. The CO₂ solubility study was performed by bubbling CO₂ into the absorbent in a solubility cell and the absorption capacity was measured based on pressure differential in the cell. The CO₂ utilization study was performed by adding 1 mol of ethanol into the CO₂ saturated absorbent. The solids obtained were characterized by using FTIR and XPS.

CHAPTER 4

RESULTS AND DISCUSSION

4.1 Overview

Experimental results were collected based on three main objectives as identified in Section 1.3 and the outcomes of the study were discussed in this chapter. The results for physical properties were reported in this chapter, accompanied by correlation studies which indicated the effects of temperature and concentration of the absorbent on its density, refractive index, surface tension, and viscosity. The absorbent obtained through neutralization of DMAPA with glycine were identified based on the surface functional group found in the absorbent. The performance of the absorbent as a potential absorbent for CO₂ capture was also discussed in this chapter. The CO₂ loading capacity of absorbent was compared with other absorbents such as monoethanolamine (MEA) and glycine neutralized with potassium hydroxide (GLY-KOH). In the last section of this chapter, the results obtained for CO₂ utilization study were highlighted. The CO₂ utilization product was analyzed using FTIR and XPS which suggest the formation of carbamate compound during the utilization process.

4.2 Characterization of Absorbent

The absorbent was characterized by physically by measuring the density, viscosity, surface tension, and refractive index as reported in Section 4.2.1, followed by correlation study based on the physical properties of the absorbent (Section 4.2.2). The absorbent was also analyzed chemically by using FTIR spectroscopy to identify the surface functional groups found in the absorbent.

4.2.1 Physical properties of the absorbent

The instruments used to measure the physical properties of the absorbent were calibrated by using deionized water. The results obtained were compared with previous literatures as shown in Appendix A. The densities, refractive indices, surface tensions, and viscosities of 0.1 M, 1.0 M, and 2.0 M of the absorbent, were measured from 298.15 to 323.15 K. The relationships between temperature and concentration of the absorbent with its physical properties are presented graphically as shown in Figures 4.1 to 4.4, in which the solid lines represent the empirical correlations as outlined in Section 3.4.2.5.

Based on Figures 4.1 to 4.4, the physical properties of the absorbent showed a decreasing trend as temperature of the absorbent increased. When the absorbent was heated, the kinetic energy within the molecules increased. As the molecules vibrated and moved further apart, density of the solution decreased. The increase in void spaces between the molecules as temperature increased reduced the interactions between light and absorbent molecules, thus the solution recorded a lower refractive index. Moreover, the increased in kinetic energy of the absorbent molecules resulted in weakening of hydrogen bonding, and thus causing more molecules to accumulate near the surface of the liquid which lead to lower surface tension of the solution [133, 141]. The viscosity of absorbent also decreased as the temperature increased, since the molecules are able to move freely against an opposing motion due to lack of interaction between molecules within the absorbent. The relationship between temperature and physical properties of absorbent was commonly observed in aqueous solution, namely amino acid salt solutions [133, 142], amine amino acid salt solution [143], and DMAPA solution [141], such that density, refractive index, surface tension, and viscosity decreased as temperature of the absorbent increased.

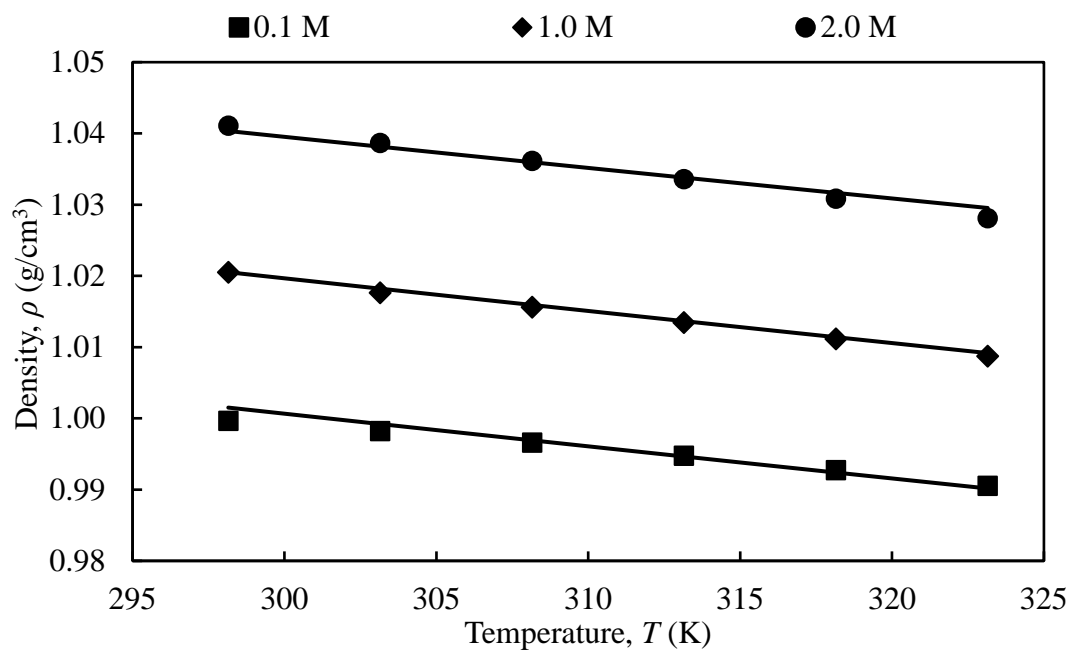


Figure 4.1: Densities of the absorbent at different temperatures.

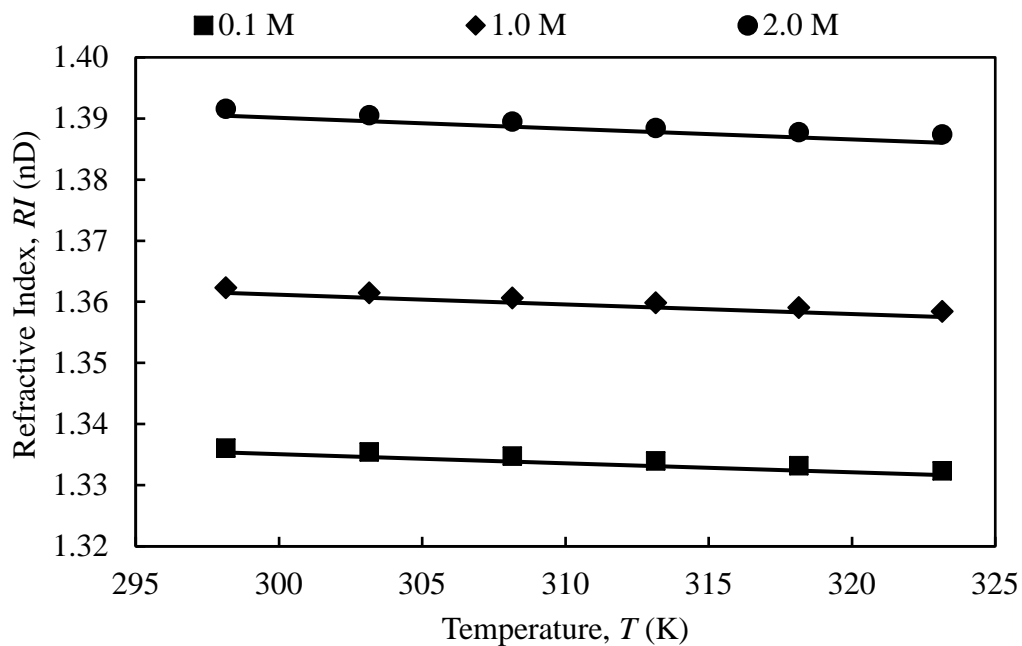


Figure 4.2: Refractive indices of the absorbent at different temperatures.

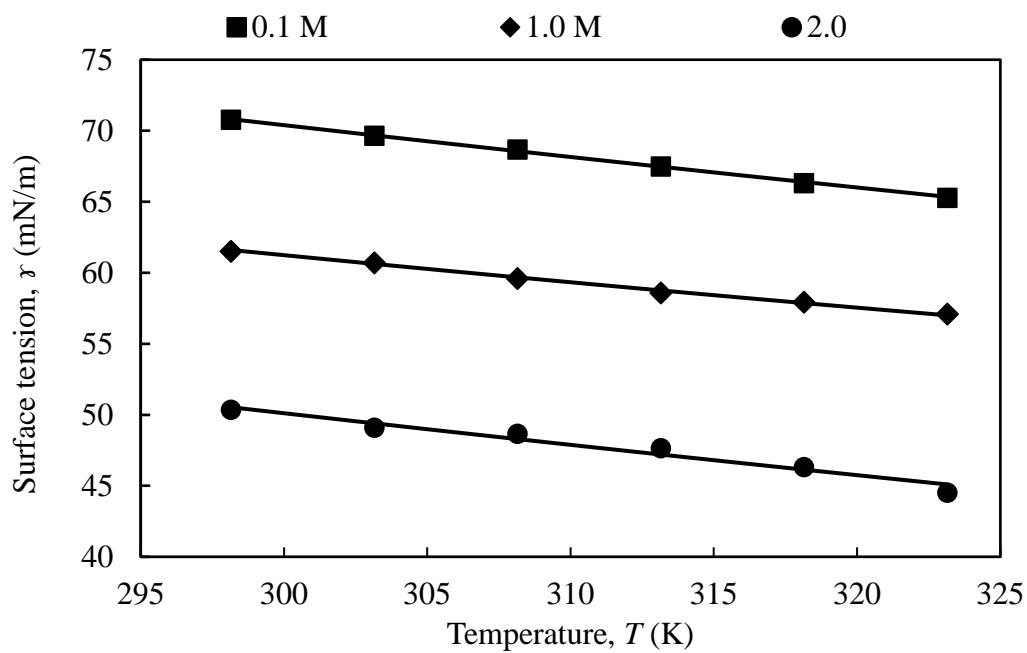


Figure 4.3: Surface tensions of absorbent at different temperatures.

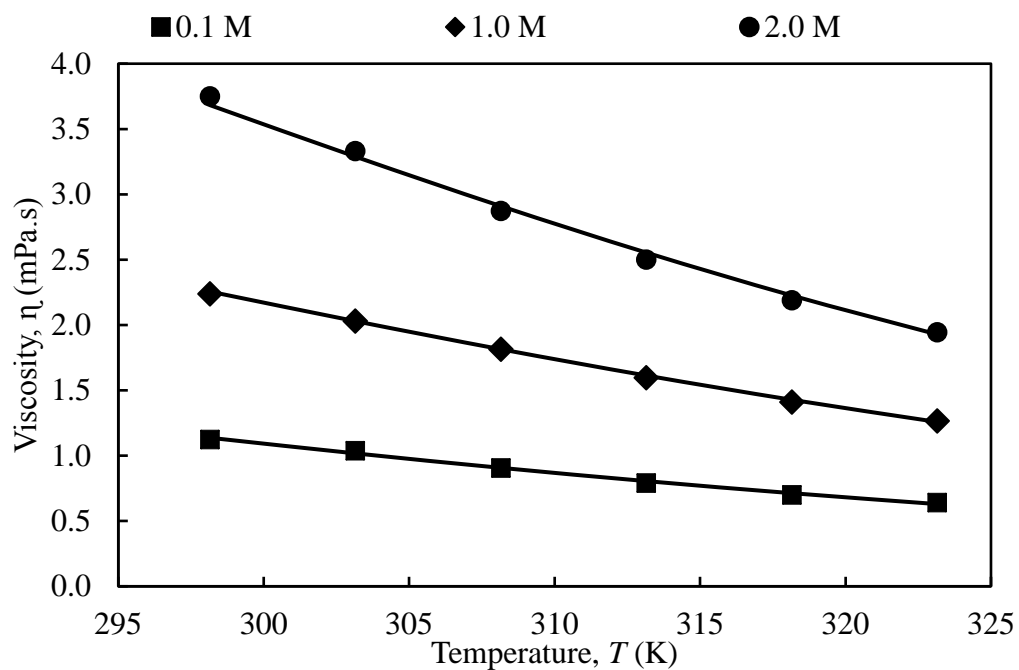


Figure 4.4: Viscosities of absorbent at different temperatures.

Figures 4.1 to 4.4 also indicated that the density, refractive index, and viscosity of the absorbent increased as the concentration of the absorbent increased. At a constant temperature, the effect of concentration of the absorbent on density and viscosity were consistent with the results reported by Aronu et al. [143] for aqueous amine amino acid salt solution. On top of that, the refractive index followed a similar trend to aqueous amino acid salt solution [133, 142]. The increased in number of molecules within the solution contributed to higher density. In addition, the presence of more absorbent molecules which interacted with light passing through the solution which caused the refractive index to increased. The large number of molecules also restricted the motion of molecules within the absorbent, resulting in higher viscosity of the absorbent. On the other hand, the surface tension exhibited an opposite trend such that, the surface tension decreased as the concentration of the absorbent increased. According to a study conducted by Blanco et al. [141], aqueous DMAPA also reported similar behavior such that DMAPA molecules accumulated at the surface of the gas-liquid interface as the concentration of the absorbent increased, thus reducing the surface tension of the absorbent [141]. This could be due to lack of hydrogen bonding effects within the solution, which could be due to packing effect [141].

4.2.2. Correlation studies for physical properties of the absorbent

Data obtained from the physical studies were represented by using empirical correlations based on temperature and concentration of the absorbent. The density, refractive index, and surface tension of the absorbent were fitted based on Equation (3.2). Meanwhile, the viscosity of the absorbent was predicted based on Equations (3.3) and (3.4). Studies reported by previous authors [133, 138, 139] suggested that the empirical correlations provided good representations of the physical properties of an aqueous system. The empirical coefficients, A_1 to A_6 (Equation (3.2)) for the selected physical properties of absorbent are tabulated in Table 4.1. The empirical correlation parameters for viscosity of the absorbent were given in Table 4.2.

Table 4.1: A_i values based on Equation (3.2) for density, refractive index, and surface tension of the absorbent.

i	A_i		
	Density, ρ (g/cm ³)	Refractive index, RI (nD)	Surface tension, γ (mN/m)
1	-72.860	-4.708	2.834
2	0.090	-0.035	0.059
3	46.540	0.790	-0.869
4	1.269	1.417	233.600
5	-0.016	-0.005	-9.366
6	0.028	0.023	-34.590

Table 4.2: Fitting parameters based on Equations (3.3) and (3.4) to predict viscosity of the absorbent.

j	Parameters		
	$b_{j,0}$	$b_{j,1}$	$b_{j,2}$
1	-21.27	-1.15	-1.56
2	10750.00	1494.00	722.40
3	-1.31 x 10 ⁶	-2.61 x 10 ⁵	-8.96 x 10 ⁴

The standard deviations (σ) and regression coefficient (R^2) values for the physical properties of the absorbent solutions were presented in Table 4.3. The small standard deviations recorded indicated that the experimental data were in good agreement with the correlations. Moreover, the regression coefficient (R^2) values were close to 1, which also suggested that the experimental data fitted well within the empirical correlations.

Table 4.3: Standard deviations (σ) and regression coefficients (R^2) of the physical properties of the absorbent.

Physical properties	Regression coefficients (R^2)	Standard deviations (σ)
Density, ρ (g/cm ³)	0.9984	8.66 x 10 ⁻⁴
Refractive Index, RI (nD)	0.9999	9.27 x 10 ⁻⁴
Surface tension, γ (mN/m)	0.9960	0.39
Viscosity, η (mPa.s)	0.9993	0.03

The data obtained can be further analyzed by comparing the experimental data with the results predicted by the empirical correlations as illustrated in Figures 4.5 to 4.8. The plots indicated that the deviations between experimental and predicted values were very small which confirmed that the data were well represented by the empirical correlations for density, surface tension, refractive index, and viscosity.

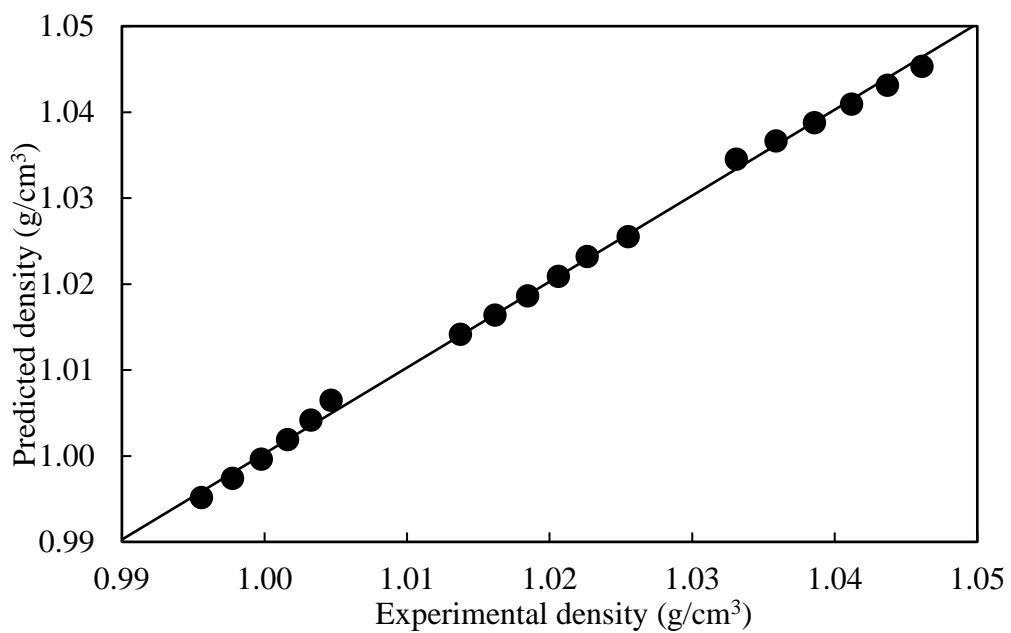


Figure 4.5: Comparison between experimental and predicted density of the absorbent.

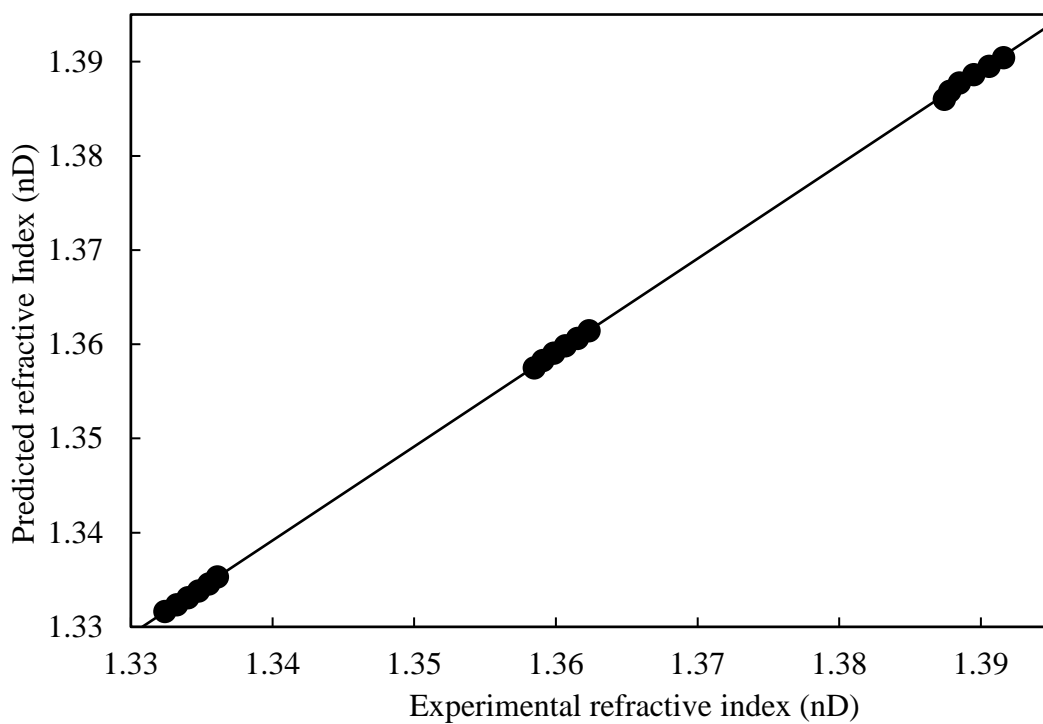


Figure 4.6: Comparison between experimental and predicted refractive index (RI) of the absorbent.

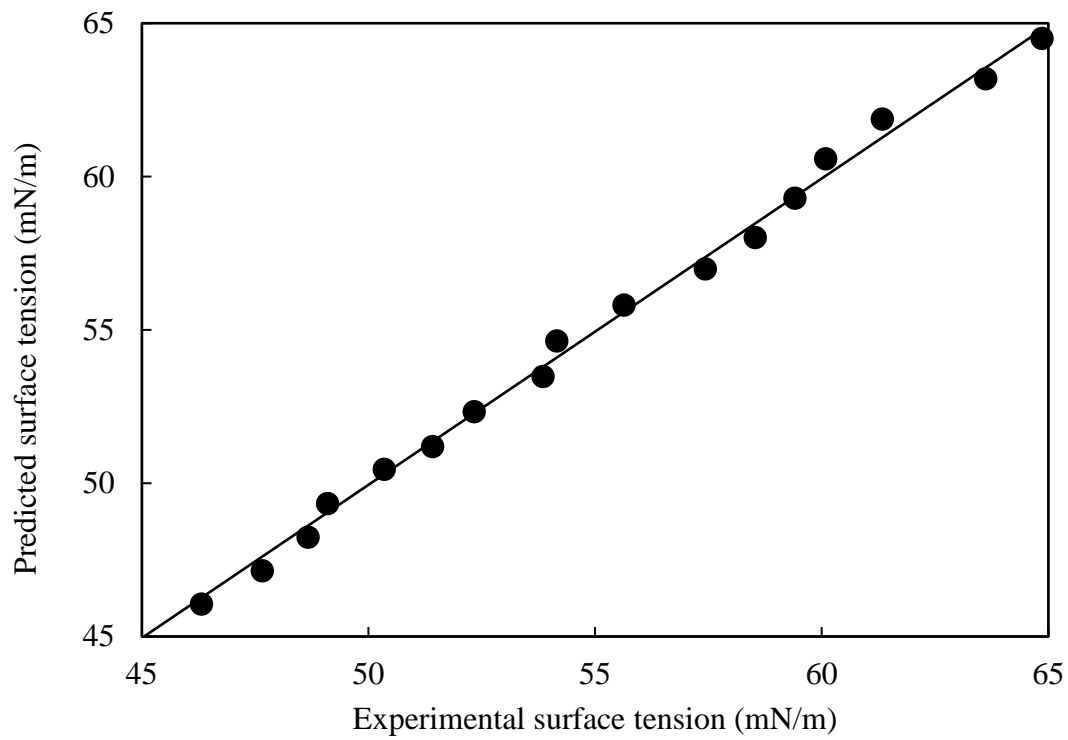


Figure 4.7: Comparison between experimental and predicted surface tension of the absorbent.

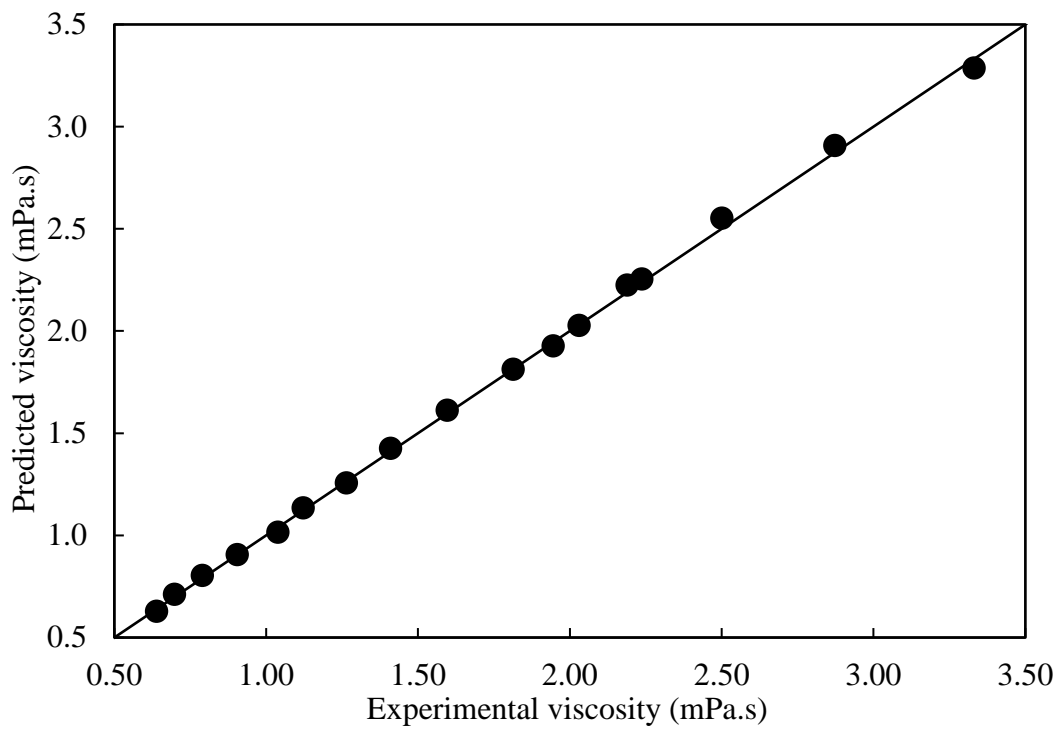


Figure 4.8: Comparison between experimental and predicted viscosity of the absorbent.

4.2.3 Surface functional groups of the absorbent

The possible interaction between GLY and DMAPA molecules is given in Figure 4.9. The proposed structure was based on the reaction between -OH functional group from glycine molecule with primary amine of the DMAPA molecule. Several studies [144, 145] also suggested similar behavior such that the reaction between carboxylic acid and secondary amine was more dominant compared to tertiary amine, since the former is more nucleophilic compared to the latter. Moreover, the hindrance effect of the two methyl groups attached to nitrogen atom may prevented the reaction between the tertiary amine of DMAPA molecules with larger molecules.

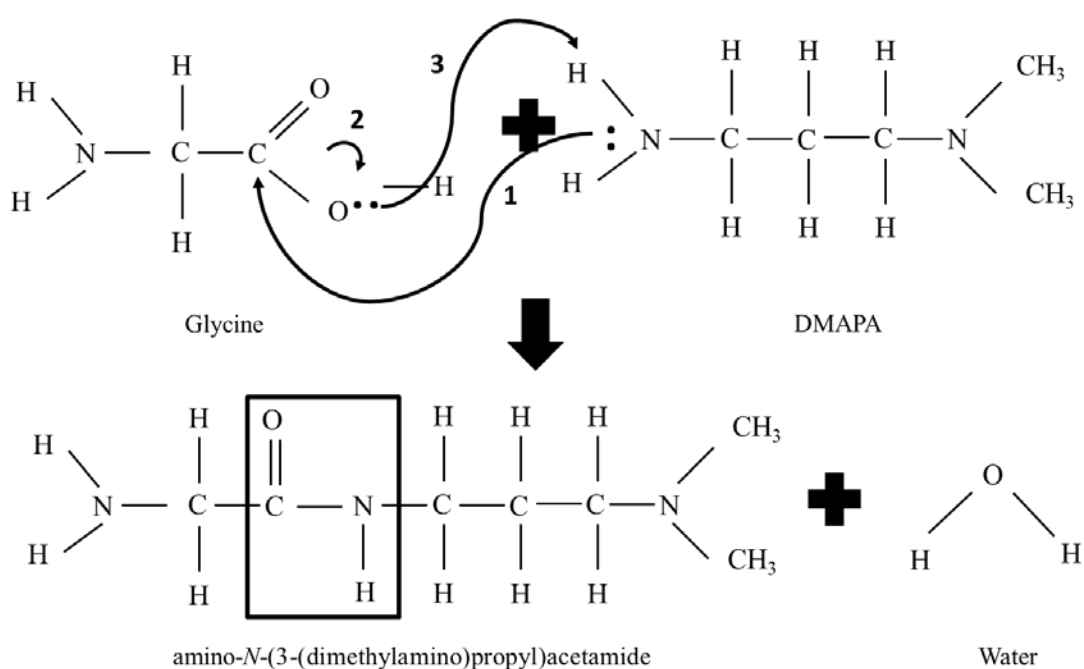


Figure 4.9: The proposed interaction between glycine (GLY) and DMAPA molecules.

The FTIR spectra of GLY, DMAPA, and the absorbent are presented as shown in Figure 4.10. The disintegration of some characteristic peaks followed by formation of new peaks in the FTIR spectra suggested possible chemical interactions between GLY and DMAPA molecules. The surface functional groups present in the aqueous glycine, aqueous DMAPA, and the absorbent were identified based on the respective wavenumbers as indicated in Table 4.4.

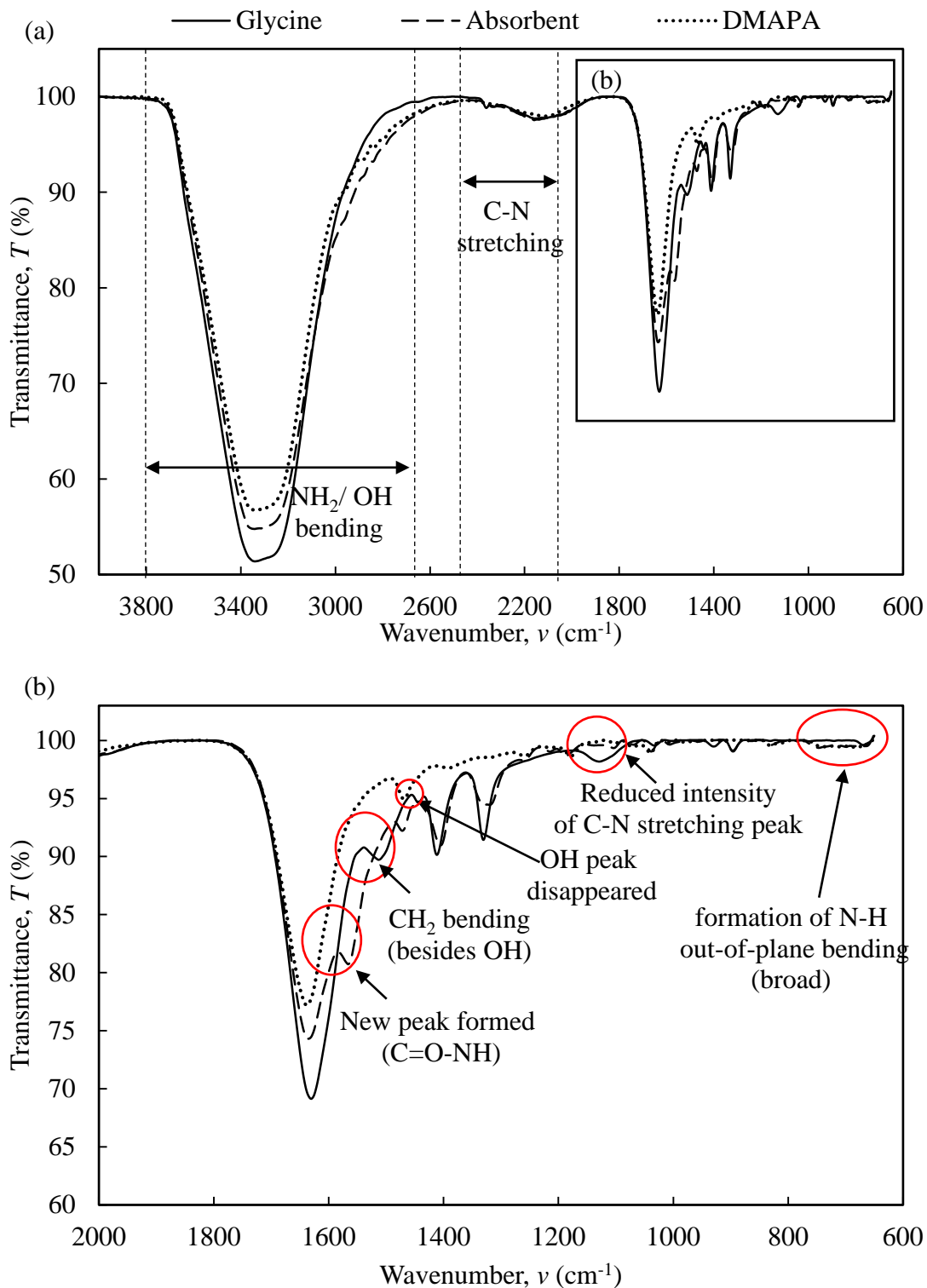


Figure 4.10: The FTIR spectra of (a) aqueous glycine (GLY), DMAPA, and the absorbent, amino-N-(3-(dimethylamino)propyl)acetamide and (b) close-up spectra between 2000 to 600 cm^{-1} .

Table 4.4: Surface functional groups and vibration modes for each peak detected in the FTIR spectra of aqueous GLY, DMAPA, and the absorbent.

Wavenumbers, ν (cm^{-1})			Surface functional groups	Vibration modes
GLY	DMAPA	Absorbent		
3270	3270	3314	NH ₂ /OH	Stretching
2100	2100	2100	C-N	Stretching
1631	1635	1618	NH ₂	Scissors
1631	-	1618	C=O	Asymmetric stretching
-	-	1565	N-H	In-plane bending
1527	-	-	CH ₂ (besides OH)	In-plane bending
-	1469	1473	C-CH ₂	Scissors
1433	-	-	OH	In-plane bending
1410	-	1400	C=O	Symmetric stretching
-	1386	-	C-N	Stretching
1329	-	1317	C-O	Stretching
1123	1105	1105	C-N-C	Stretching
-	750-860	600-750	N-H	Out-of-plane bending
669	-	-	O-H	Out-of-plane bending

The chemical interactions between GLY and DMAPA were suggested based on the changes in several characteristic peaks at wavenumbers ranging from 1800 to 1000 cm^{-1} . The formation of a new peak at wavenumber 1565 cm^{-1} was detected in the absorbent corresponded to the N-H in-plane bending from a secondary amide functional group [146]. This indicated the formation of an amide linkage (-H-N-C=O), when GLY reacted with DMAPA. The formation of amide linkage was supported by the change in the wavelength range for N-H out of plane bending peak from 750 - 860 cm^{-1} (primary amine from DMAPA molecules) to 600 - 750 cm^{-1} (secondary amide) [146]. The peak observed in GLY spectrum at wavenumber 1527 cm^{-1} represented CH₂ bending besides an OH functional group [147]. The disintegration of the peak 1527 cm^{-1} indicated possible reaction between the OH functional group with the amino functional group from DMAPA molecules. This was supported by the disappearance of OH functional group in GLY molecules detected at wavenumber 1433 cm^{-1} . Another change in characteristic peak was observed at 1386 cm^{-1} whereby the intensity of the C-N

stretching peak found in the DMAPA molecules were reduced, which could be due to change in the C-N environment of the DMAPA molecules, when the N-H besides the C-N functional group reacted with GLY molecules. The FTIR spectra also suggested the reaction between -OH (from glycine) and N-(CH₃)₂ from DMAPA molecule was insignificant as no peak was observed at approximately 1505 cm⁻¹. According to Smith [146], a medium intensity peak at 1505 cm⁻¹ was usually detected in tertiary amide due to C-N-(CH₃)₂ stretching. This showed lack of interaction between -OH and N-(CH₃)₂ from glycine and DMAPA, which could be due to high reactivity of secondary amino group compared to primary amino group [144, 145]. In general, the reaction between GLY and DMAPA leads to the formation of amino-N-(3-(dimethylamino)propyl)acetamide as shown in Figure 4.9.

4.3 CO₂ Solubility Study

The CO₂ solubility study is divided into three sections which covers the experimental data for CO₂ solubility study, comparison of the CO₂ solubilities with other absorbents, and also the possible interactions between CO₂ and the amino-N-(3-(dimethylamino)propyl)acetamide absorbent.

4.3.1 Experimental data for CO₂ solubility study

The reliability of the high pressure solubility cell in generating experimental results for the CO₂ solubility study was evaluated as per Appendix C, by comparing the experimental results of CO₂ solubility of 5.0 M MEA and 1.0 M GLY-KOH with previous data available from the literatures [105, 132, 148]. The small standard deviations recorded indicated high consistency of the CO₂ loading capacity results obtained by using the solubility cell.

Figure 4.11 indicate the CO₂ loading capacity (α) of 1.0 M amino-N-(3-(dimethylamino)propyl)acetamide measured at different temperatures. It was found that increasing the temperature of the absorbent from 303.15 K to 323.15 K resulted in decreased in CO₂ loading capacity of the absorbent. This trend was observed mainly because CO₂ absorption is an exothermic process which released heat when CO₂ interacted with the absorbent molecules and hence dissolved in the absorbent. When

external heat is added into the system, it will cause the equilibrium reaction to be reversible, thus reducing the CO₂ solubility in the absorbent [96]. In addition, the influence of pressure on the CO₂ loading capacity can also be seen from Figure 4.11, such that the latter increased as the former increased. The trend observed is based on the increase in the amount of CO₂ in the gas phase as the pressure increased. Thus, more CO₂ molecules are able to react with the absorbent. The behaviors were commonly observed for other absorbents such as MEA [105, 132, 148] and GLY-KOH [126].

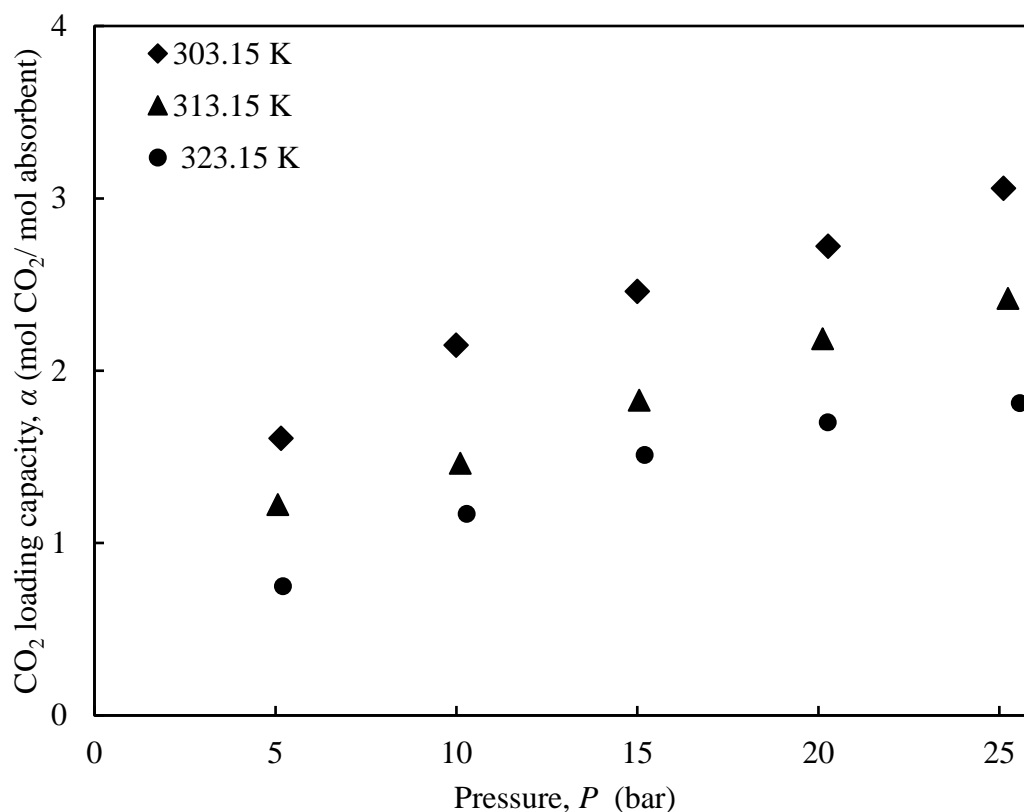


Figure 4.11: CO₂ loading capacities of 1.0 M amino-*N*-(3-(dimethylamino)propyl)acetamide at different temperatures.

Based on the high CO₂ loading capacity obtained at the temperature of 303.15 K, the effect of concentrations of absorbent on CO₂ solubility was studied at this temperature by varying the concentrations of the absorbent from 0.1 M to 2.0 M. The CO₂ loading capacity of the amino-*N*-(3-(dimethylamino)propyl)acetamide absorbent measured at different pressure are presented in Figure 4.12. It was observed that, the CO₂ solubility decreased as the concentration of the absorbent increased. This was in line with the presence of additional molecules within the absorbent as the concentration increased which increases the viscosity of the absorbent, causing limited

the diffusion of CO₂ molecules into the solution. The influence of concentration of the absorbent on the CO₂ loading capacity were consistent with the findings reported by other authors [126, 132, 148].

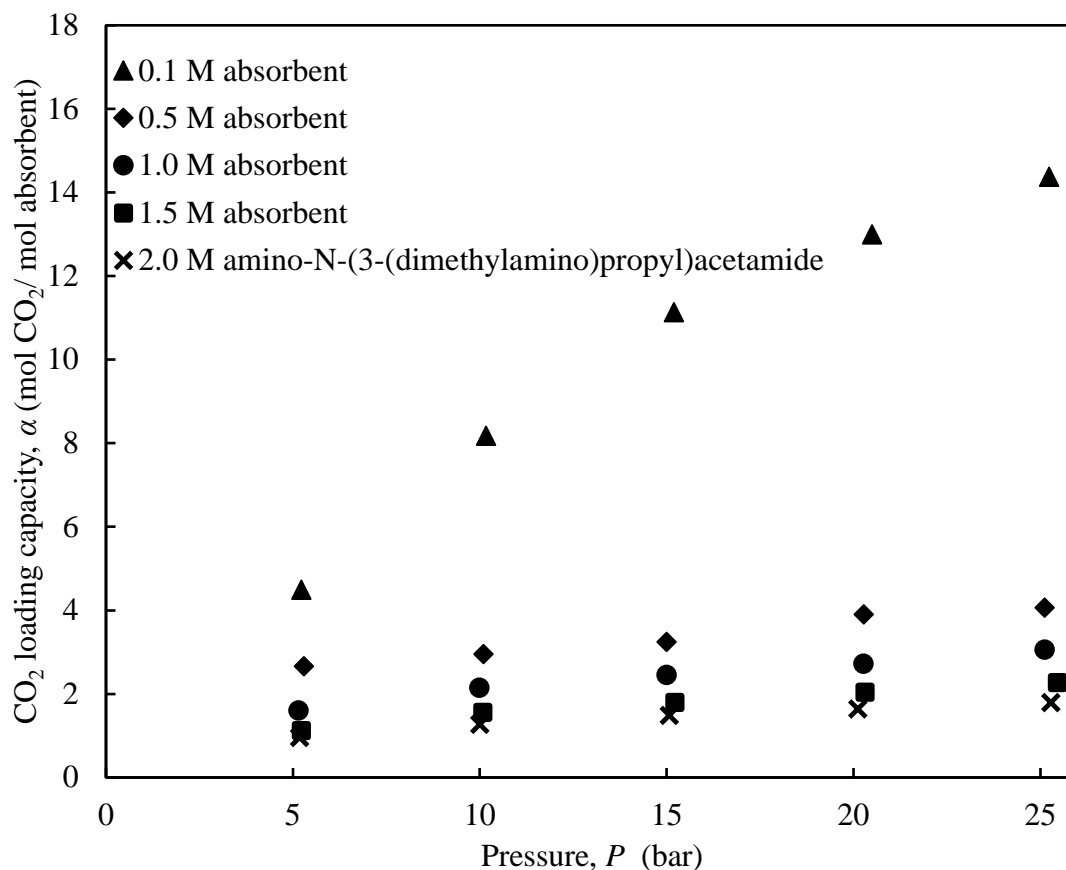


Figure 4.12: CO₂ loading capacity of different concentrations of the absorbent (Temperature: 303.15 K).

Despite the fact that 0.1 M amino-N-(3-(dimethylamino)propyl)acetamide exhibited the highest CO₂ loading capacity, theoretically the net CO₂ absorbed by the solution was the lowest due to low amount of molecules present in the solution which participated in the CO₂ absorption process. This is can be seen from Figure 4.13 (Detailed calculations on the total mole of CO₂ absorbed by the absorbent can be found in Appendix E), such that the net CO₂ absorbed by amino-N-(3-(dimethylamino)propyl)acetamide solution showed an opposite trend compared to the CO₂ loading capacity of the absorbent. The same observation was reported by Harris et al. [148] for 0.1 M sodium glycinate. The authors indicated that the total amount of CO₂ absorbed by the solution at fixed volume increased when concentration increased [148].

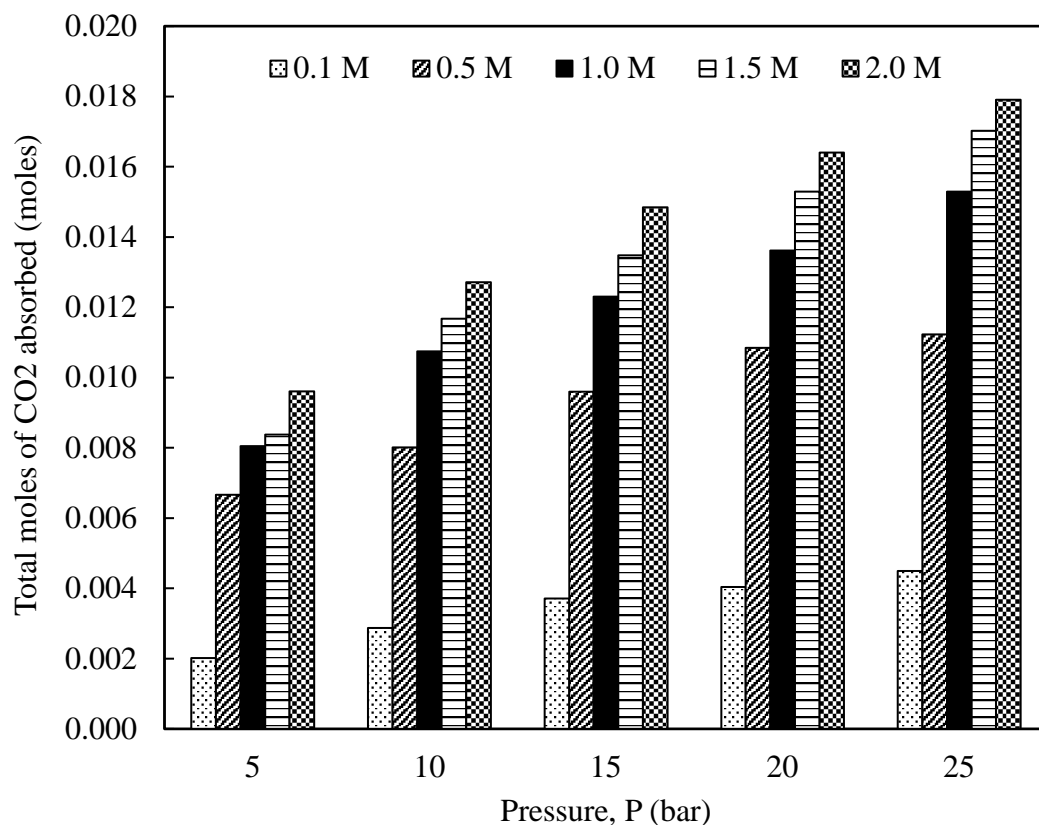


Figure 4.13: Net CO₂ absorbed by the absorbent (Temperature: 303.15 K).

4.3.2 Comparison of CO₂ solubilities of the absorbent with other absorbents

The CO₂ loading capacity of the absorbent was compared with 30 w/w % MEA (5.0 M MEA), which is the conventional absorbent used as bench mark in various CO₂ absorption studies [19, 126, 132]. Based on Figure 4.14, it was deduced that the CO₂ solubility of amino-N-(3-(dimethylamino)propyl)acetamide is generally higher than then conventional MEA absorbent. It is also observed that smaller concentration of amino-N-(3-(dimethylamino)propyl)acetamide contributed to higher CO₂ loading capacity compared to 5.0 M MEA. This results suggested amino-N-(3-(dimethylamino)propyl)acetamide can be used as a potential absorbent for CO₂ capture since smaller amount of absorbent is required to achieve high absorption capacity.

Amino acid neutralized with inorganic base (GLY-KOH) was reported as a potential absorbent for CO₂ capture [122, 126]. Since the absorbent amino-N-(3-(dimethylamino)propyl)acetamide which was made up of amino acid (GLY) neutralized with organic base (DMAPA), the results obtained in this work was

compared with GLY-KOH [126] to study the performance of the absorbent in comparison to amino acid neutralized with inorganic base. Figure 4.15 indicated that amine neutralized with organic base has higher CO₂ loading capacity compared to amino acid neutralized with inorganic base. The neutralization of amino acid with organic base resulted in the formation of amide linkage which provides additional sites for CO₂ attachments along with amino group from the amino group from the glycine molecules as shown in Figure 4.9. In comparison, amino acid neutralized with inorganic base only has one active site available from amino group of the glycine molecules. This result is in agreement with the work reported by Aronu et al. [22], such that amine amino acid salt absorbed larger amount of CO₂ in contrast to its KOH counter parts.

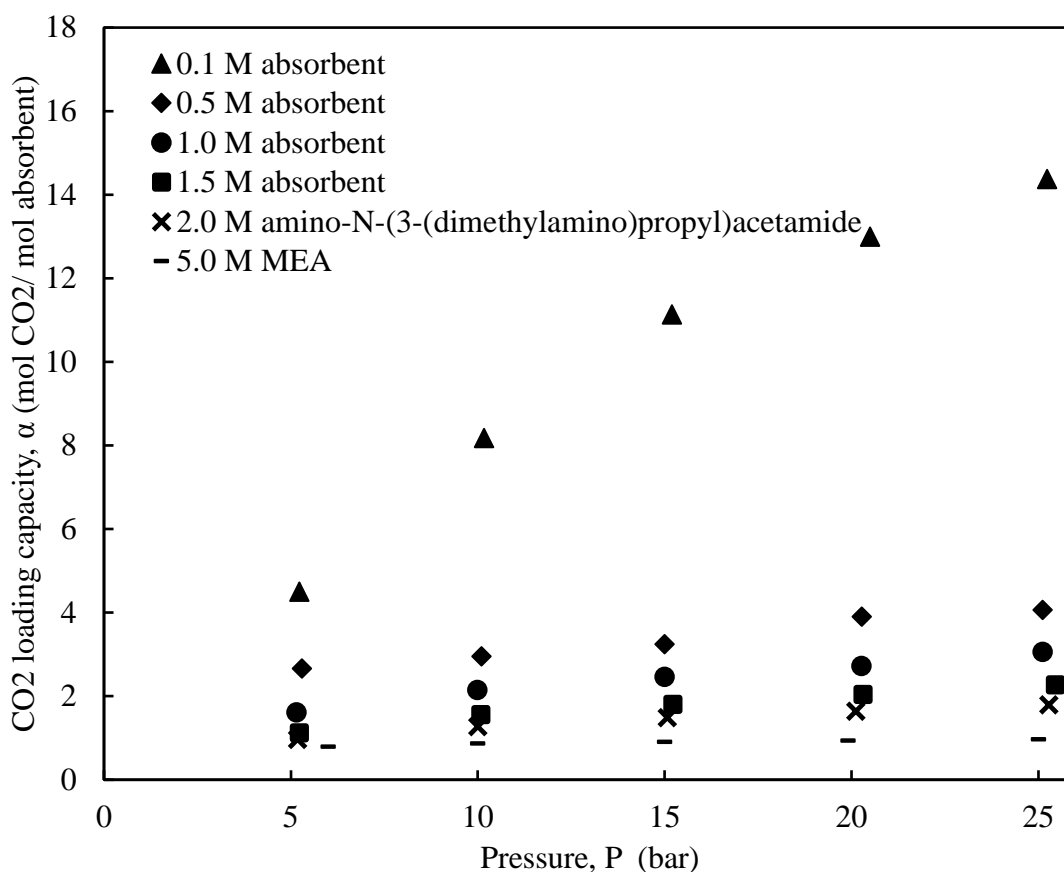


Figure 4.14: CO₂ loading capacity of amino-N-(3-(dimethylamino)propyl)acetamide absorbent in comparison with 30 w/w % MEA measured at 303.15 K.

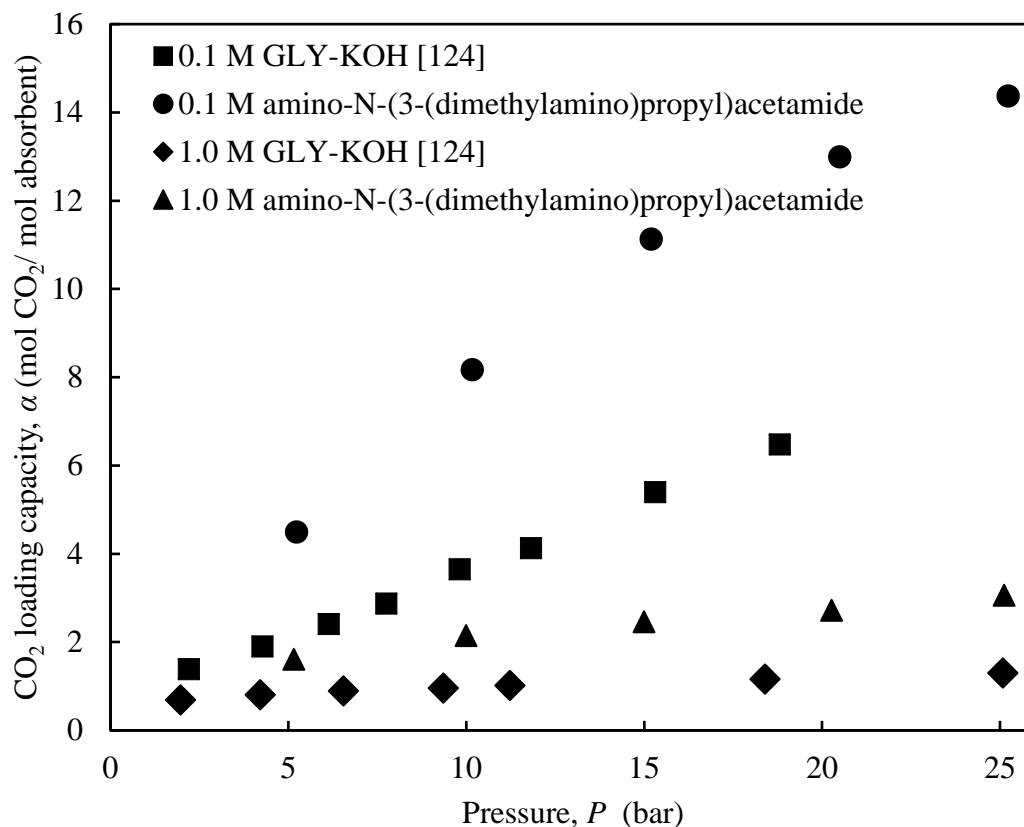


Figure 4.15: The CO₂ loading capacity of 0.1 and 1.0 M amino-N-(3-(dimethylamino)propyl)acetamide measured at 303.15 K, in comparison with GLY-KOH.

4.3.3 Interactions between CO₂ and the absorbent

The chemical interactions between the absorbent, amino-N-(3-(dimethylamino)propyl)acetamide and CO₂ were analyzed by studying the FTIR spectra of the absorbent before and after CO₂ capture process as illustrated in Figure 4.16. The characteristic peaks detected in the FTIR spectra before and after the absorption process are listed in Table 4.5. Based on the structure of amino-N-(3-(dimethylamino)propyl)acetamide (Figure 4.9), CO₂ molecules is expected to react with amide linkage (HN-C=O) to produce imide, respectively. The interaction between CO₂ molecules and the amide linkage can be justified based on the disintegration of broad -NH wagging peak at wavenumber between 600 – 750 cm⁻¹ [146], as observed from Figure 4.15(b). Moreover, the dissolution of amide bond was also indicated by degeneration of N-H peak at 1565 cm⁻¹ [146]. The presence of imide functional groups can be detected at wavelengths 1505 cm⁻¹ and 1137 cm⁻¹, which corresponded to N-H in-plane bending and C-N stretching, respectively.

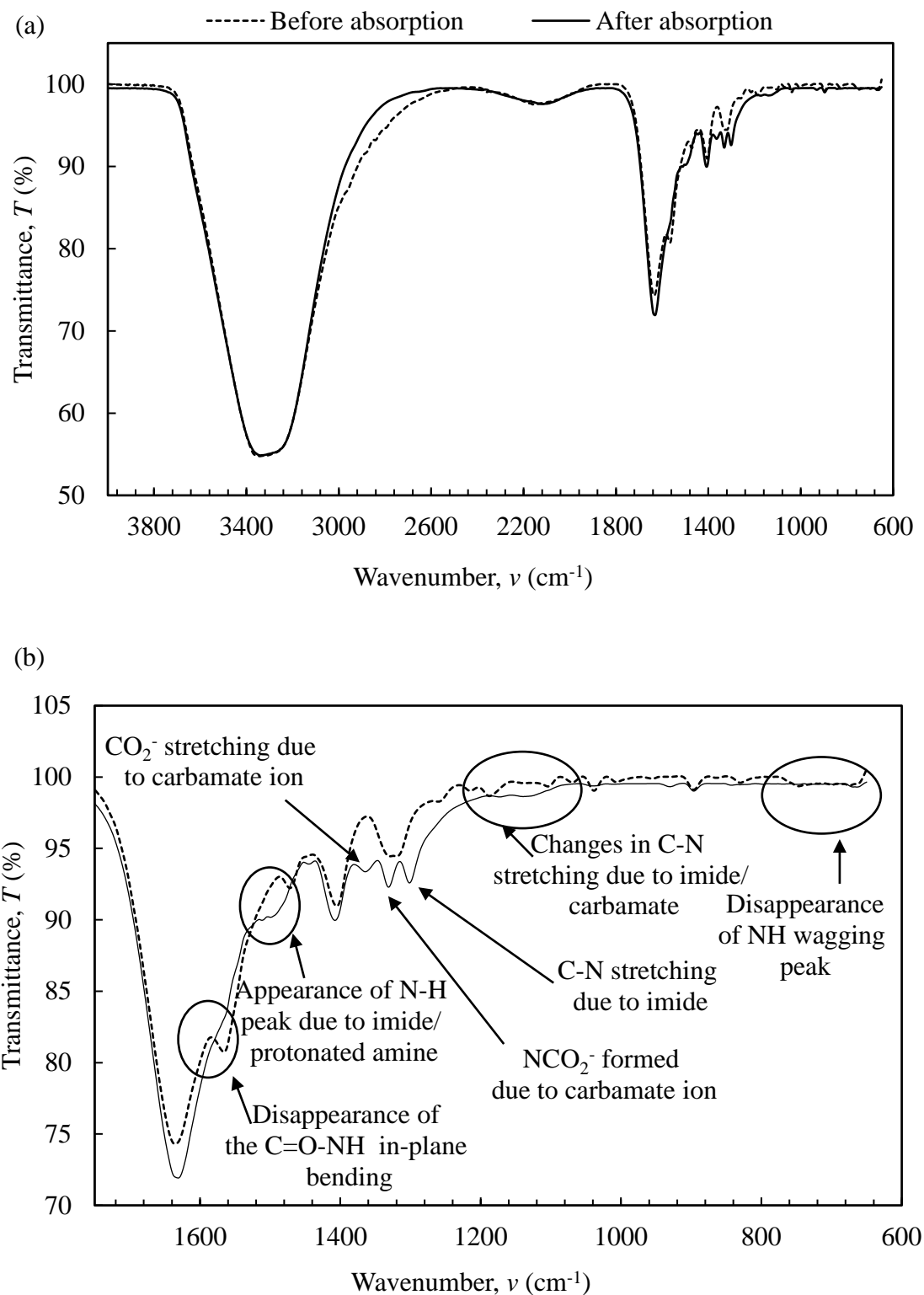


Figure 4.16: FTIR spectra of (a) the absorbent before and after the absorption process (b) close-up spectra between 1750 to 600 cm^{-1} .

Table 4.5: The characteristics peaks of the absorbent before and after CO₂ absorption process.

Wavenumbers (cm ⁻¹)		Assignments	Remarks
Before CO ₂ absorption	After CO ₂ absorption		
3314	3314	O-H stretch	-OH molecules from water molecules
2825-2801; 2775-2765	2825-2801; 2775-2765	N-(CH ₃) symmetric C-H stretch/ N-H	Difficult to identify the exact functional groups due to overlapping of functional groups. The peaks smoothen and the intensity decreased after the CO ₂ absorption process.
2100	2100	C-N stretch	No changes observed at this wavelength
1618	1631	C=O asymmetric stretch	COO ⁻ functional group from amide bond and possible attachments of CO ₂
1565	-	N-H in-plane bend	N-H bending from CHNO functional group of secondary amide
1473	-	C-CH ₂ scissors	This peak corresponds to CH ₂ functional group. This peak was not detected after CO ₂ capture due to overlapping with N-H in-plane bending
-	1505	N-H in-plane bend	Peak was present after CO ₂ absorption. The N-H bending is specific to nitrogen atom attached to two carbonyl groups (imide)
1400	1407	C=O symmetric stretch	COO ⁻ functional group from amide bond and possible attachment of CO ₂
-	1361	C=O symmetric stretch	COO ⁻ functional group from carbamate ion
-	1329	N-CO ₂ ⁻	This peak was detected after CO ₂ capture due to skeletal vibrations of N-CO ₂ ⁻

Table 4.5: The characteristics peaks of the absorbent before and after CO₂ absorption process (continued).

Wavenumbers (cm ⁻¹)		Assignments	Remarks
Before CO ₂ absorption	After CO ₂ absorption		
1317	-	C-O stretch	C-O stretching from carboxylic acid functional group. Peak is very weak, could be contributed by the presence of unreacted glycine during sample preparation
-	1300	C-N stretch	C-N stretching from secondary amide.
-	1137	C-N stretch	C-N stretching from imides
600- 750	-	NH wag	This peak is contributed by NH from secondary amide [146]. The disappeared of this peak after CO ₂ absorption process indicating the interaction between amide and CO ₂

The primary amine group from amino-N-(3-(dimethylamino)propyl)acetamide is also predicted to react with CO₂ molecules to produce carbamate ion. While it is difficult to distinguish the N-H functional groups of the primary amine and the N-H functional group from the amide functional group, the interaction between CO₂ with primary amine can be justified through the formation of carbamate ions detected in the FTIR spectrum through the formation of new characteristics peaks at 1329 cm⁻¹ due to skeletal vibrations of N-CO₂⁻ [71]. Moreover the COO⁻ functional group from carbamate ions can also be detected at wavenumber 1361 cm⁻¹.

For the tertiary amino group forum within the amino-N-(3-(dimethylamino)propyl)acetamide molecule, the lack of proton leads inhibit direct reaction between CO₂ molecules and the amino group. However, CO₂ will react with water molecule to form carbamic acid which will interact with tertiary amine group to produce protonated amine [80]. The presence of protonated amine may be deduced through the formation of a new characteristic peaks at 1505 cm⁻¹.

In general, the FTIR spectra provided evident of possible interactions between CO₂ molecules and the amino-N-(3-(dimethylamino) propyl) acetamide absorbent. The dissolution of the amide linkage and the formation of additional peaks from the FTIR spectra suggested that occurrence of chemical reactions during the CO₂ absorption process. However, the further analysis is required to determine the exact mechanism for the CO₂ capture process.

4.4 CO₂ Utilization and Characterization Study

The CO₂ utilization study was carried out at low pressure condition to evaluate the possibility of CO₂ conversion at low pressure condition (5 bar). The performances of CO₂ utilization were evaluated in this section. The product obtained from CO₂ capture was then characterized using FTIR and XPS.

4.4.1 CO₂ utilization performances

In this work, the CO₂ utilization study was conducted at 5 bar in order to study the possibility of CO₂ conversion at low pressure condition. The conversion process was carried out through addition of 1 mol ethanol into CO₂-saturated solution at 303.15 K. Formation of white precipitate was observed after three hours. The mass of solids recovered during the conversion process are indicated in Figure 4.17. The experiments were repeated three times and the average values along with standard deviations were listed in Appendix G. Formation of solids were not detected when 0.1 M amino-N-(3-(dimethylamino)propyl)acetamide was used as an absorbent. This result was consistent with the CO₂ absorption capacity results reported in Section 4.3.1 which suggested that the net amount of CO₂ absorbed by 0.1 M amino-N-(3-(dimethylamino) propyl) acetamide was minimum. This is based on the low amount of solute found in the absorbent, contributing to negligible solid formation. However, as the concentration of amino-N-(3-(dimethylamino)propyl)acetamide increased from 0.5 to 2.0 M, the amount of solids recovered also increased from 15 to 95 mg solid/ g absorbent.

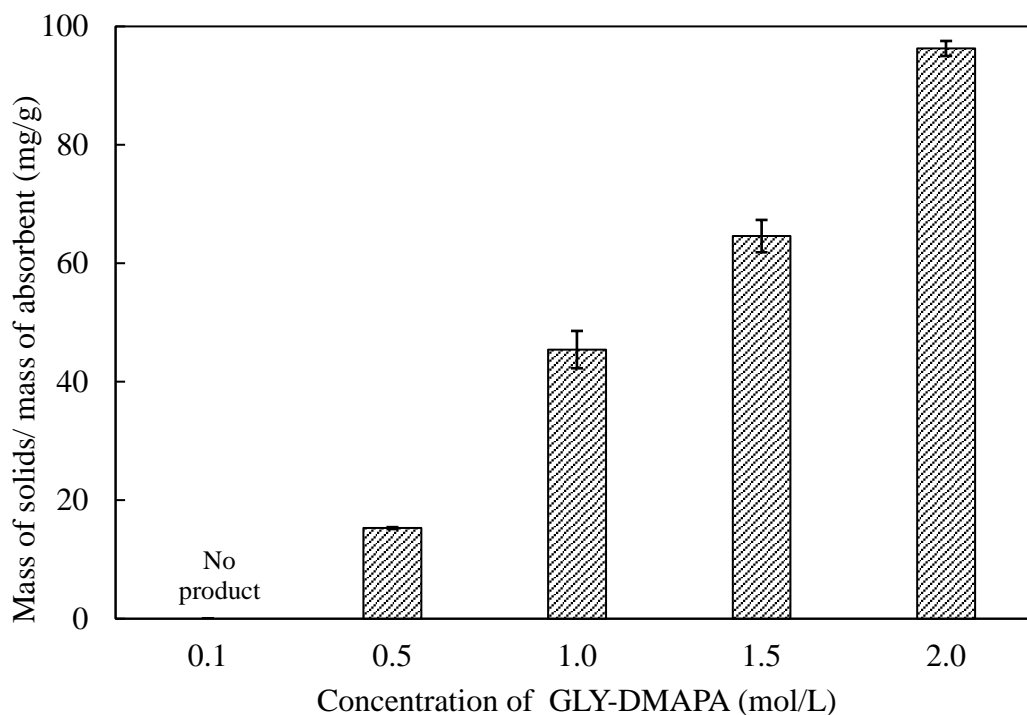


Figure 4.17: Amount of solids from CO₂ utilization based on different concentrations of absorbent (Ethanol concentration: 1 mol).

The concentration of absorbent selected for the CO₂ capture process is dependent on both the amount of products recovered and the CO₂ loading capacity of the absorbent. Despite the high solid formations at higher concentration of absorbent, the CO₂ loading capacity of the absorbent decreased as the concentration of the absorbent increased, as indicated in Figure 4.18. The highest CO₂ loading capacity was recorded at 0.1 M amino-N-(3-(dimethylamino)propyl)acetamide. However, no product was obtained at this concentration. From 0.5 to 1.0 M amino-N-(3-(dimethylamino)propyl)acetamide, the CO₂ loading capacity decreased by 40%. In contrast, the amount of product recovered increased by 196%. The higher increment in product formation outweighs the decrease in the CO₂ loading capacity of the absorbent. Moreover, The CO₂ loading capacity at 1.0 M was reasonably higher than the CO₂ loading capacity of 1.0 M GLY-KOH which was reported to be between 0.8 to 0.9 mol CO₂/ mol of absorbent, measured at 4.2 and 6.5 bar, respectively [126]. Hence, 1.0 M amino-N-(3-(dimethylamino)propyl)acetamide was used as a basis for further CO₂ utilization study.

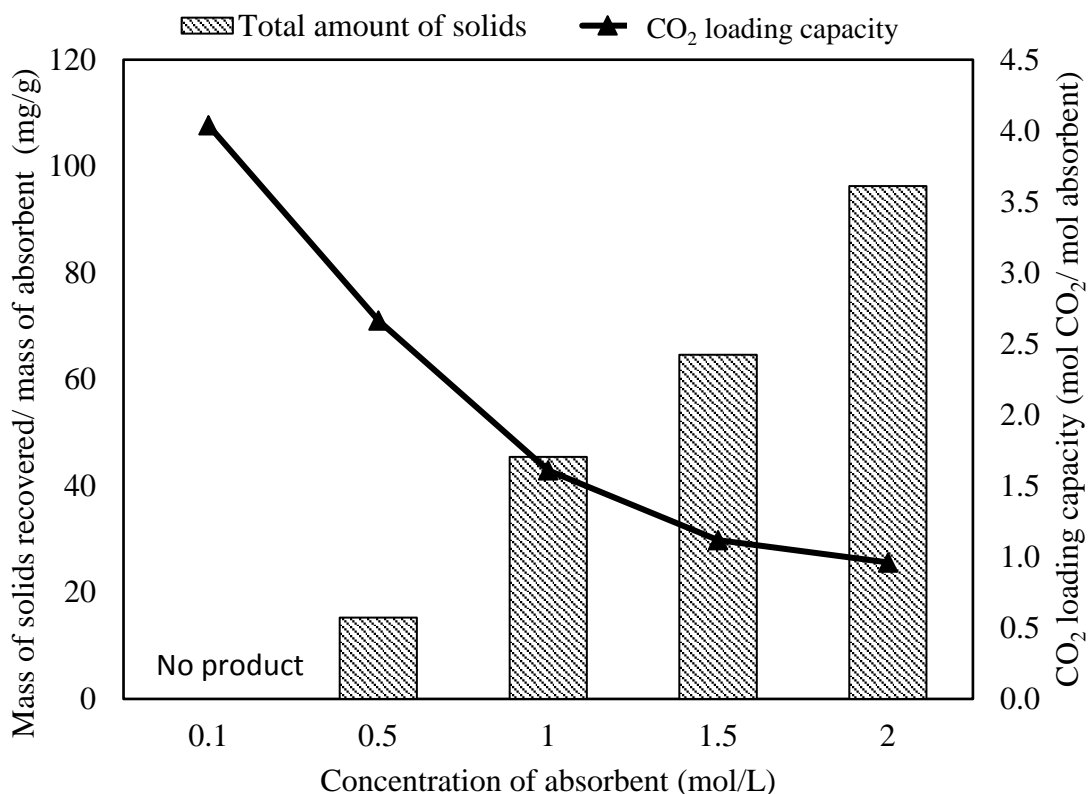


Figure 4.18: CO₂ loading capacities and the total amount of solids recovered during utilization process.

The effect of amount of ethanol on the absorbent was evaluated by varying the moles of ethanol added during the CO₂ utilization process. Based on Figure 4.19, it was observed that the amount of solids recovered increased when the number of moles of ethanol added increased from 0.5 to 1.0 M. However, beyond 1 M, the amount of solids recovered decreased. The initial increase the product formation is due to the increase in number of molecules that are able to participate in the CO₂ conversion process. However, after 1.0 M, the CO₂ conversion activity decreased due to excess amount of reagent, which shifted the chemical reaction to the left, thus producing less solids. This trend is also reported by [79-81], such that excess reactant causes the yield during CO₂ conversion process to decrease.

Figure 4.20 shows the conversion time for the CO₂ utilization process, which indicated that the CO₂ utilization process requires at least one hour to reach equilibrium. Based on the findings, the optimum amount of product for CO₂ utilization was 45 mg/g, which was attained by using 1.0 M absorbent, and 1.0 mol ethanol after 1 hour. Meanwhile the CO₂ loading capacity recorded was 1.6 mol CO₂/ mol of absorbent.

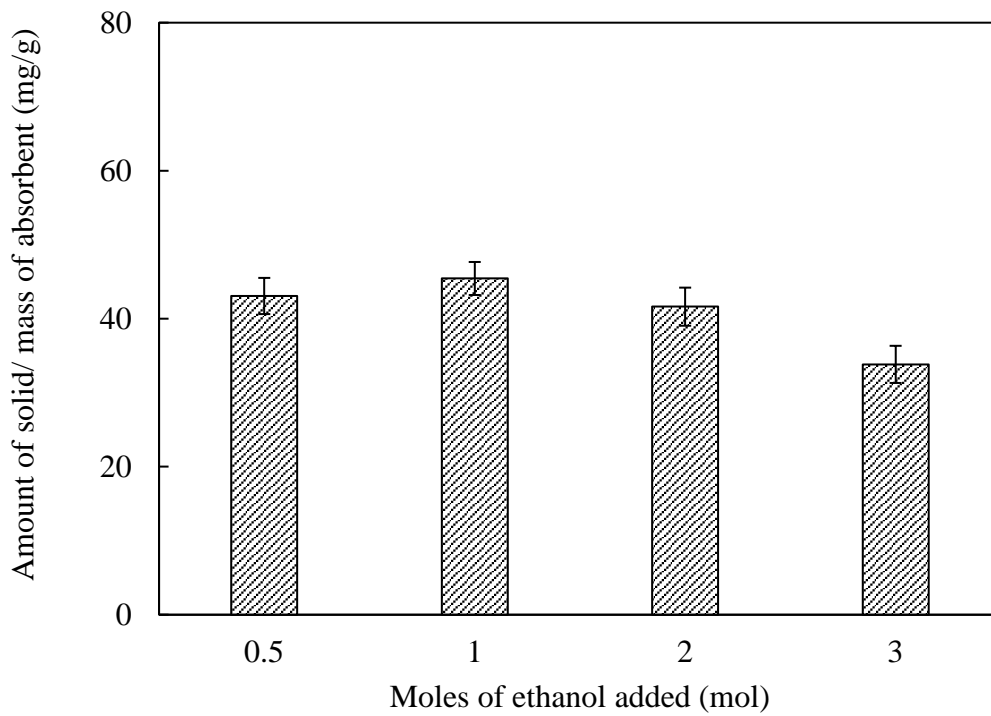


Figure 4.19: The effect of amount of ethanol on the product formation (absorbent concentration = 1 mol; time = 3 hours).

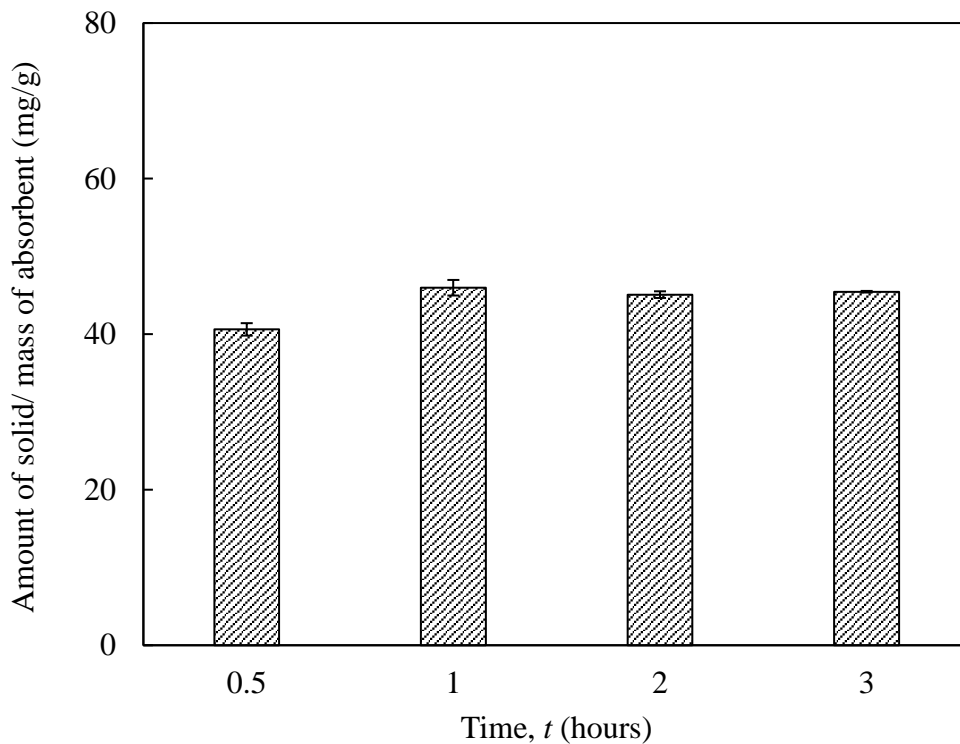


Figure 4.20: The effect of conversion time on the product formation (absorbent concentration = 1 mol; ethanol concentration = 1 mol).

4.4.2 Characterization of solid particles

The solid particles were characterized by using the Fourier transform infrared spectroscopy to identify the surface functional group of the absorbent. Furthermore, x-ray photoelectron spectroscopy (XPS) was also used to identify the surface chemical binding of the solid product.

4.4.2.1 Surface functional group

The FTIR spectra of ethanol was compared with the solid products obtained after the CO₂ utilization process as illustrated in Figure 4.21. The interactions between ethanol and the CO₂-saturated absorbent were suggested based on the changes in the main characteristic peaks found in the CO₂-saturated absorbent and ethanol. For the ethanol and CO₂-saturated absorbent spectra, the main changes were observed at wavenumber 3302 cm⁻¹. In the CO₂-saturated absorbent, this peak is contributed by the presence of water molecules in the absorbent. However, in ethanol, this peak corresponded to the OH functional group found in the alcohol. The shifting of the in the OH functional group at wavenumber 3302 cm⁻¹ after the addition of ethanol in the CO₂-saturated absorbent may be due to the interaction between the OH group and the absorbent, to produce a different functional group.

A close up FTIR spectrum of the solids was provided in Figure 4.22 to identify the surface functional group present in the solid particles. The characteristic peaks of the solids are listed in Table 4.6. The FTIR spectrum suggested the presence of carbamate compound based on the functional groups based on the carbamate moiety in the solid precipitates. The characteristic peak at wavenumber 1332 cm⁻¹ was detected in the FTIR spectrum corresponded to N-COO⁻ stretching vibrations. In a study conducted by Sun and Dutta [148], the same characteristic peak corresponding to carbamate peak (1332 cm⁻¹) was detected in the presence of MEA carbamate. Moreover, the peak NHCOO⁻ is also observed at wavenumber 1517 cm⁻¹, which suggested the N-H in-plane bending next to a COO⁻ functional group [145]. This two peaks provide evident on the formation of carbamate salt during CO₂ utilization process. On top of that, the COO⁻ stretching detected at wavenumber 1606 cm⁻¹ and 1134 cm⁻¹ are also contributed by carbamate functional group.

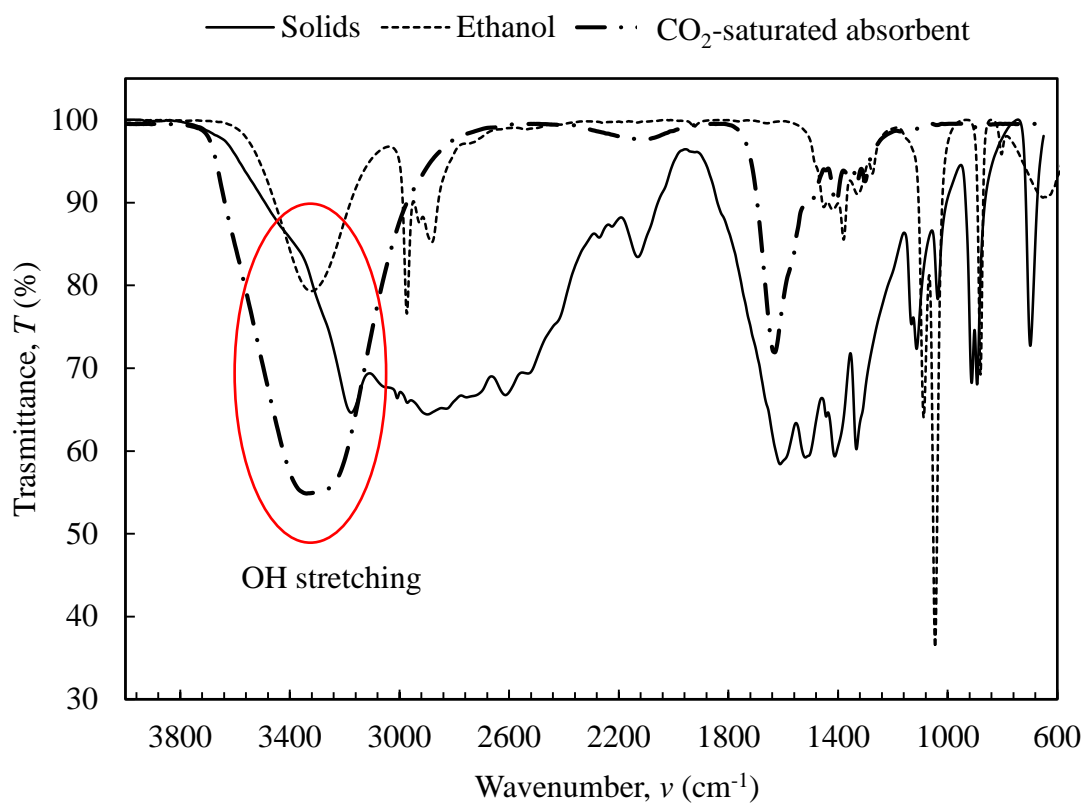


Figure 4.21: Full FTIR spectra of the solids, ethanol, and CO₂-saturated absorbent, for wavenumber ranging from 4000 to 600 cm⁻¹.

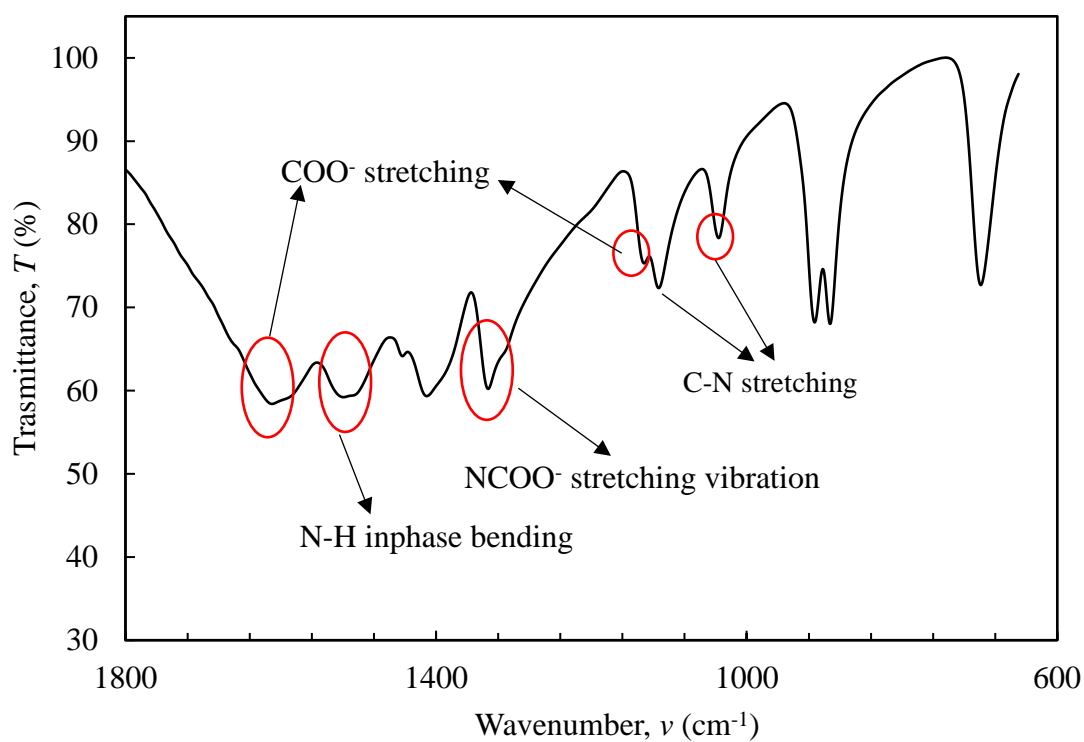


Figure 4.22: The close up spectra of the solid products at wavenumber ranging from 1800 cm⁻¹ to 600 cm⁻¹.

Table 4.6: The characteristics peaks of solids obtained after addition of ethanol.

Wavenumbers (cm ⁻¹)	Assignments	Remarks
2200 - 3450	NH ₃ ⁺ stretching summation bands	NH ₃ ⁺ may be due to the formation of carbamate salt
2124	C-N stretch	The peak indicated the presence of amine group
1608	C=O asymmetric stretch	The C=O is due to COO ⁻ from carbamate salt. For organic carbonates, this peak should be detected at 1740 cm ⁻¹
1517	N-H in-plane bend/ COO ⁻ stretching	This peak corresponded to secondary amide which is contributed by carbamate functional group NHCOO ⁻
1431	C-CH ₂ stretching	This peak is based on the CH ₂ carbon chain
1414	C=O symmetric stretching	This peak is mainly due to COO ⁻ functional group from carbamate salt
1121	C-O stretching	The C-O stretching was contributed by the carbamate group. For organic carbonates this peak should be visible at 1280 – 1240 cm ⁻¹
1332	N-CO ₂ ⁻	Skeletal vibrations of N-CO ₂ ⁻ from carbamate ion
1111	C-N stretch	Due to RNHCOO ⁻

Apart from identifying the carbamate functional groups, analysis was also carried out to identify the presence of inorganic carbonate in the FTIR spectrum. The inorganic carbonate functional groups are usually detected at wavenumbers 1740 cm⁻¹ and 1280 cm⁻¹ which correspond to C=O stretching and O-C-O stretching, respectively [146]. However, the characteristic peaks corresponding to inorganic carbonates were not detected in the FTIR spectrum of the solids presented in Figure 4.22, which suggested inorganic carbonates may not be formed during the reaction between alcohol and CO₂-saturated amino-N-(3-(dimethylamino)propyl)acetamide. However, this needs to be confirmed by other types of analysis. Nonetheless, the FTIR results indicated the presence the carbamate compound in the solid particles.

4.4.2.2 Surface chemical binding

The XPS spectra of the solid products obtained from CO₂ utilization are as illustrated in Figure 4.23. Three main elements were detected in the spectra namely oxygen (525 – 545 eV), nitrogen (392 – 410 eV) and carbon (280 – 294 eV). The chemical bindings found in each element were studied through a more detailed scan as shown in Figure 4.24. The specific chemical moiety represented by the binding energies are listed in Table 4.7, for each of the elements found in the spectra.

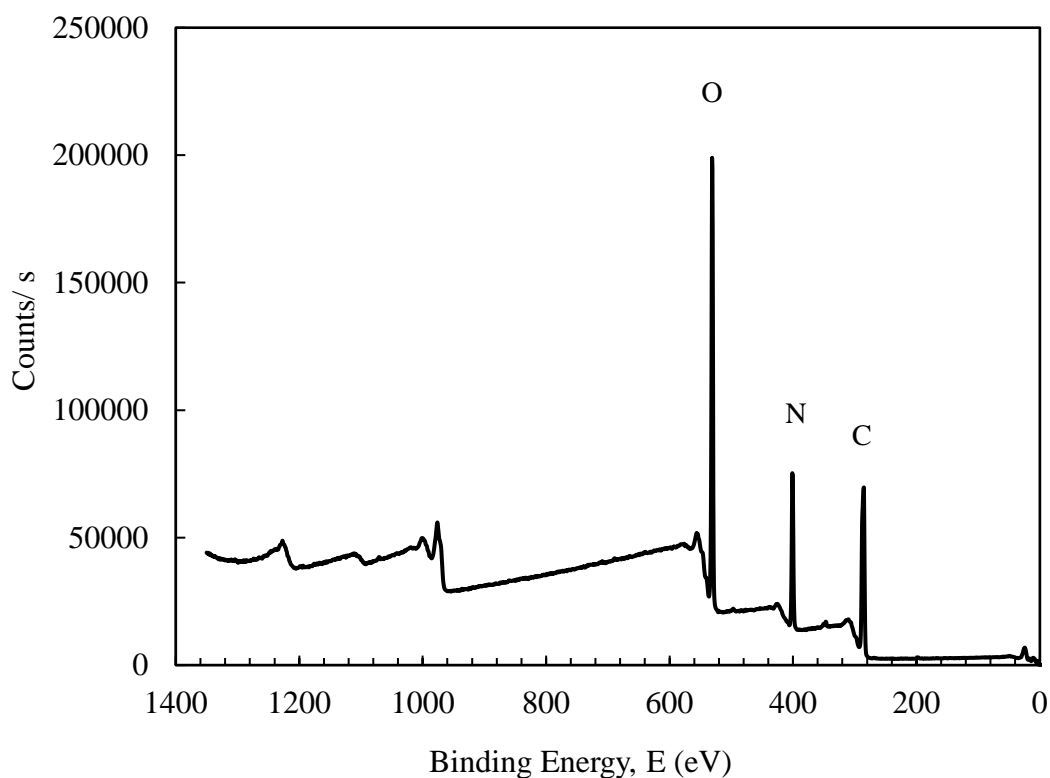


Figure 4.23: XPS spectrum of solids obtained after addition of ethanol into CO₂-saturated solution.

Table 4.7: Binding energy detected by the XPS spectra and the corresponding moiety.

Elements	Binding Energy (eV)	Moiety
Carbon (C)	285.6	C-C/ C-H
	287.9	C=O
	288.9	O-C=O
Nitrogen (N)	399.1	NH-C(=O) ⁻
	400.8	(O=C)-N-(C=O)
	401.8	(NR ₄) ⁺
Oxygen (O)	530.9	C=O
	532.6	C-O

For the carbon element, the main peak corresponded to C-C and C-H were observed at 285.6 eV. Meanwhile the carbamate functional group (COO⁻) was identified at binding energies 287.9 eV and 288.8 eV based on the presence of C=O and O-C=O linkage, respectively. The XPS spectra also detected three types of bonding for the nitrogen atom. The imide functional group was identified at binding energy of 400.8 eV, whereas C-N was observed at 399.1 eV, and finally the peak at 401.8 eV corresponded to (NR₄)⁺ which might be detected due to the presence of unreacted protonated amine found on the surface of the solid particles. Two peaks were observed for oxygen at 530.9 eV and 532.6 eV which corresponded to C-O and C=O bonding, respectively.

The presence of carbamate compound in the were confirmed by comparing the results obtained with the work reported by Edere et al. [149], which employed XPS to characterize polyurethane nanomaterials which contained carbamate functional group. The carbamate functional group corresponding to NHCOO⁻ were detected at approximately 289.0 eV, which is close to 288.8 eV (Table 4.7). This suggest the presence of carbamate compound in the solid particles was obtained, when CO₂-saturated amino-N-(3-(dimethylamino)propyl)acetamide was reacted with ethanol.

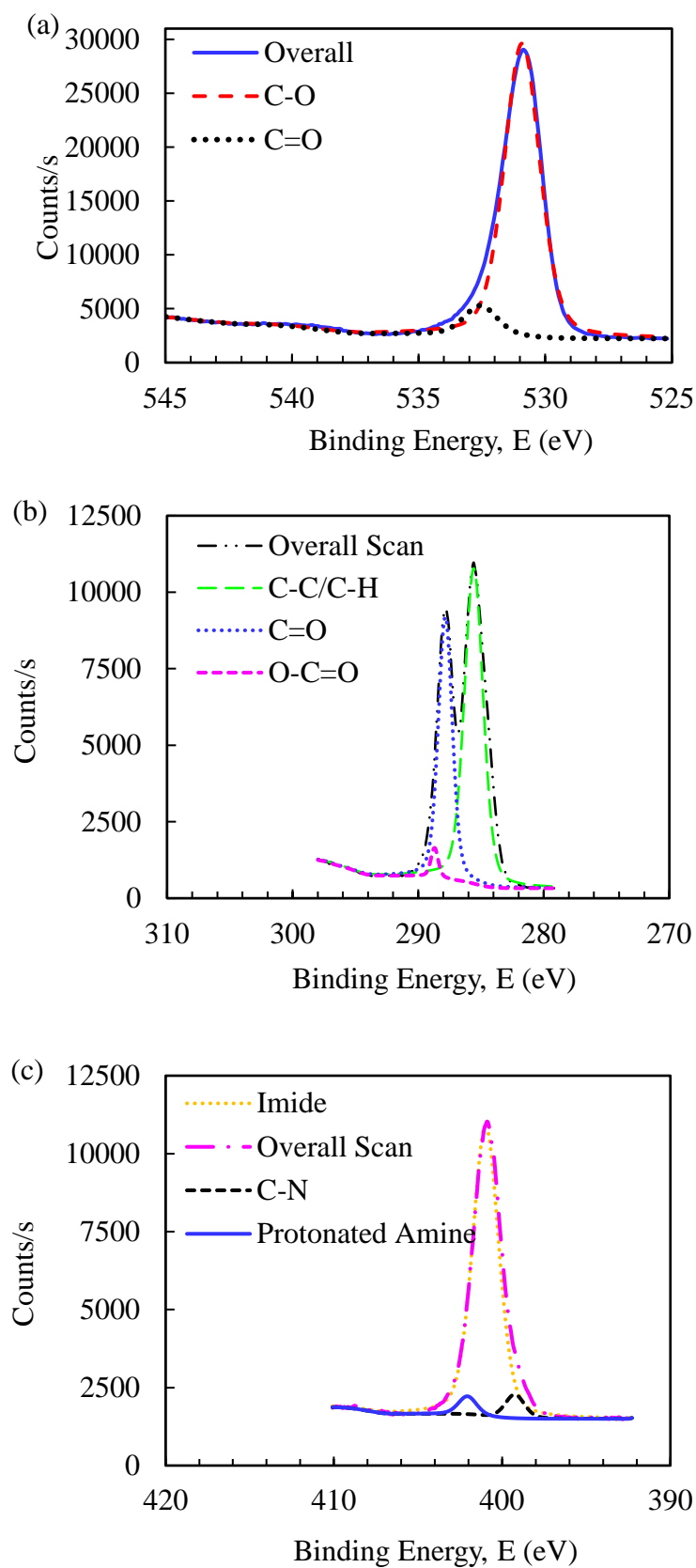


Figure 4.24: XPS spectra of (a) oxygen; (b) carbon; and (c) nitrogen, of the solids.

4.5 Summary

In this chapter, the performance of amino-N-(3-(dimethylamino) propyl)acetamide as a potential absorbent for CO₂ capture was reported. The absorbent was formed through neutralization of 3-dimethylaminopropylamine (DMAPA) with glycine. FTIR analysis confirmed that the neutralization of diamine with amino acid formed amide linkage. The CO₂ loading capacity of the absorbent was also reported in this chapter. The results indicated that the CO₂ absorption capacity of the absorbent was significantly higher than the conventional MEA absorbent. The CO₂ utilization study suggested the possibility of using two-steps CO₂ capture and conversion process contributed to formation of solid products. The FTIR and XPS analysis provide evidences that the solid particles contained carbamate compound. However, further analysis is required to confirm the structure of the carbamate salt.

This page is intentionally left blank

CHAPTER 5

CONCLUSION

5.1 Conclusion

Carbon capture and utilization is regarded as a promising option for reducing CO₂ emissions in the atmosphere, parallel with the efforts to reduce the impacts of global warming. Based on the literature reviews, chemical absorption was identified as one of the methods for CO₂ mitigation by capturing CO₂ from large point sources. Monoethanolamine is widely used in the CO₂ capture industry. However, the main drawback of using MEA is limited CO₂ loading capacity of the absorbent and the high energy requirement during CO₂ desorption process. Moreover, CO₂ utilization process also requires high energy input to overcome the high thermodynamic stability of the CO₂ molecules during the conversion process. In this study, the possibility of integrating CO₂ absorption with the CO₂ utilization process was evaluated to eliminate the energy intensive CO₂ desorption and CO₂ conversion process.

The first part of this study focused on the preparation and characterization of an absorbent for CO₂ capture. The absorbent was prepared through neutralization of 3-dimethylaminopropylamine (DMAPA) with glycine. The density, viscosity, surface tension, and refractive index were measured at temperature ranging from 298.15 to 323.15 K. The results revealed that the physical properties of the absorbent decreased as the temperature of the absorbent increased. At constant temperature, density, refractive index, and viscosity of the absorbent increased as the concentration of the absorbent increased. In contrast, the surface tension decreased with increased in the concentration of the absorbent. The experimental data for the physicochemical study were successfully represented by using empirical correlations. The FTIR results indicated the formation of amino-N-(3-(dimethylamino)propyl)acetamide when glycine was added into DMAPA solution.

Based on the CO₂ solubility study, amino-N-(3-(dimethylamino)propyl)acetamide was reported to be significantly higher in comparison to the conventional MEA absorbent. Moreover, the absorption capacity of amino-N-(3-(dimethylamino)propyl)acetamide was reported to be higher than glycine neutralized with amino acid salt. The effects of temperature, pressure, and concentration of the absorbent were also investigated in this study. The CO₂ loading capacity of the absorbent increased when temperature and concentration of the absorbent decreased. In addition, the CO₂ loading capacity was found to increase in parallel with pressure of CO₂.

The results obtained from the CO₂ utilization study revealed that the addition of ethanol into CO₂ saturated absorbent was able to generate solid products. 1.0 M amino-N-(3-(dimethylamino)propyl)acetamide was used as a basis for the CO₂ utilization study based on its high CO₂ loading capacity (1.6 mol CO₂/ mol of absorbent). The product obtained was analyzed using FTIR and XPS which suggest the presence of carbamate salt. The experimental results obtained in this study suggested that amino-N-(3-(dimethylamino)propyl)acetamide has a potential to be developed as an absorbent for CO₂ capture. The integration of CO₂ capture with CO₂ utilization provide suggested that the highly intensive solvent regeneration process can be eliminated from the CO₂ absorption technology. This will reduce the overall energy requirement for CO₂ capture process. Moreover, the study on CO₂ utilization indicated the possibility of CO₂ capture and conversion at lower temperature and pressure conditions.

5.2 Recommendations

This study focused on CO₂ capture at pressure ranging from 5 to 25 bar, for pre-combustion CO₂ capture application. Based on the high CO₂ loading capacity of the amino-N-(3-(dimethylamino)propyl)acetamide absorbent, the study can be extended for higher pressure applications particularly for natural gas purification process. Apart from that, kinetic studies should also be included to evaluate the rate of CO₂ absorption, which is another important criterion for selection of absorbent for CO₂ removal process. Based on the solids generated at low pressure, the CO₂ utilization study should also be evaluated at higher pressure to study the effect of pressure on the conversion process. On top of that, further characterization on the solids obtained from the CO₂ utilization process needs to be carried out to provide a better understanding on the mechanisms

involved during the conversion process. The fundamental studies on the amino-N-(3-(dimethylamino)propyl)acetamide absorbent for CO₂ capture and utilization is performed through batch processes, using small amount of absorbent. This is crucial to properly investigate the behavior of the absorbent, before proceeding to continuous study which usually involves larger quantity of absorbent.

REFERENCES

- [1] G. T. Rochelle, "Amine scrubbing for CO₂ capture," *Science*, vol. 325, no. 5948, pp. 1652-1654, 2009.
- [2] I. Hinkov, F. D. Lamari, P. Langlois, M. Dicko, C. Chilev, and I. Pentchev, "Carbon dioxide capture by adsorption," *Journal of Chemical Technology & Metallurgy*, vol. 51, no. 6, 2016.
- [3] A. Basile, A. Iulianelli, F. Gallucci, and P. Morrone, "7 - Advanced membrane separation processes and technology for carbon dioxide (CO₂) capture in power plants A2 - Maroto-Valer, M. Mercedes," in *Developments and Innovation in Carbon Dioxide (CO₂) Capture and Storage Technology*, vol. 1: Woodhead Publishing, 2010, pp. 203-242.
- [4] G. Xu, F. Liang, Y. Yang, Y. Hu, K. Zhang, and W. Liu, "An improved CO₂ separation and purification system based on cryogenic separation and distillation theory," *Energies*, vol. 7, no. 5, pp. 3484-3502, 2014.
- [5] R. R. Bottoms, "Process for separating acidic gases," 1930. [Online]. Available: <https://www.google.com/patents/US1783901>
- [6] M. T. Ravanchi and S. Sahebdehfar, "Carbon dioxide capture and utilization in petrochemical industry: potentials and challenges," *Applied Petrochemical Research*, vol. 4, no. 1, pp. 63-77, 2014.
- [7] Y. E. Kim, J. A. Lim, S. K. Jeong, Y. I. Yoon, S. T. Bae, and S. C. Nam, "Comparison of carbon dioxide absorption in aqueous MEA, DEA, TEA, and AMP solutions," *Bulletin of the Korean Chemical Society*, vol. 34, no. 3, pp. 783-787, 2013.
- [8] M. Hasib-ur-Rahman, M. Siaj, and F. Larachi, "Ionic liquids for CO₂ capture—Development and progress," *Chemical Engineering and Processing: Process Intensification*, vol. 49, no. 4, pp. 313-322, 2010.
- [9] W. Li, X. Zhang, B. Lu, C. Sun, S. Li, and S. Zhang, "Performance of a hybrid solvent of amino acid and ionic liquid for CO₂ capture," *International Journal of Greenhouse Gas Control*, vol. 42, pp. 400-404, 2015.
- [10] T. Wang *et al.*, "Solvent regeneration by novel direct non-aqueous gas stripping process for post-combustion CO₂ capture," *Applied Energy*, vol. 205, pp. 23-32, 2017.
- [11] Y. Li, J. Cheng, L. Hu, J. Liu, J. Zhou, and K. Cen, "Phase-changing solution PZ/DMF for efficient CO₂ capture and low corrosiveness to carbon steel," *Fuel*, vol. 216, pp. 418-426, 2018.
- [12] D. Kang, M.-G. Lee, H. Jo, Y. Yoo, S.-Y. Lee, and J. Park, "Carbon capture and utilization using industrial wastewater under ambient conditions," *Chemical Engineering Journal*, vol. 308, pp. 1073-1080, 2017.

- [13] X. Luo, K. Chen, H. Li, and C. Wang, "The capture and simultaneous fixation of CO₂ in the simulation of fuel gas by bifunctionalized ionic liquids," *International Journal of Hydrogen Energy*, vol. 41, no. 21, pp. 9175-9182, 2016.
- [14] M. Peters, B. Köhler, W. Kuckshinrichs, W. Leitner, P. Markewitz, and T. E. Müller, "Chemical technologies for exploiting and recycling carbon dioxide into the value chain," *ChemSusChem*, vol. 4, no. 9, pp. 1216-1240, 2011.
- [15] E. Alper and O. Yuksel Orhan, "CO₂ utilization: Developments in conversion processes," *Petroleum*, vol. 3, no. 1, pp. 109-126, 2017.
- [16] A. Ion, C. Van Doorslaer, V. Parvulescu, P. Jacobs, and D. De Vos, "Green synthesis of carbamates from CO₂, amines and alcohols," *Green Chemistry*, vol. 10, no. 1, pp. 111-116, 2008.
- [17] A. K. Ghosh and M. Brindisi, "Organic carbamates in drug design and medicinal chemistry," *Journal of medicinal chemistry*, vol. 58, no. 7, pp. 2895-2940, 2015.
- [18] S. Shen, Y. Bian, and Y. Zhao, "Energy-efficient CO₂ capture using potassium proline/ethanol solution as a phase-changing absorbent," *International Journal of Greenhouse Gas Control*, vol. 56, pp. 1-11, 2017.
- [19] M. R. Abu-Zahra, Z. Abbas, P. Singh, and P. Feron, "Carbon dioxide post-combustion capture: solvent technologies overview, status and future directions," *Materials and processes for energy: communicating current research and technological developments*, vol. 1, pp. 923-934, 2013.
- [20] R. Zhang *et al.*, "Toward Efficient CO₂ Capture Solvent Design by Analyzing the Effect of Chain Lengths and Amino Types to the Absorption Capacity, Bicarbonate/Carbamate, and Cyclic Capacity," *Energy & Fuels*, vol. 31, no. 10, pp. 11099-11108, 2017.
- [21] U. E. Aronu, E. T. Hessen, T. Haug-Warberg, K. A. Hoff, and H. F. Svendsen, "Equilibrium absorption of carbon dioxide by amino acid salt and amine amino acid salt solutions," *Energy Procedia*, vol. 4, pp. 109-116, 2011.
- [22] U. E. Aronu, H. F. Svendsen, and K. A. Hoff, "Investigation of amine amino acid salts for carbon dioxide absorption," *International Journal of Greenhouse Gas Control*, vol. 4, no. 5, pp. 771-775, 2010.
- [23] H.-J. Song, S. Park, H. Kim, A. Gaur, J.-W. Park, and S.-J. Lee, "Carbon dioxide absorption characteristics of aqueous amino acid salt solutions," *International Journal of Greenhouse Gas Control*, vol. 11, pp. 64-72, 2012.
- [24] S.-J. Han and J.-H. Wee, "Carbon Dioxide Fixation via the Synthesis of Sodium Ethyl Carbonate in NaOH-Dissolved Ethanol," *Industrial & Engineering Chemistry Research*, vol. 55, no. 46, pp. 12111-12118, 2016.
- [25] The Australian National University. "Humans affect Earth system more than natural forces." <http://www.anu.edu.au/news/all-news/humans-affect-earth-system-more-than-natural-forces> (accessed February 16, 2017).

- [26] S. Bouzalakos and M. M. Maroto-Valer, "1 - Overview of carbon dioxide (CO₂) capture and storage technology," in *Developments and Innovation in Carbon Dioxide (CO₂) Capture and Storage Technology*, vol. 2: Woodhead Publishing, 2010, pp. 1-24.
- [27] J. F. P. Gomes, *Carbon Dioxide Capture and Sequestration: An Integrated Overview of Available Technologies*. Nova Science Publishers, Incorporated, 2013.
- [28] C. Song, "CO₂ Conversion and Utilization: An Overview," in *CO₂ Conversion and Utilization*, vol. 809, (ACS Symposium Series, no. 809): American Chemical Society, 2002, ch. 1, pp. 2-30.
- [29] S. A. Rackley, *Carbon Capture and Storage*. Butterworth-Heinemann/Elsevier, 2010.
- [30] (2016). *Climate Change Indicators: Greenhouse Gases*. [Online] Available: <https://www.epa.gov/climate-indicators/greenhouse-gases>
- [31] Global CCS Institute, "The Global Status of CCS: 2014," Melbourne, Australia, 2014.
- [32] S. M. Al-Fattah *et al.*, *Carbon capture and storage: technologies, policies, economics, and implementation strategies*. CRC Press, 2012.
- [33] Global CCS Institute. "Large Scale CCS Projects." <https://www.globalccsinstitute.com/projects/large-scale-ccs-projects> (accessed February 16, 2017).
- [34] J. D. Figueroa, T. Fout, S. Plasynski, H. McIlvried, and R. D. Srivastava, "Advances in CO₂ capture technology—The U.S. Department of Energy's Carbon Sequestration Program," *International Journal of Greenhouse Gas Control*, vol. 2, no. 1, pp. 9-20, 2008.
- [35] IPCC, "Climate change 2013: the physical science basis: Working Group I contribution to the Fifth assessment report of the Intergovernmental Panel on Climate Change," Cambridge University Press, 110705799X, 2013. [Online]. Available: http://www.climatechange2013.org/images/report/WG1AR5_Frontmatter_FIN_AL.pdf
- [36] B. Metz, O. Davidson, H. De Coninck, M. Loos, and L. Meyer, "IPCC special report on carbon dioxide capture and storage," Intergovernmental Panel on Climate Change, Geneva (Switzerland). Working Group III, 2005.
- [37] B. Shimekit and H. Mukhtar, "Natural Gas Purification Technologies - Major advances for CO₂ Separation and Future Directions," in *Advances in Natural Gas Technology*, H. Al-Megren Ed.: InTech, 2012, ch. Chapter 9.
- [38] J. A. Gibson *et al.*, "Adsorption materials and processes for carbon capture from gas-fired power plants: AMPGas," *Industrial & Engineering Chemistry Research*, vol. 55, no. 13, pp. 3840-3851, 2016.

- [39] M. Younas, M. Sohail, L. K. Leong, M. J. Bashir, and S. Sumathi, "Feasibility of CO₂ adsorption by solid adsorbents: a review on low-temperature systems," *International Journal of Environmental Science and Technology*, journal article vol. 13, no. 7, pp. 1839-1860, 2016.
- [40] Y. Alcheikhhamdon and M. Hoorfar, "Natural gas purification from acid gases using membranes: A review of the history, features, techno-commercial challenges, and process intensification of commercial membranes," *Chemical Engineering and Processing: Process Intensification*, vol. 120, pp. 105-113, 2017.
- [41] K. Dalane, Z. Dai, G. Mogseth, M. Hillestad, and L. Deng, "Potential applications of membrane separation for subsea natural gas processing: A review," *Journal of Natural Gas Science and Engineering*, vol. 39, pp. 101-117, 2017.
- [42] T. E. Rufford *et al.*, "The removal of CO₂ and N₂ from natural gas: A review of conventional and emerging process technologies," *Journal of Petroleum Science and Engineering*, vol. 94-95, pp. 123-154, 2012.
- [43] A. S. Holmes and J. M. Ryan, "Cryogenic distillative separation of acid gases from methane," ed: Google Patents, 1982.
- [44] V. Singh, E. J. Grave, P. S. Northrop, and N. Sundaram, "Integrated controlled freeze zone (CFZ) tower and dividing wall (DWC) for enhanced hydrocarbon recovery," ed: Google Patents, 2012.
- [45] D. Y. C. Leung, G. Caramanna, and M. M. Maroto-Valer, "An overview of current status of carbon dioxide capture and storage technologies," *Renewable and Sustainable Energy Reviews*, vol. 39, pp. 426-443, 2014.
- [46] M. K. Mondal, H. K. Balsora, and P. Varshney, "Progress and trends in CO₂ capture/separation technologies: A review," *Energy*, vol. 46, no. 1, pp. 431-441, 2012.
- [47] W. M. Budzianowski, "Explorative analysis of advanced solvent processes for energy efficient carbon dioxide capture by gas-liquid absorption," *International Journal of Greenhouse Gas Control*, vol. 49, pp. 108-120, 2016.
- [48] M. R. Abu-Zahra, Z. Abbas, P. Singh, and P. Feron, "Carbon dioxide post-combustion capture: solvent technologies overview, status and future directions," in *Materials and processes for energy: communicating current research and technological developments*, vol. 1, A. Méndez-Vilas Ed., 2013, pp. 923-934.
- [49] W. M. Budzianowski, "Single solvents, solvent blends, and advanced solvent systems in CO₂ capture by absorption: a review," *International Journal of Global Warming*, vol. 7, no. 2, pp. 184-225, 2015.
- [50] R. Idem *et al.*, "Practical experience in post-combustion CO₂ capture using reactive solvents in large pilot and demonstration plants," *International Journal of Greenhouse Gas Control*, vol. 40, pp. 6-25, 2015.

- [51] M.-G. Lee, D. Kang, Y. Yoo, H. Jo, H.-J. Song, and J. Park, "Continuous and Simultaneous CO₂ Absorption, Calcium Extraction, and Production of Calcium Carbonate Using Ammonium Nitrate," *Industrial & Engineering Chemistry Research*, vol. 55, no. 45, pp. 11795-11800, 2016.
- [52] E. I. Koytsoumpa, C. Bergins, and E. Kakaras, "The CO₂ economy: Review of CO₂ capture and reuse technologies," *The Journal of Supercritical Fluids*, vol. 132, pp. 3-16, 2018.
- [53] Q. Zhu, "Developments on CO₂-utilization technologies," *Clean Energy*, vol. 3, no. 2, pp. 85-100, 2019.
- [54] M. De Falco, G. Iaquaniello, and G. Centi, *CO₂: a valuable source of carbon*. Springer, 2013.
- [55] A. Rafiee, K. Rajab Khalilpour, D. Milani, and M. Panahi, "Trends in CO₂ conversion and utilization: A review from process systems perspective," *Journal of Environmental Chemical Engineering*, vol. 6, no. 5, pp. 5771-5794, 2018.
- [56] P. Brinckerhoff, "Accelerating the uptake of CCS: industrial use of captured carbon dioxide," *Global CCS Institute*, p. 260, 2011.
- [57] R. M. Cuéllar-Franca and A. Azapagic, "Carbon capture, storage and utilisation technologies: A critical analysis and comparison of their life cycle environmental impacts," *Journal of CO₂ Utilization*, vol. 9, pp. 82-102, 2015.
- [58] S. K. Ritter. (2007, 30 April 2007) What can we do with Carbon Dioxide? *Chemical and Engineering News*. 11-17.
- [59] S. Moret, P. J. Dyson, and G. Laurenczy, "Direct synthesis of formic acid from carbon dioxide by hydrogenation in acidic media," *Nature communications*, vol. 5, 2014.
- [60] D. Chaturvedi, "Recent developments on the carbamation of amines," *Current Organic Chemistry*, vol. 15, no. 10, pp. 1593-1624, 2011.
- [61] Z.-Z. Yang, L.-N. He, J. Gao, A.-H. Liu, and B. Yu, "Carbon dioxide utilization with C–N bond formation: carbon dioxide capture and subsequent conversion," *Energy & Environmental Science*, vol. 5, no. 5, pp. 6602-6639, 2012.
- [62] S. Park, M.-G. Lee, and J. Park, "CO₂ (carbon dioxide) fixation by applying new chemical absorption-precipitation methods," *Energy*, vol. 59, pp. 737-742, 2013.
- [63] J. L. Galvez-Martos *et al.*, "Environmental assessment of aqueous alkaline absorption of carbon dioxide and its use to produce a construction material," *Resources, Conservation and Recycling*, vol. 107, pp. 129-141, 2016.
- [64] R. H. Heyn, "Chapter 7 - Organic Carbonates," in *Carbon Dioxide Utilisation*, P. Styring, E. A. Quadrelli, and K. Armstrong Eds. Amsterdam: Elsevier, 2015, pp. 97-113.

- [65] S.-J. Han and J.-H. Wee, "Carbon Dioxide Fixation by Combined Method of Physical Absorption and Carbonation in NaOH-Dissolved Methanol," *Energy & Fuels*, vol. 31, no. 2, pp. 1747-1755, 2017.
- [66] F. Barzagli, F. Mani, and M. Peruzzini, "From greenhouse gas to feedstock: formation of ammonium carbamate from CO₂ and NH₃ in organic solvents and its catalytic conversion into urea under mild conditions," *Green Chemistry*, 10.1039/C0GC00674B vol. 13, no. 5, pp. 1267-1274, 2011.
- [67] S. Zheng, M. Tao, Q. Liu, L. Ning, Y. He, and Y. Shi, "Capturing CO₂ into the Precipitate of a Phase-Changing Solvent after Absorption," *Environmental Science & Technology*, vol. 48, no. 15, pp. 8905-8910, 2014.
- [68] J. Sim *et al.*, "Isolation and Crystal Structure Determination of Piperazine Dicarbamate Obtained from a Direct Reaction between Piperazine and Carbon Dioxide in Methanol," *Bulletin of the Korean Chemical Society*, vol. 37, no. 11, pp. 1854-1857, 2016.
- [69] V. Barbarossa, F. Barzagli, F. Mani, S. Lai, P. Stoppioni, and G. Vanga, "Efficient CO₂ capture by non-aqueous 2-amino-2-methyl-1-propanol (AMP) and low temperature solvent regeneration," *RSC Advances*, 10.1039/C3RA40933C vol. 3, no. 30, pp. 12349-12355, 2013.
- [70] Y. Yoo, D. Kang, I. Kim, and J. Park, "Characteristics of Metal Cation Carbonation and Carbon Dioxide Utilization Using Seawater-Based Industrial Wastewater," *ChemistrySelect*, vol. 3, no. 32, pp. 9284-9292, 2018.
- [71] B. Guo, T. Zhao, F. Sha, F. Zhang, Q. Li, and J. Zhang, "A novel CCU approach of CO₂ by the system 1,2-ethylenediamine+1,2-ethylene glycol," *Korean Journal of Chemical Engineering*, Article vol. 33, no. 6, pp. 1883-1888, 2016.
- [72] S.-J. Han, M. Yoo, D.-W. Kim, and J.-H. Wee, "Carbon dioxide capture using calcium hydroxide aqueous solution as the absorbent," *Energy & Fuels*, vol. 25, no. 8, pp. 3825-3834, 2011.
- [73] J. T. Yeh, K. P. Resnik, K. Rygle, and H. W. Pennline, "Semi-batch absorption and regeneration studies for CO₂ capture by aqueous ammonia," *Fuel Processing Technology*, vol. 86, no. 14-15, pp. 1533-1546, 2005.
- [74] F. Kozak, A. Petig, E. Morris, R. Rhudy, and D. Thimsen, "Chilled ammonia process for CO₂ capture," *Energy Procedia*, vol. 1, no. 1, pp. 1419-1426, 2009.
- [75] D. Sutter, M. Gazzani, J.-F. Pérez-Calvo, C. Leopold, F. Milella, and M. Mazzotti, "Solid formation in ammonia-based processes for CO₂ capture—Turning a challenge into an opportunity," *Energy Procedia*, vol. 114, pp. 866-872, 2017.
- [76] P. Kumar, M. Varyani, P. K. Khatri, S. Paul, and S. L. Jain, "Post combustion capture and conversion of carbon dioxide using histidine derived ionic liquid at ambient conditions," *Journal of Industrial and Engineering Chemistry*, vol. 49, pp. 152-157, 2017.

- [77] M. Liu, L. Liang, X. Li, X. Gao, and J. Sun, "Novel urea derivative-based ionic liquids with dual-functions: CO₂ capture and conversion under metal- and solvent-free conditions," *Green Chemistry*, vol. 18, no. 9, pp. 2851-2863, 2016.
- [78] M. S. Fonari, S. Antal, R. Castaneda, C. Ordonez, and T. V. Timofeeva, "Crystalline products of CO₂ capture by piperazine aqueous solutions," *CrystEngComm*, 10.1039/C6CE01083K vol. 18, no. 33, pp. 6282-6289, 2016.
- [79] A. Uma Maheswari and K. Palanivelu, "Alkyl amine and vegetable oil mixture—a viable candidate for CO₂ capture and utilization," *Environmental Science and Pollution Research*, pp. 1-13, 2016.
- [80] A. Uma Maheswari and K. Palanivelu, "Absorption of carbon dioxide in alkanolamine and vegetable oil mixture and isolation of 2-amino-2-methyl-1-propanol carbamate," *Journal of CO₂ Utilization*, vol. 6, pp. 45-52, 2014.
- [81] A. Uma Maheswari and K. Palanivelu, "Carbon Dioxide Capture and Utilization by Alkanolamines in Deep Eutectic Solvent Medium," *Industrial & Engineering Chemistry Research*, vol. 54, no. 45, pp. 11383-11392, 2015.
- [82] M. Hasib-ur-Rahman, M. Siaj, and F. Larachi, "CO₂ capture in alkanolamine/room-temperature ionic liquid emulsions: A viable approach with carbamate crystallization and curbed corrosion behavior," *International Journal of Greenhouse Gas Control*, vol. 6, pp. 246-252, 2012.
- [83] A. Dindi, D. V. Quang, N. E. Hadri, A. Rayer, A. Abdulkadir, and M. R. M. Abu-Zahra, "Potential for the Simultaneous Capture and Utilization of CO₂ Using Desalination Reject Brine: Amine Solvent Selection and Evaluation," *Energy Procedia*, vol. 63, pp. 7947-7953, 2014.
- [84] D. Kang, S. Park, H. Jo, and J. Park, "Carbon fixation using calcium oxide by an aqueous approach at moderate conditions," *Chemical Engineering Journal*, vol. 248, pp. 200-207, 2014.
- [85] T. Zhao, B. Guo, F. Zhang, F. Sha, Q. Li, and J. Zhang, "Morphology control in the synthesis of CaCO₃ microspheres with a novel CO₂-storage material," *ACS applied materials & interfaces*, vol. 7, no. 29, pp. 15918-15927, 2015.
- [86] S. Park, J.-H. Bang, K. Song, C. W. Jeon, and J. Park, "Barium carbonate precipitation as a method to fix and utilize carbon dioxide," *Chemical Engineering Journal*, vol. 284, pp. 1251-1258, 2016.
- [87] M. Arti, M. H. Youn, K. T. Park, H. J. Kim, Y. E. Kim, and S. K. Jeong, "Single Process for CO₂ Capture and Mineralization in Various Alkanolamines Using Calcium Chloride," *Energy & Fuels*, vol. 31, no. 1, pp. 763-769, 2017.
- [88] F. Sha *et al.*, "Direct non-biological CO₂ mineralization for CO₂ capture and utilization on the basis of amine-mediated chemistry," *Journal of CO₂ Utilization*, vol. 24, pp. 407-418, 2018.
- [89] V. Darde, K. Thomsen, W. J. Van Well, and E. H. Stenby, "Chilled ammonia process for CO₂ capture," *Energy Procedia*, vol. 1, no. 1, pp. 1035-1042, 2009.

- [90] A. Gaur, J.-W. Park, and J.-H. Jang, "Metal-carbonate formation from ammonia solution by addition of metal salts—An effective method for CO₂ capture from landfill gas (LFG)," *Fuel Processing Technology*, vol. 91, no. 11, pp. 1500-1504, 2010.
- [91] Z.-Z. Yang, L.-N. He, Y.-N. Zhao, B. Li, and B. Yu, "CO₂ capture and activation by superbase/polyethylene glycol and its subsequent conversion," *Energy & Environmental Science*, vol. 4, no. 10, pp. 3971-3975, 2011.
- [92] Z. H. Liang *et al.*, "Recent progress and new developments in post-combustion carbon-capture technology with amine based solvents," *International Journal of Greenhouse Gas Control*, vol. 40, pp. 26-54, 2015.
- [93] J. Ejenstam, "The lime industry, a potential business area for Kanthal," ed, 2010.
- [94] L. M. Diamante and T. Lan, "Absolute Viscosities of Vegetable Oils at Different Temperatures and Shear Rate Range of 64.5 to 4835 per second," *Journal of Food Processing*, vol. 2014, p. 6, 2014, Art no. 234583.
- [95] H. Nouredini, B. Teoh, and L. Davis Clements, "Viscosities of vegetable oils and fatty acids," *Journal of the American Oil Chemists' Society*, vol. 69, no. 12, pp. 1189-1191, 1992.
- [96] A. Shamiri, M. Shafeeyan, H. Tee, C. Leo, M. Aroua, and N. Aghamohammadi, "Absorption of CO₂ into aqueous mixtures of glycerol and monoethanolamine," *Journal of Natural Gas Science and Engineering*, vol. 35, pp. 605-613, 2016.
- [97] S. Leclaire, M. Reggio, and J.-Y. Trépanier, "Progress and investigation on lattice Boltzmann modeling of multiple immiscible fluids or components with variable density and viscosity ratios," *Journal of Computational Physics*, vol. 246, pp. 318-342, 2013.
- [98] M. Yoo, S.-J. Han, and J.-H. Wee, "Carbon dioxide capture capacity of sodium hydroxide aqueous solution," *Journal of Environmental Management*, vol. 114, pp. 512-519, 2013.
- [99] T. Ma *et al.*, "A process simulation study of CO₂ capture by ionic liquids," *International Journal of Greenhouse Gas Control*, vol. 58, pp. 223-231, 2017.
- [100] Z. Huang *et al.*, "Investigation of glycerol-derived binary and ternary systems in CO₂ capture process," *Fuel*, vol. 210, pp. 836-843, 2017.
- [101] P. Luis, "Use of monoethanolamine (MEA) for CO₂ capture in a global scenario: Consequences and alternatives," *Desalination*, vol. 380, pp. 93-99, 2016.
- [102] E. Sanchez Fernandez *et al.*, "Conceptual design of a novel CO₂ capture process based on precipitating amino acid solvents," *Industrial & Engineering Chemistry Research*, vol. 52, no. 34, pp. 12223-12235, 2013.
- [103] M. Hasib-ur-Rahman and F. Larachi, "CO₂ Capture in Alkanolamine-RTIL Blends via Carbamate Crystallization: Route to Efficient Regeneration," *Environmental Science & Technology*, vol. 46, no. 20, pp. 11443-11450, 2012.

- [104] R. Zhang, Q. Yang, B. Yu, H. Yu, and Z. Liang, "Toward to efficient CO₂ capture solvent design by analyzing the effect of substituent type connected to N-atom," *Energy*, vol. 144, pp. 1064-1072, 2018.
- [105] K. P. Shen and M. H. Li, "Solubility of carbon dioxide in aqueous mixtures of monoethanolamine with methyldiethanolamine," *Journal of Chemical & Engineering Data*, vol. 37, no. 1, pp. 96-100, 1992.
- [106] F. Harris, K. A. Kurnia, M. I. A. Mutalib, and M. Thanapalan, "Solubilities of Carbon Dioxide and Densities of Aqueous Sodium Glycinate Solutions before and after CO₂ Absorption," *Journal of Chemical & Engineering Data*, vol. 54, no. 1, pp. 144-147, 2009.
- [107] M. Haji-Sulaiman, M. Aroua, and A. Benamor, "Analysis of equilibrium data of CO₂ in aqueous solutions of diethanolamine (DEA), methyldiethanolamine (MDEA) and their mixtures using the modified Kent Eisenberg model," *Chemical Engineering Research and Design*, vol. 76, no. 8, pp. 961-968, 1998.
- [108] S. Jamaludin and R. Salleh, "Absorption of Carbon Dioxide in the aqueous solution of Diethanolamine (DEA) blended with 1-Butyl-1-Methylpyrrolidinium Trifluoromethanesulfonate [BmPyr][OTf] at high pressure," in *IOP Conference Series: Materials Science and Engineering*, 2018, vol. 334, no. 1: IOP Publishing, p. 012055.
- [109] P.-Y. Chung, A. N. Soriano, R. B. Leron, and M.-H. Li, "Equilibrium solubility of carbon dioxide in the amine solvent system of (triethanolamine+piperazine+water)," *The Journal of Chemical Thermodynamics*, vol. 42, no. 6, pp. 802-807, 2010.
- [110] S. N. Khan, S. M. Hailegiorgis, Z. Man, and A. M. Shariff, "High pressure solubility of carbon dioxide (CO₂) in aqueous solution of piperazine (PZ) activated N-methyldiethanolamine (MDEA) solvent for CO₂ capture," in *AIP Conference Proceedings*, 2017, vol. 1891, no. 1: AIP Publishing, p. 020081.
- [111] I.-S. Jane and M.-H. Li, "Solubilities of mixtures of carbon dioxide and hydrogen sulfide in water+ diethanolamine+ 2-amino-2-methyl-1-propanol," *Journal of Chemical & Engineering Data*, vol. 42, no. 1, pp. 98-105, 1997.
- [112] P. Tontiwachwuthikul, A. Meisen, and C. J. Lim, "Solubility of carbon dioxide in 2-amino-2-methyl-1-propanol solutions," *Journal of chemical and engineering data*, vol. 36, no. 1, pp. 130-133, 1991.
- [113] G. G. Murshid, K. Lau, and F. F. Ahmad, "Solubility of CO₂ in aqueous solutions of 2-amino-2-methyl-1-propanol at high pressure," *World Academy of Science, Engineering and Technology*, vol. 6, 2011.
- [114] M. W. Arshad, H. F. Svendsen, P. L. Fosbøl, N. von Solms, and K. Thomsen, "Equilibrium total pressure and CO₂ solubility in binary and ternary aqueous solutions of 2-(diethylamino) ethanol (DEEA) and 3-(methylamino) propylamine (MAPA)," *Journal of Chemical & Engineering Data*, vol. 59, no. 3, pp. 764-774, 2014.

- [115] B. Yu *et al.*, "Characterisation and kinetic study of carbon dioxide absorption by an aqueous diamine solution," *Applied Energy*, vol. 208, pp. 1308-1317, 2017.
- [116] D. Nath, "Solubility of Carbon Dioxide (CO₂) in Aqueous 3-(Dimethylamino)-1-Propylamine," in *14th Greenhouse Gas Control Technologies Conference Melbourne*, 2018, pp. 21-26.
- [117] Y. Mergler, R. Rumley-van Gurp, P. Brassler, M. de Koning, and E. Goetheer, "Solvents for CO₂ capture. Structure-activity relationships combined with vapour-liquid-equilibrium measurements," *Energy Procedia*, vol. 4, pp. 259-266, 2011.
- [118] S. P. Verevkin and Y. Chernyak, "Vapor pressure and enthalpy of vaporization of aliphatic propanediamines," *The Journal of Chemical Thermodynamics*, vol. 47, pp. 328-334, 2012.
- [119] V. A. Pozdeev and S. P. Verevkin, "Vapor pressure and enthalpy of vaporization of linear aliphatic alkanediamines," *The Journal of Chemical Thermodynamics*, vol. 43, no. 12, pp. 1791-1799, 2011.
- [120] N. Yang, H. Yu, D. y. Xu, W. Conway, M. Maeder, and P. Feron, "Amino acids/NH₃ Mixtures for CO₂ Capture: Effect of Neutralization Methods on CO₂ Mass Transfer and NH₃ Vapour Loss," *Energy Procedia*, vol. 63, pp. 773-780, 2014.
- [121] U. E. Aronu, A. F. Ciftja, I. Kim, and A. Hartono, "Understanding Precipitation in Amino Acid Salt systems at Process Conditions," *Energy Procedia*, vol. 37, pp. 233-240, 2013.
- [122] A. F. Portugal, P. W. J. Derks, G. F. Versteeg, F. D. Magalhães, and A. Mendes, "Characterization of potassium glycinate for carbon dioxide absorption purposes," *Chemical Engineering Science*, vol. 62, no. 23, pp. 6534-6547, 2007.
- [123] A. F. Portugal, J. M. Sousa, F. D. Magalhães, and A. Mendes, "Solubility of carbon dioxide in aqueous solutions of amino acid salts," *Chemical Engineering Science*, vol. 64, no. 9, pp. 1993-2002, 2009.
- [124] M. S. Shaikh, M. S. Azmi, M. A. Bustam, and G. Murshid, "Study of CO₂ Solubility in Aqueous Blend of Potassium Carbonate Promoted with Glycine," in *Applied Mechanics and Materials*, 2014, vol. 625: Trans Tech Publ, pp. 19-23.
- [125] H. Thee, N. J. Nicholas, K. H. Smith, G. da Silva, S. E. Kentish, and G. W. Stevens, "A kinetic study of CO₂ capture with potassium carbonate solutions promoted with various amino acids: Glycine, sarcosine and proline," *International Journal of Greenhouse Gas Control*, vol. 20, no. Supplement C, pp. 212-222, 2014.
- [126] M. E. Hamzehie and H. Najibi, "Experimental and theoretical study of carbon dioxide solubility in aqueous solution of potassium glycinate blended with

- piperazine as new absorbents," *Journal of CO₂ Utilization*, vol. 16, pp. 64-77, 2016.
- [127] A. F. Ciftja, A. Hartono, and H. F. Svendsen, "Selection of Amine Amino Acids Salt Systems for CO₂ Capture," *Energy Procedia*, vol. 37, no. Supplement C, pp. 1597-1604, 2013.
- [128] U. E. Aronu, E. T. Hessen, T. Haug-Warberg, K. A. Hoff, and H. F. Svendsen, "Equilibrium absorption of carbon dioxide by amino acid salt and amine amino acid salt solutions," *Energy Procedia*, vol. 4, no. Supplement C, pp. 109-116, 2011.
- [129] M. Caplow, "Kinetics of carbamate formation and breakdown," *Journal of the American Chemical Society*, vol. 90, no. 24, pp. 6795-6803, 1968.
- [130] B. Arstad, R. Blom, and O. Swang, "CO₂ Absorption in Aqueous Solutions of Alkanolamines: Mechanistic Insight from Quantum Chemical Calculations," *The Journal of Physical Chemistry A*, vol. 111, no. 7, pp. 1222-1228, 2007.
- [131] B. Yu *et al.*, "Postcombustion Capture of CO₂ by Diamines Containing One Primary and One Tertiary Amino Group: Reaction Rate and Mechanism," *Energy & Fuels*, vol. 33, no. 8, pp. 7500-7508, 2019.
- [132] A. M. Shariff, M. S. Shaikh, M. A. Bustam, S. Garg, N. Faiqa, and A. Aftab, "High-pressure Solubility of Carbon Dioxide in Aqueous Sodium L- Proline Solution," *Procedia Engineering*, vol. 148, pp. 580-587, 2016.
- [133] S. Garg, A. M. Shariff, M. S. Shaikh, B. Lal, A. Aftab, and N. Faiqa, "Selected Physical Properties of Aqueous Potassium Salt of L-Phenylalanine as a Solvent for CO₂ Capture," *Chemical Engineering Research and Design*, vol. 113, pp. 169-181, 2016.
- [134] S. Garg, A. Shariff, M. Shaikh, B. Lal, A. Aftab, and N. Faiqa, "Surface tension and derived surface thermodynamic properties of aqueous sodium salt of l-phenylalanine," *Indian Journal of Science and Technology*, vol. 9, no. 29, 2016.
- [135] F. Koohyar, "Refractive Index and Its Applications," *Journal of Thermodynamics and Catalysis*, vol. 4, no. 2, 2013.
- [136] M. S. Shaikh, A. M. Shariff, M. A. Bustam, and G. Murshid, "Physicochemical properties of aqueous solutions of sodium glycinate in the non-precipitation regime from 298.15 to 343.15 K," *Chinese Journal of Chemical Engineering*, vol. 23, no. 3, pp. 536-540, 2015.
- [137] T. A. Graber, H. R. Galleguillos, C. Céspedes, and M. E. Taboada, "Density, refractive index, viscosity, and electrical conductivity in the Na₂CO₃+ Poly (ethylene glycol)+ H₂O system from (293.15 to 308.15) K," *Journal of Chemical & Engineering Data*, vol. 49, no. 5, pp. 1254-1257, 2004.
- [138] L.-A. Tirona, R. B. Leron, A. N. Soriano, and M.-H. Li, "Densities, viscosities, refractive indices, and electrical conductivities of aqueous alkali salts of α -

- alanine," *The Journal of Chemical Thermodynamics*, vol. 77, pp. 116-122, 2014.
- [139] P.-Y. Lin, A. N. Soriano, R. B. Leron, and M.-H. Li, "Electrolytic conductivity and molar heat capacity of two aqueous solutions of ionic liquids at room-temperature: Measurements and correlations," *The Journal of Chemical Thermodynamics*, vol. 42, no. 8, pp. 994-998, 2010.
- [140] A. Aftab, A. M. Shariff, S. Garg, B. Lal, M. S. Shaikh, and N. Faiqa, "Solubility of CO₂ in aqueous sodium β-alaninate: Experimental study and modeling using Kent Eisenberg model," *Chemical Engineering Research and Design*, 2017.
- [141] A. Blanco, A. García-Abuín, D. Gómez-Díaz, and J. M. Navaza, "Density, Speed of Sound, Viscosity and Surface Tension of 3-Dimethylamino-1-propylamine + Water, 3-Amino-1-propanol + 3-Dimethylamino-1-propanol, and (3-Amino-1-propanol + 3-Dimethylamino-1-propanol) + Water from T = (293.15 to 323.15) K," *Journal of Chemical & Engineering Data*, vol. 62, no. 8, pp. 2272-2279, 2017.
- [142] M. S. Shaikh, A. M. Shariff, M. A. Bustam, and G. Murshid, "Measurement and prediction of physical properties of aqueous sodium l-prolinate and piperazine as a solvent blend for CO₂ removal," *Chemical Engineering Research and Design*, vol. 102, pp. 378-388, 2015.
- [143] U. E. Aronu, A. Hartono, and H. F. Svendsen, "Density, viscosity, and N₂O solubility of aqueous amino acid salt and amine amino acid salt solutions," *The Journal of Chemical Thermodynamics*, vol. 45, no. 1, pp. 90-99, 2012.
- [144] S. M. Shaban, "N-(3-(Dimethyl benzyl ammonio)propyl)alkanamide chloride derivatives as corrosion inhibitors for mild steel in 1 M HCl solution: experimental and theoretical investigation," *RSC Advances*, 10.1039/C6RA00252H vol. 6, no. 46, pp. 39784-39800, 2016.
- [145] W. Phakhodee, S. Wangngae, and M. Pattarawarapan, "Metal-free amidation of carboxylic acids with tertiary amines," *RSC Advances*, vol. 6, no. 65, pp. 60287-60290, 2016.
- [146] B. C. Smith, *Infrared spectral interpretation: a systematic approach*. CRC press, 1998.
- [147] M. Ibrahim, A. Nada, and D. E. Kamal, "Density functional theory and FTIR spectroscopic study of carboxyl group," 2005.
- [148] F. Harris, K. A. Kurnia, M. I. A. Mutalib, and M. Thanapalan, "Solubilities of carbon dioxide and densities of aqueous sodium glycinate solutions before and after CO₂ absorption," *Journal of Chemical & Engineering Data*, vol. 54, no. 1, pp. 144-147, 2008.
- [149] J. Ederer *et al.*, "Determination of amino groups on functionalized graphene oxide for polyurethane nanomaterials: XPS quantitation vs. functional speciation," *RSC Advances*, vol. 7, no. 21, pp. 12464-12473, 2017.

APPENDIX A

Physical properties of absorbent

The equipment used to measure the physical properties of the absorbent were calibrated by using deionized water. The density, refractive index, surface tension, and viscosity of the deionized water were compared with previous literature [133] as shown in Table A1. The average absolute deviations (AAD) recorded were less than 3%, mainly attributed to the uncertainty in measurements, variations in purity of deionized water, and different types of equipment used in the experiment. Nonetheless, the small AAD reported indicated that the experimental results were within close proximity to the work reported by Garg et al. [133].

Table A1: Comparison of experimental (Exp.) physical properties of deionized water with previous literature (Lit.) [133] at various temperatures (T).

T (K)	Density, ρ (g/cm³)		Refractive index, RI (nD)		Surface tension, γ (mN/m)		Viscosity, η (mPa.s)	
	Exp.	Lit.	Exp.	Lit.	Exp.	Lit.	Exp.	Lit.
298.15	0.99704	0.99696	1.332531	1.33243	71.76	71.79	0.897	0.895
303.15	0.99564	0.99587	1.331931	1.33187	71.26	71.10	0.817	0.797
308.15	0.99402	0.99425	1.331291	1.33124	70.32	70.25	0.747	0.719
313.15	0.99221	0.99243	1.330565	1.33054	69.58	69.42	0.684	0.653
318.15	0.99020	0.99043	1.329778	1.32973	68.68	68.66	0.624	0.596
323.15	0.98803	0.98826	1.328937	1.32889	67.69	67.75	0.557	0.547
AAD (%)	0.02		0.01		0.12		2.95	

Table A2: Densities of the absorbent at different temperatures (T).

T (K)	Density, ρ (g/cm³)		
	0.1 M	1.0 M	2.0 M
298.15	0.9997	1.0188	1.0411
303.15	0.9982	1.0176	1.0387
308.15	0.9966	1.0156	1.0362
313.15	0.9948	1.0135	1.0339
318.15	0.9928	1.0112	1.0309
323.15	0.9906	1.0087	1.0281

Table A3: Refractive indices of the absorbent at different temperatures (T).

T (K)	Refractive index, RI (nD)		
	0.1 M	1.0 M	2.0 M
298.15	1.33610	1.36232	1.39159
303.15	1.33548	1.36152	1.39056
308.15	1.33477	1.36065	1.38949
313.15	1.33401	1.35985	1.38847
318.15	1.33323	1.35908	1.38779
323.15	1.33239	1.35846	1.38740

Table A4: Surface tensions of the absorbent at different temperatures (T).

T (K)	Surface tension, σ (mN/m)		
	0.1 M	1.0 M	2.0 M
298.15	70.8	61.5	53.9
303.15	69.6	60.7	52.4
308.15	68.7	59.6	51.7
313.15	67.5	58.6	50.6
318.15	66.3	57.9	49.6
323.15	65.3	57.1	48.8

Table A5: Viscosities of GLY-DMAPA at different temperatures (T).

T (K)	Viscosity, η (mPa.s)		
	0.1 M	1.0 M	2.0 M
298.15	1.122	2.237	3.620
303.15	1.038	2.030	3.330
308.15	0.904	1.812	2.872
313.15	0.790	1.596	2.500
318.15	0.698	1.409	2.188
323.15	0.639	1.264	1.944

Appendix B

Sample calculation for CO₂ loading capacity

The CO₂ loading capacity of 5.0 M MEA at 5 bar was determined based the following steps:

- 1) Data was collected from the computer (Figure B1)

$$P_i = 5.52 \text{ bar}; \quad P_f = 5.41 \text{ bar}; \quad P_T = 3.95 \text{ bar};$$

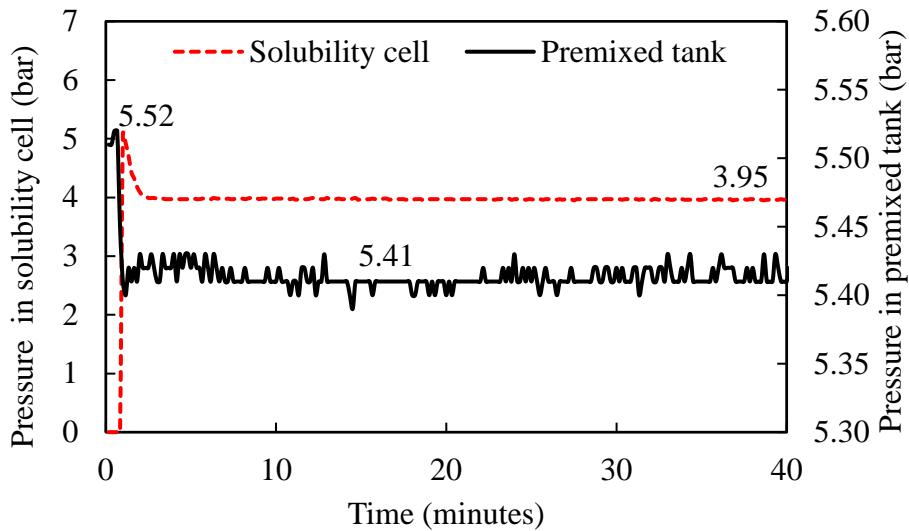


Figure B1: Pressure in solubility cell and premixed tank during the CO₂ absorption process.

- 2) The compressibility factor (Z) at respective pressure was calculated by using Peng Robinson Equation of State as per Equation B1.
(Example was based on $P_i = 5.52 \text{ bar} = 0.552 \text{ MPa}$)

$$Z^3 - (1 - B)Z^2 + (A - 3B^2 - 2B)Z - (AB - B^2 - B^3) = 0 \quad (\text{B1})$$

$$A = \frac{aP}{R^2T^2} \quad (\text{B2})$$

$$B = \frac{bP}{RT} \quad (\text{B3})$$

$$a(T_c) = 0.45724 \frac{R^2T_c^2}{P_c} \quad (\text{B4})$$

$$b(T_c) = 0.07780 \frac{RT_c}{P_c} \quad (\text{B5})$$

For carbon dioxide, $T_c = 304.2 \text{ K}$; $P_c = 7.382 \text{ MPa}$;

The values T_c and P_c were substituted into Equations B4 and B5.

The values $P = 0.552 \text{ Mpa}$, along with a and b previously determined from Equations B4 and B5 were then substituted into Equations B2 and B3. The variables a , b , A , and B are given in Table B1.

Table B1: Variables a , b , A , and B based on Peng Robinson Equation.

Variables	Values
a	396194.7
b	26.655
A	0.023
B	0.004

The variables in Table B1 were then substituted into Equation A1 to form a cubic equation $Z^3 + a_2Z^2 + a_1Z + a_0 = 0$. The values of a_2 , a_1 , and a_0 are given in Table B2.

Table B2: Variables a_2 , a_1 , and a_0 based on cubic equation $Z^3 + a_2Z^2 + a_1Z + a_0 = 0$.

Variables	Values
a_2	-0.99435
a_1	0.0202
a_0	-0.00015

The goal seek method in Microsoft Excel was then used to solve the equation, which gives $z = 0.97376$, when $P = 5.52 \text{ bar}$.

- 3) The amount of CO_2 transferred from the mixing vessel into the solubility cell was determined based on the pressure change in the pre-mixed tank based on the following equation:

$$n_{\text{CO}_2} = \frac{V_{pt}}{RT_{pt}} \left(\frac{P_i}{z_i} - \frac{P_f}{z_f} \right)$$

Data required for the calculation are as follows;

$$V_{pt} = 5 \text{ L}; \quad R = 8.314 \text{ m}^3 \cdot \text{Pa} \cdot \text{K}^{-1} \cdot \text{mol}^{-1}; \quad T_{pt} = 313.15 \text{ K}$$

$$P_i = 5.52 \text{ bar}; \quad z_i = 0.97376; \quad P_f = 5.41 \text{ bar}; \quad z_f = 0.97429;$$

number of moles of CO_2 transferred from premixed tank to solubility cell,

$$n_{\text{CO}_2} = \frac{5 \text{ L}}{8.314 \text{ m}^3 \cdot \text{Pa} \cdot \text{K}^{-1} \cdot \text{mol}^{-1} \times 313.15 \text{ K}} \left(\frac{5.52}{0.97376} - \frac{5.41}{0.97429} \right) \times \frac{1 \text{ m}^3}{1000 \text{ L}} \times \frac{10^5 \text{ Pa}}{1 \text{ bar}}$$

$$= \mathbf{0.0222749 \text{ mol}}$$

- 4) The CO₂ equilibrium pressure in the solubility cell, P_{CO₂} was determined. In this experiment, the vapor pressure was assumed to be negligible.

Hence $P_{CO_2} = P_T = 3.95 \text{ bar}$

- 5) The amount of CO₂ in the gas phase was calculated based on the following equation;

$$n_{CO_2(g)} = \frac{V_g P_{CO_2}}{z_{CO_2} RT}$$

Data required for the calculation are as follows;

$V_g = 0.045 \text{ L}$; $P_{CO_2} = 3.95 \text{ bar}$; $z_{CO_2} = 0.98128$;

$R = 8.314 \text{ m}^3 \cdot \text{Pa} \cdot \text{K}^{-1} \cdot \text{mol}^{-1}$; $T = 313.15 \text{ K}$

Number of CO₂ in the gas phase,

$$n_{CO_2(g)} = \frac{0.045 \text{ L} \times 3.95 \text{ bar}}{0.98128 \times 8.314 \text{ m}^3 \cdot \text{Pa} \cdot \text{K}^{-1} \cdot \text{mol}^{-1} \times 313.15 \text{ K}} \times \frac{1 \text{ m}^3}{1000 \text{ L}} \times \frac{10^5 \text{ Pa}}{1 \text{ bar}}$$

$$= \mathbf{0.0069575 \text{ mol}}$$

- 6) The amount of CO₂ dissolved in the absorbent (liquid phase) was determined from the following equation ($n_{CO_2(l)} = n_{CO_2} - n_{CO_2(g)}$)

$$n_{CO_2(l)} = 0.0222748 - 0.0067575 = \mathbf{0.01531 \text{ mol}}$$

- 7) CO₂ loading capacity (α) is determined by the following equation:

$$\alpha = \frac{n_{CO_2(l)}}{n_{liquid}}$$

Volume of absorbent = 5 mL.

No of moles in liquid, $n_{liquid} = \frac{5 \text{ mol}}{1000 \text{ ml}} \times 5 \text{ mL} = 0.0249 \text{ mol}$

Hence, the CO₂ loading capacity, $\alpha = \frac{0.015314}{0.0249} = \mathbf{0.616 \text{ mol CO}_2 / \text{mol MEA}}$

- 8) Steps 1 to 6 were repeated three times and the average values were reported as per Table B3.

Table B3: Data and measured values for determination of CO₂ loading capacity of 5.0 M MEA.

Exp	P_i	z_i	P_f	z_f	P_{CO_2}	z_{CO_2}	n_{CO_2}	$n_{CO_2(g)}$	$n_{CO_2(l)}$	α
1	5.52	0.9738	5.41	0.9743	3.95	0.9813	0.0223	0.0070	0.0153	0.6164
2	5.37	0.9745	5.26	0.9750	3.83	0.9819	0.0223	0.0067	0.0155	0.6237
3	5.48	0.9740	5.36	0.9745	4.43	0.9790	0.0243	0.0078	0.0165	0.6627

Average CO₂ loading capacity of 5.0 M MEA measured at 5 bar,

$$\alpha_{average} = \frac{0.6164 + 0.6237 + 0.6627}{3} = \mathbf{0.634 \text{ mol CO}_2 / \text{mol MEA}}$$

APPENDIX C

Verification of solubility cell for measuring CO₂ solubility

To confirm the reliability of the solubility cell used in this study, the CO₂ loading capacities of 5.0 M MEA (30 w/w %) and 1.0 M GLY-KOH were measured at pressure ranging from 5 to 25 bar and temperature of 313.15 K are presented in Figure C1. The experiments were repeated three times and the average standard deviations for pressure and CO₂ loading capacities were reported for pressure and CO₂ solubility were less than 0.15 bar and 0.05 mol CO₂/ mol absorbent, respectively (Table C1 and C2). The small standard deviations suggested that the equipment have high reliability in measuring the CO₂ solubility of the absorbent.

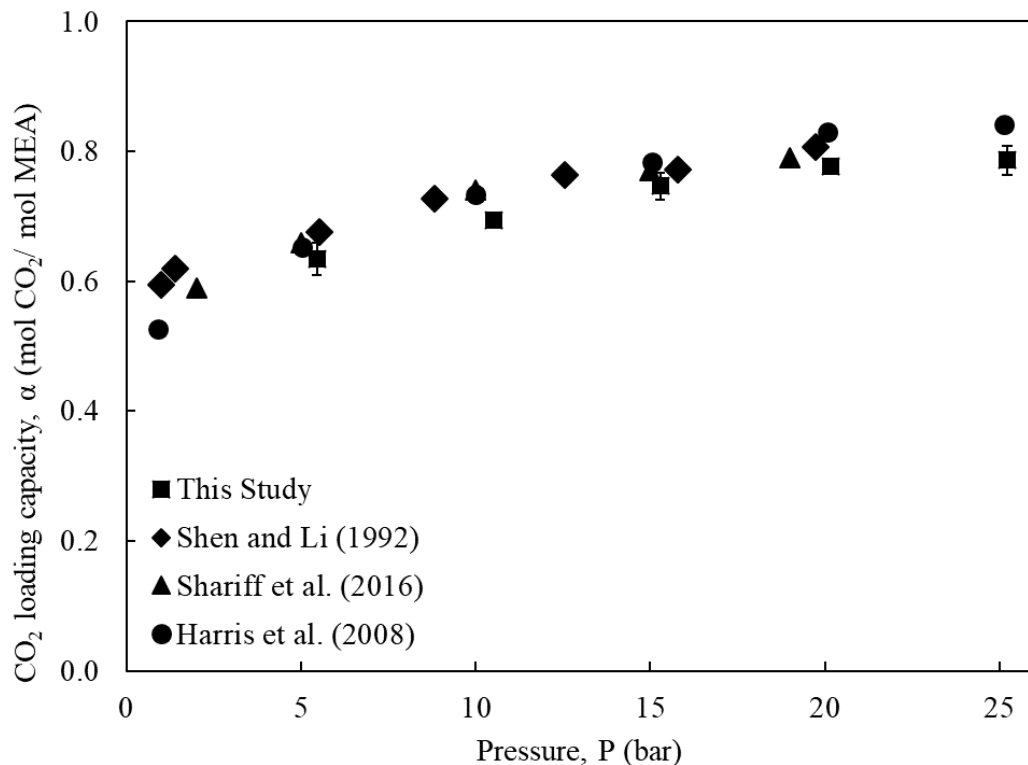


Figure C1: CO₂ loading capacities of 5.0 M monoethanolamine (MEA) in comparison with previous literatures (Temperature: 313.15 K).

Table C1: The standard deviations for pressure and CO₂ loading capacities of 5.0 MEA measured at 313.15 K.

Pressure (bar)			CO ₂ loading capacities (mol CO ₂ / mol MEA)		
Measured values	Average values	Standard deviations	Measured values	Average values	Standard deviations
5.52			0.616		
5.37	5.46	0.08	0.624	0.634	0.025
5.48			0.663		
10.62			0.694		
10.48	10.51	0.10	0.698	0.695	0.004
10.43			0.692		
15.09			0.748		
15.31	15.28	0.18	0.725	0.746	0.020
15.44			0.766		
20.01			0.779		
20.34	20.17	0.17	0.769	0.778	0.003
20.17			0.785		
25.35			0.810		
25.15	25.21	0.12	0.784	0.786	0.021
25.14			0.766		
Average standard deviation		0.13	Average standard deviation		0.015

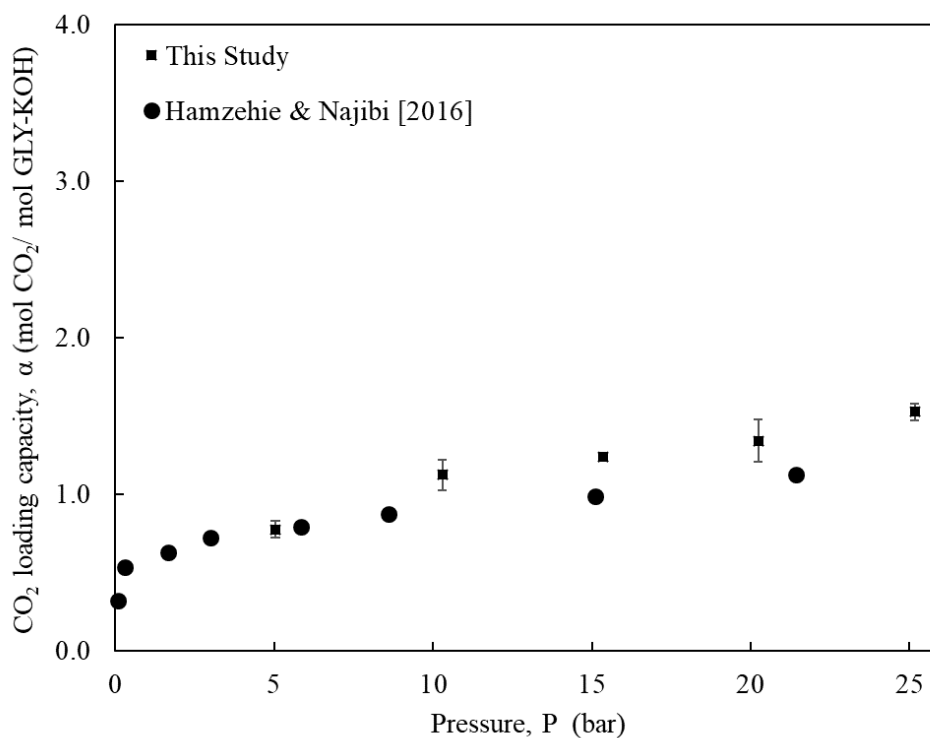


Figure C2: CO₂ loading capacities of 1.0 M GLY-KOH in comparison with previous literature (Temperature: 313.15 K).

Table C2: The standard deviations for pressure and CO₂ loading capacity of 1.0 M GLY-KOH measured at 313.15 K.

Pressure (bar)			CO₂ loading capacities (mol CO₂/ mol GLY-KOH)		
Measured values	Average values	Standard deviations	Measured values	Average values	Standard deviations
5.02			0.780		
5.06	5.03	0.03	0.810	0.815	0.039
5.01			0.857		
10.31			1.120		
10.22	10.29	0.07	1.048	1.062	0.053
10.35			1.016		
15.30			1.248		
15.44	15.35	0.08	1.218	1.242	0.021
15.31			1.260		
20.23			1.407		
20.15	20.23	0.09	1.470	1.412	0.056
20.32			1.358		
25.29			1.566		
25.10	25.17	0.11	1.467	1.528	0.054
25.11			1.551		
Average standard deviation		0.07	Average standard deviation		0.045

APPENDIX D

Experimental data on CO₂ solubility study at different temperature and pressure

Table D1: The CO₂ loading capacities (α) of 1.0 M amino-N-(3 (dimethylamino)propyl) acetamide measured at different temperature and pressure (P).

Temperature					
303.15 K		313.15 K		323.15 K	
P	α	P	α	P	α
5.15	1.609	5.07	1.224	5.21	0.749
9.99	2.149	10.10	1.463	10.28	1.169
15.00	2.460	15.05	1.829	15.20	1.512
20.27	2.723	20.12	2.186	20.26	1.749
25.11	3.058	25.24	2.419	25.57	1.963

Table D2: The CO₂ loading capacities (α) of 0.1 M to 2.0 M amino-N-(3-(dimethylamino)propyl)acetamide measure at different pressure (P) and 303.15 K.

Concentration of GLY-DMAPA									
0.1 M		0.5 M		1.0 M		1.5 M		2.0 M	
P	α	P	α	P	α	P	α	P	α
5.08	4.038	5.30	2.664	5.15	1.609	5.23	1.117	5.18	0.961
10.16	5.748	10.10	3.203	9.99	2.149	10.09	1.556	10.00	1.271
15.23	7.419	15.01	3.838	15.00	2.460	15.23	1.797	15.07	1.484
20.49	8.072	20.27	4.337	20.27	2.723	20.32	2.039	20.11	1.640
25.26	8.997	25.11	4.493	25.11	3.058	25.46	2.269	25.38	1.791

APPENDIX E

Total moles of CO₂ absorbed by the absorbent

Table E1: Total moles of CO₂ absorbed by the absorbent.

Pressure	Number of moles of absorbent (mol)	CO ₂ loading capacity, α (mol CO ₂ / mol absorbent)	Net CO ₂ absorbed* (mol)
5	0.10	4.498	0.45
	0.50	2.664	1.33
	1.00	1.609	1.61
	1.50	1.117	1.68
	2.00	0.961	1.92
10	0.10	8.177	0.82
	0.50	2.664	1.33
	1.00	2.149	2.15
	1.50	1.556	2.33
	2.00	1.271	2.54
15	0.10	11.133	1.11
	0.50	3.244	1.62
	1.00	2.460	2.46
	1.50	1.797	2.70
	2.00	1.484	2.97
20	0.10	12.995	1.30
	0.50	3.903	1.95
	1.00	2.723	2.72
	1.50	2.039	3.06
	2.00	1.640	3.28
25	0.10	14.377	1.44
	0.50	4.064	2.03
	1.00	3.058	3.06
	1.50	2.269	3.40
	2.00	1.791	3.58

Sample calculation:

$$\begin{aligned}
 \text{Net CO}_2 \text{ absorbed} &= \text{Number of moles of absorbent} \times \text{CO}_2 \text{ loading capacity} \\
 &= 0.1 \times 4.498 \text{ mol} \\
 &= 0.45 \text{ mol}
 \end{aligned}$$

APPENDIX F

Mass of solids recovered from CO₂ utilization process

Table F1: The average mass of solids recovered and standard deviations based on 1 mol ethanol.

Concentration of GLY-DMAPA (mol/L)	Mass of solids recovered/ mass of absorbent (mg/g)				Standard deviations
	1	2	3	averages	
0.1	0.00	0.00	0.00	0.00	0.00
0.5	15.48	15.70	14.72	15.30	0.16
1.0	43.16	47.62	45.53	45.43	3.15
1.5	68.00	64.13	61.66	64.59	2.73
2.0	95.41	95.68	97.73	96.27	1.27

APPENDIX G

Permission to reprint Figure 2.10

10/21/2019

Rightslink® by Copyright Clearance Center



RightsLink®

Home

Account Info

Help



Title:

Toward Efficient CO₂ Capture Solvent Design by Analyzing the Effect of Chain Lengths and Amino Types to the Absorption Capacity, Bicarbonate/Carbamate, and Cyclic Capacity

Author:

Rui Zhang, Qi Yang, Zhiwu Liang, et al

Publication: Energy & Fuels

Publisher: American Chemical Society

Date: Oct 1, 2017

Copyright © 2017, American Chemical Society

Logged in as:

Hanan Mohamed Mohsin

Account #:

3001522853

LOGOUT

PERMISSION/LICENSE IS GRANTED FOR YOUR ORDER AT NO CHARGE

This type of permission/license, instead of the standard Terms & Conditions, is sent to you because no fee is being charged for your order. Please note the following:

- Permission is granted for your request in both print and electronic formats, and translations.
- If figures and/or tables were requested, they may be adapted or used in part.
- Please print this page for your records and send a copy of it to your publisher/graduate school.
- Appropriate credit for the requested material should be given as follows: "Reprinted (adapted) with permission from (COMPLETE REFERENCE CITATION). Copyright (YEAR) American Chemical Society." Insert appropriate information in place of the capitalized words.
- One-time permission is granted only for the use specified in your request. No additional uses are granted (such as derivative works or other editions). For any other uses, please submit a new request.

If credit is given to another source for the material you requested, permission must be obtained from that source.

BACK

CLOSE WINDOW

Copyright © 2019 [Copyright Clearance Center, Inc.](#) All Rights Reserved. [Privacy statement](#). [Terms and Conditions](#). Comments? We would like to hear from you. E-mail us at customercare@copyright.com

APPENDIX H

Publications

H. M. Mohsin, A.M. Shariff, K. Johari. (2019). 3-Dimethylaminopropylamine (DMAPA) mixed with glycine (GLY) as an absorbent for carbon dioxide capture and subsequent utilization. *Separation and Purification Technology*. 222, 297 – 308.

H. M. Mohsin, K. Johari, A.M. Shariff (2019). Absorbents, media, and reagents for carbon dioxide capture and utilization, *Sustainable Agriculture Reviews* 38 (pp. 41-62): Springer.

H. M. Mohsin, K. Johari, A.M. Shariff. (2018). Virgin coconut oil (VCO) and potassium glycinate (PG) mixture as absorbent for carbon dioxide capture. *Fuel*. 232, 454-462.